GLYCOGEN ENHANCEMENT AUGMENTS OVERLOAD-INDUCED PROTEIN SYNTHESIS, GROWTH, AND MYOGENESIS IN AGED SKELETAL MUSCLE

by

Marcus Michael Lawrence

A dissertation submitted to the faculty of
The University of North Carolina at Charlotte
in partial fulfillment of the requirements
for the degree of Doctor of Philosophy in
Biology

Charlotte

2017

Approved by:

_____
Dr. Scott Gordon

_____
Dr. Susan Tsivitse Arthur

_____
Dr. Didier Dréau

_____
Dr. Joseph Marino

_____
Dr. Jeanette Bennett

ABSTRACT

MARCUS MICHAEL LAWRENCE. Glycogen Enhancement Augments Overload-Induced Protein Synthesis, Growth, and Myogenesis in Aged Skeletal Muscle. (Under the direction of DR. SCOTT E. GORDON)

Age-related skeletal muscle (SkM) wasting is associated with elevated 5'-AMP-Activated Protein Kinase (AMPK) activity, which inhibits overload-induced (OI) SkM protein synthesis (MPS) and growth. Glycogen, an inhibitor of AMPK, is reduced in aged SkM. We performed a series of experiments to examine the effects of manipulating glycogen on AMPK, MPS and related signaling, and OI-growth in aged SkM. Mutant glycogen synthase (GS; designed to enhance SkM glycogen content [GC]) or empty-vector plasmids were electrotransferred into fast-twitch plantaris muscles prior to 21-day synergist ablation-induced unilateral overload in young adult (8 mo.; empty vector; YE) and old (33 mo.; empty vector, OE; or mutant GS, OM) male FBN rats. Contralateral limbs underwent SHAM ablations with no plasmid. There were significant increases in OI-(all vs. SHAM) MPS and hypertrophy in YE and OM groups only. As expected, mutant GS expression and GC were significantly higher in OM overloaded muscles (the only muscles receiving the mutant GS plasmid) vs. SHAM OM muscles or vs. both SHAM or overloaded YE and OE muscles. Markers of AMPK activity and other signaling intermediates affecting MPS were largely unaltered by glycogen enhancement. Subsequent experiments in which the mutant GS vs. empty-vector plasmid were transfected into cultured C2C12 skeletal muscle myotubes also confirmed a positive effect of enhanced GC on MPS with little change in underlying signaling intermediates affecting MPS. However, there was a strong and significant effect of enhancing GC (via mutant GS vs. empty vector plasmid) on myogenic regulatory factors, embryonic myosin

heavy chain-positive fibers, and total fiber number in aged muscle under conditions of overload in vivo. Thus, enhancing GC may lead to enhanced MPS and OI growth in aged SkM. This effect may be due, in part, to an enhanced myogenesis.

DEDICATIONS

To my parents, Anne and Mike, fiancé and future wife, Marissa, and sisters, Katie and Lucy, this work is dedicated to you.

ACKNOWLEDGEMENTS

This work was entirely made possible by the expert tutelage and support of Dr. Scott Gordon throughout my time at UNC Charlotte. I want to express my utmost gratitude for your valued guidance, knowledge, and critique. I would also like to thank my committee members, Dr. Susan Tsivitse Arthur, Dr. Didier Dréau, Dr. Joseph Marino, and Dr. Jeanette Bennett for your important feedback and support. Thank you to the members of the Laboratory of Systems Physiology, Dr. Reuben Howden, Benjamin Gordon, Dr. Yvette Huet, Dr. Susan Tsivitse Arthur, Joshua Huot, Dr. Joseph Marino, Jonathan Petrocelli, and Bailey Peck for their assistance and camaraderie. Thank you to Dr. Peter Roach and Dr. Alexander Skurat for providing the pCMV4 plasmids. Thank you to Dr. Adam Reitzel and Eric Kane for providing materials and expertise in plasmid molecular biology techniques. I would like to thank The University of North Carolina at Charlotte Graduate School for the Graduate Assistant Support award that funded me to perform this work and The American College of Sports Medicine for the ACSM Doctoral Student Research Award that partially funded this research. Also, I would like to thank the National Institutes of Aging for supplying the animals at no cost for use in this work. Lastly, I would like to acknowledge my parents, Anne and Mike, fiancé and future wife, Marissa, sisters, Katie and Lucy, and friends for their patience and everlasting support throughout my doctoral studies.

TABLE OF CONTENTS

LIST OF TABLES

LIST OF FIGURES

LIST OF ABBREVIATIONS

ACC	Acetyl-Coenzyme A Carboxylase
AMP/ADP/ATP	Adenosine Monophosphate/Diphosphate/Triphosphate
AMPK	5'-AMP-Activated Protein Kinase
Akt1	Protein Kinase B-1
BCAA	Branched Chain Amino Acid
CMV	Cytomegalovirus promoter
eIF4E	Eukaryotic Initiation Factor 4E
eEF2/eEF2K	Eukaryotic Elongation Factor 2/eEF2 Kinase
eMyHC	Embryonic Myosin Heavy Chain
FOXO3A	Forkhead Box Transcription Factor 3A
GBD	Glycogen Binding Domain
GDP/GTP	Guanidine Diphosphate/Triphosphate
GH	Growth Hormone
GS	Glycogen Synthase
GSK3	Glycogen Synthase Kinase 3
IGF-1	Insulin-like Growth Factor 1
IRS-1	Insulin Receptor Substrate-1
MAFbx	Muscle Atrophy F-box
MPS	Muscle Protein Synthesis
MPB	Muscle Protein Breakdown
mTOR	Mechanistic (formerly mammalian) Target of Rapamycin
MuRF1	Muscle Ring-Finger 1

PA	Phosphatidic Acid
PDK1	3-Phosphoinositide-Dependent Kinase
PI3K	Phosphoinositide 3-Kinase
PIP2	Phosphatidylinositol (3,4)-bisphosphate
PIP3	Phosphatidylinositol (3,4,5)-triphosphate
PYGM	Muscle-specific Glycogen Phosphorylase
p70S6K	70-kDa Ribosomal Protein S6 Kinase
Rag	Ras-related GTP binding
RE	Resistance Exercise
Rheb	Ras homolog enriched in brain
rpS6	Ribosomal Protein S6
TSC1/TSC2	Tuberous Sclerosis Complex
4EBP1	eIF4E Binding Protein 1

CHAPTER 1: PROPOSED RESEARCH

1.1 Background and significance

Skeletal muscle mass and function decline greatly with age; known interventions are relatively ineffective in combatting this problem. Aging is associated with a progressive loss of skeletal muscle mass and function (sarcopenia), particularly in fast-twitch (i.e., type II) skeletal muscle fibers, and leads to an inability to perform activities of daily living, reduction in overall quality of life, and significantly increases the risk for all-cause mortality (94). The consequential burden on healthcare costs in our rapidly expanding national and global older adult population is large. Sarcopenia-related disabilities were estimated to cost >$18 billion in the year 2000 in the U.S. (90). As our older adult (65+ years of age) population is projected to double to 70 million in the year 2030 compared to 35 million in the year 2000, this will likely lead to a doubling in the prevalence and associated costs of sarcopenia. Unfortunately, interventions such as resistance exercise (RE) training [loading of the muscle; (34, 35)] and amino acid supplementation (28, 33, 134) are not completely effective at combatting chronic condition.

Following an acute bout of RE in aged skeletal muscle, there is suppressed muscle protein synthesis (MPS) and anabolic protein translational signaling (through the protein kinase B (Akt)-mechanistic (formerly mammalian) target of rapamycin (mTOR)-70-kDa ribosomal protein S6 kinase (p70S6k); Akt-mTOR-p70S6k pathway; (54); see Figure 1.1

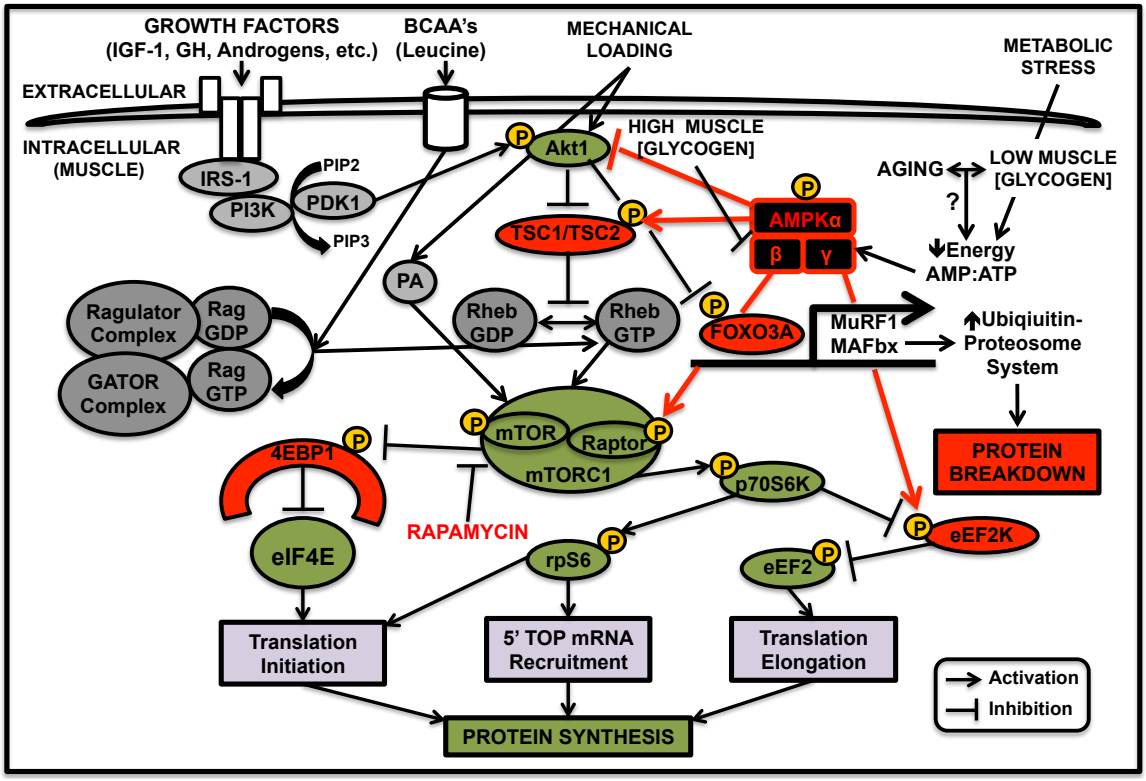

Figure 1.1 Overview of potential muscle protein synthesis (MPS) and muscle protein breakdown (MPB) regulation by 5'-AMP-activated protein kinase (AMPK). Note: red arrows and lines indicate direct effects of AMPK. This figure also includes simplistic inputs by branched-chain amino acids (BCAAs); IGF-1, insulin-like growth factor 1; GH, growth hormone; androgens; mechanical loading; and metabolic stress. Factors that inhibit protein synthesis and/or lead to protein breakdown are in red, whereas, factors involved in protein synthesis and/or inhibit protein breakdown are in green. Note: Aging is associated with low muscle [glycogen], which may be the cause of the negative energy (high AMP:ATP) balance leading to activation of AMPK. IRS-1, insulin receptor substrate 1; PI3k, phosphoinositide 3-kinase; PIP2, phosphatidylinositol (3,4)-bisphosphate; PIP3, phosphatidylinositol (3,4,5)-triphosphate; PDK1, 3-phosphoinositide-dependent protein kinase 1; PA; phosphatidic acid; Akt1, protein kinase B 1; TSC1/TSC2, tuberous sclerosis complex; Rheb, Ras homolog enriched in brain; Rag, Ras-related GTP binding; GATOR, GAP activity toward Rags; FOXO3A, forkhead box transcription factor 3A; mTOR, mechanistic (formerly mammalian) target of rapamycin; mTORC1, mTOR complex 1; MuRF1, muscle ring-finger 1; MAFbx, muscle atrophy F-box; eIF4E, eukaryotic initiation factor 4E; 4EBP1, eIF4E binding protein; p70S6k, 70-kDa ribosomal protein S6 (rpS6) kinase; eEF2K, eukaryotic elongation factor 2 (eEF2) kinase; 5' TOP, 5' terminal oligopyrimidine tract.

below for acronym definitions) with an upregulation in muscle protein breakdown (MPB) and catabolic signaling (e.g., "atrogenes" such as forkhead box transcription factor 3A (FOXO3A), muscle ring finger-1 (MuRF1), and muscle atrophy f-box (MAFbx); the ubiquitin-proteasome system (107); Figure 1.1), resulting in a diminished increase in muscle mass (i.e., with RE training) versus young adult muscle (65). The Gordon laboratory has observed highly similar detriments in MPS and anabolic signaling in aged vs. young adult rat skeletal muscle (42, 126-129). This occurs both in response to an

acute bout of RE via high-frequency electrical stimulation (HFES), a model of acute RE (126, 127), and in response to chronic overloading of the muscle via synergistic ablation/tenotomy (42, 128, 129) leading to a blunted muscle growth with age. Importantly, these findings closely model similar findings in aged humans (34, 65).

Aged skeletal muscle displays a blunted protein turnover and anabolic response. Skeletal muscle mass is maintained by the intricate balance of protein turnover that involves MPS and MPB (134). As discussed above, aged skeletal muscle is associated with a reduction in anabolic signaling/MPS and an upregulation in catabolic signaling/MPB, leading to a net protein loss (11, 65). These losses have been predominantly found to affect fast-twitch (type II) fibers (42, 69). Additionally, in response to anabolic stimuli (i.e., RE, amino acids, growth factors, etc.) aged muscle has a blunted ability to hypertrophy (28, 42, 65). This diminished ability to maintain or increase muscle fiber size/mass occurs both in aged humans (65, 107) and in rats (11, 42). Importantly, the Gordon laboratory found that an enzyme within skeletal muscle fibers called 5'-AMP-activated protein kinase (AMPK) plays a major role in the suppression of acute (31, 126) and chronic MPS/anabolic signaling (42, 128, 129) and thus, impaired growth in aged muscle (42, 128, 129).

Negative energy balance in aged skeletal muscle chronically activates AMPK. Aged skeletal muscle displays a negative energy balance compared to young (i.e., a higher ratio of AMP to ATP or AMP:ATP; Figure 1.1), which is known to activate AMPK (50), and may do so on a chronic basis in aged muscle (42, 128). AMPK exists in a 3-subunit complex containing 7 isoforms: α_1, α_2, β_1, β_2, γ_1, γ_2, γ_3. In addition to being activated allosterically by elevated AMP (on its γ subunit), AMPK is also activated by

phosphorylation at Threonine-172 (Thr^{172}; the 172^{nd} amino acid) by upstream kinases (e.g., AMPK kinase) on its α subunit (the catalytic subunit; Figure 1.1). Moreover, AMPK can strongly be inhibited by glycogen binding to a glycogen-binding domain (GBD) on its β subunit [(50, 77, 78); Figure 1.2 below]. When activated, AMPK acutely upregulates pathways to supply short-term energy via glucose uptake and fat oxidation (77, 78), and chronic AMPK activation leads to long-term energy supply pathways being increased, such as mitochondrial biogenesis (50), to restore cellular energy homeostasis.

AMPK also inhibits ATP-expensive pathways such as MPS. Specifically, AMPK directly activates (via phosphorylation) TSC2 allowing for the TSC1/TSC2 (TSC) complex to form, which in turn inhibits mTOR complex 1 (mTORC1; (114); Figure 1.1). AMPK also directly inhibits mTORC1 by phosphorylating and inhibiting the mTORC1 protein Raptor [(114); Figure 1.1]. mTORC1 inactivation leads to suppression of protein translation initiation by not allowing mTORC1 to activate (via phosphorylation) both p70S6k and being unable to remove (via phosphorylation) 4E-BP1 inhibitory binding on eIF-4E (Figure 1.1). The inhibition of p70S6k by AMPK also inhibits p70S6k from recruiting 5' TOP mRNA as well as phosphorylating rpS6 (54, 114) further inhibiting protein translation initiation (Figure 1.1). Further, the inhibition of p70S6k by AMPK leads to inhibition of protein elongation by not allowing p70S6k to remove eEF2k inhibition of eEF2 [(54, 114); Figure 1.1]. AMPK has been found to directly inhibit elongation by phosphorylating eEF2k [(129); Figure 1.1]. AMPK also blocks Akt inhibition (via phosphorylation) of FOXO3A, allowing for FOXO3A translocation to the nucleus and subsequent upregulation of MuRF1 and MAFbx, leading to MPB [(54, 114); Figure 1.1]. The Gordon laboratory has observed a similar elevation of AMPK activity

and inhibition of protein translation initiation and elongation anabolic (MPS) signaling following an acute bout of RE (126, 127) and following chronic muscle overload (42, 128, 129), in conjunction with a blunted hypertrophy in aged rat skeletal muscle (42, 128, 129).

Several different stimuli that activate MPS, converge on the mTORC1 pathway and are all affected with age. mTOR exists in 2 distinct protein complexes, mTOR complex 1 (mTORC1) consists of the proteins mTOR, GβL, and Raptor, whereas, the mTOR complex 2 (mTORC2) consists of the proteins mTOR, GβL, and Rictor (41, 55). *In vivo*, rapamycin forms a complex with FK506 binding protein 12 (FKBP12), which binds to the FRB domain of mTOR and inhibits its function (41, 55). mTORC1 contains the rapamycin-sensitive protein Raptor, whereas, mTORC2 contains the rapamycin-insensitive protein Rictor (41, 55). Because mTORC2 does not seem to be directly inhibited by rapamycin, it remains to be seen if it contributes to any muscle growth-regulated effects seen with protein translation and therefore will not be further reviewed (41, 55). The mTORC1 pathway will be the only one reviewed for the remainder of this proposal.

The mTORC1 pathway regulating protein translation in muscle, can be activated via several stimuli including, but not limited to, amino acids and mechanical loading (117). All of these stressors converge on the mTORC1 pathway via several different mechanisms (Figure 1.1) to increase MPS and will be summarized briefly. Signaling through the mTORC1 pathway is tightly controlled by its association with various small GTPases, mainly Ras homolog enriched in brain (Rheb) and Ras-related GTP binding [Rag, Figure 1.1; (57, 62, 117)]. Rheb activates mTORC1 when it is bound to GTP, but

not when it is bound to GDP, and this GTP/GDP loading status of Rheb is regulated by a GTPase (GAP) complex (57, 62, 117). The activity of the GAP complex is regulated by the TSC1/2 complex, which in turn is influenced by several upstream kinases, namely Akt, extracellular-related protein kinases (ERK) 1 and 2, the 90-kDa ribosomal protein S6 kinase (p90RSK), and AMPK (57, 62, 117). Phosphorylation of TSC1/2 by Akt, ERK, or p90S6K inhibits the GAP activity leading to an increase in the GTP bound form of Rheb which leads an increase in mTORC1 activity, whereas, AMPK has the opposite effect (57, 62, 117). mTORC1 signaling is also controlled by the GTPase RagA or RagB (RagA/B) in association with RagC or RagD (RageC/D). When RagA/B is bound to GTP and RagC/D is bound to GDP, the activity of mTORC1 is increased, whereas, when RagA/B is bound to GDP and RagC/D is bound to GTP mTORC1 is inactive (57, 62, 117). Additionally, the RagA/B-RagC/D complex is also associated with an additional protein complex called Ragulator that acts as a guanine nucleotide exchange factor (GEF) for RagA/B (57, 62, 117). Ragulator helps to target the RagA/B complex to the late endosomal/lysomal [LEL; (57, 62, 117)] membrane that leads to increased mTORC1 activity.

Amino acids, mainly the branched-chain amino acid (BCAA) leucine, have been found to be a potent stimulator of mTOR and MPS (26, 36). Leucine stimulates mTORC1 signaling by activating the GEF activity of Ragulator to repress a protein complex called GAP activity toward Rags (GATOR), that in turn leads to more RagA/B in the GTP bound state (57, 62, 117). Mechanical loading leads to activation of mTORC1 signaling by activating ERK and Akt, leading to suppression of TSC1/2 and upregulation of Rheb in the GTP bound form (57, 62, 117). Also, mechanical activation

leads an increase in phosphatidic acid (PA), which is believed to lead to an increase of the GTP bound form of Rheb (57, 62, 117). Importantly, aging muscle displays a blunted ability to increase mTORC1 signaling in response to both amino acids (28, 33, 134) and mechanical loading (34, 35). These findings highlight the need for a potent countermeasure to restore the ability of aged skeletal muscle to enhance mTORC1 signaling, MPS, and ultimately growth.

Glycogen is reduced in aged skeletal muscle and this may underlie the increase in AMPK activity. Glycogen, the stored form of glucose, makes up ~500g of total skeletal muscle mass and serves as a critical energy reserve for ATP production during states of reduced cellular energy (102). Glycogen is synthesized into highly organized branched tiered granules (where the amount of glucose increases exponentially for each branched tier generated) by the main enzyme glycogen synthase (GS) and is degraded by the enzyme glycogen phosphorylase, and both work in conjunction with other enzymes (109). GS is the critical regulator of glycogen content in skeletal muscle (109). The gene GSY1 encodes GS in skeletal muscle and mostly all other tissues capable of glycogen synthesis; however, GSY2 is specific to the liver form of GS (109). GS is phosphorylated (and thus inhibited) on nine sites (serine residues) on the N- and C-termini of the enzyme, with 4 sites (2, 2a, 3a and 3b) being identified as the most critical for glycogen synthesis [(109); see Figure 1.2 below]. Important to this proposal, glycogen content is diminished in aged skeletal muscle at rest in both rats (7, 17, 23, 47) and humans (17, 82), although not consistently (53, 83, 85, 103, 108). Moreover, the contraction-induced depletion of glycogen is significantly greater in aged muscle (17, 53,

126) and there is a blunted ability to increase glycogen levels with training vs. young adult muscle in both rats (17, 53, 126) and humans (17, 82).

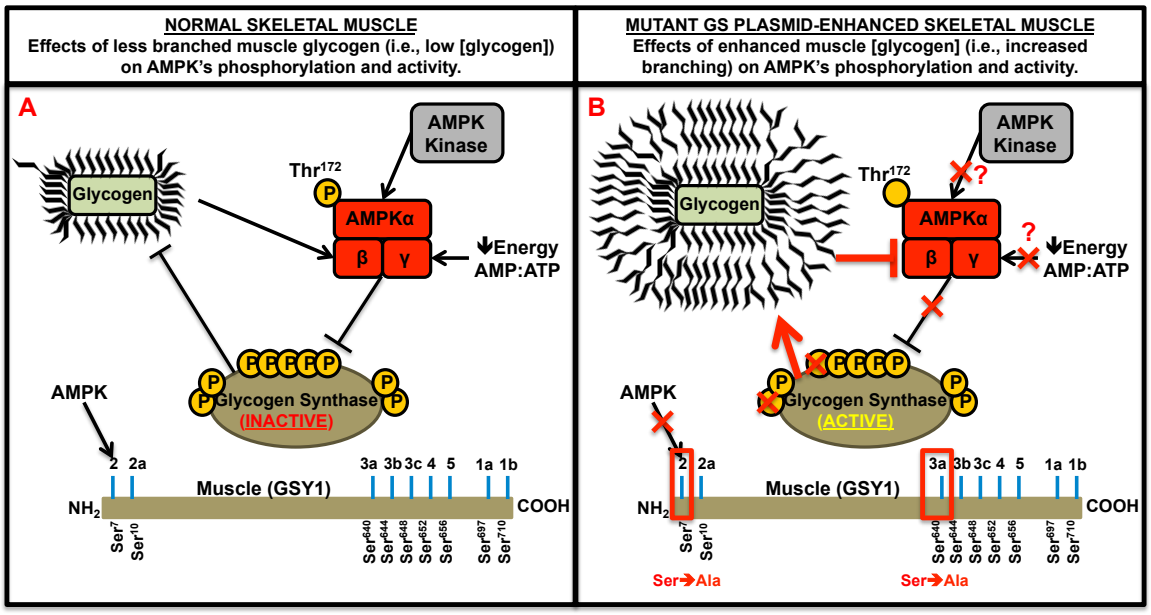

Figure 1.2. Effect of glycogen concentration ([glycogen]) on 5'-AMP-activated protein kinase (AMPK) phosphorylation and activity in muscle without (A) and with (B) muscle glycogen enhancement. A) AMPK is phosphorylated on its catalytic (α) subunit on Thr^{172} by upstream AMPK Kinase, activated by less branched glycogen on its β subunit containing the glycogen binding domain, and by low cellular energy (i.e., a high ratio of AMP:ATP) on its γ subunit. When activated AMPK, amongst other functions, inhibits Glycogen Synthase (GS). Muscle-specific glycogen synthase is encoded by GSY1 resulting in 9 phosphorylation sites from its amino (NH_2) to carboxyl (COOH) ends (sites 2, 2a, 3a, 3b, 3c, 4, 5, 1a, 1b corresponding to Ser^7, Ser^{10}, Ser^{640}, Ser^{644}, Ser^{648}, Ser^{652}, Ser^{697}, and Ser^{710}, respectively). Once phosphorylation of any of the 4 key sites (2, 2a, 3a, 3b) occurs the GS enzyme is inactive and therefore inhibits formation of glycogen with increased branching (more branching increases glucose). AMPK phosphorylates and thus inhibits the GS enzyme on site 2 (Ser^7). **B**) Introduction of plasmid DNA expressing an active GS mutated on sites 2 & 3a (Mutant GS) will produce highly branched glycogen (i.e., high [glycogen]) and induce a strong inhibition of AMPK, thereby removing AMPK inhibition of GS. NOTE: It is unknown whether the high [glycogen] produced by mutant GS will restore cellular energy (AMP:ATP) in old muscle and thereby not activate AMPK, or whether it will inhibit upstream kinases from activating it.

Further, as stated above, AMPK is directly inhibited by glycogen through its β subunit containing a GBD [(77, 78); Figure 1.2]. AMPK activity has been found to be inversely related with the level of glycogen in muscle *in vivo*, with its activity being dramatically suppressed with high levels of glycogen and an increased AMPK activity with low levels of glycogen in both rats (138) and humans (123), however, these findings have been recently challenged (122, 140, 141). These findings of an AMPKβ-glycogen interaction have also been supported *in vitro*, where large synthesized branched

oligosaccharides (i.e., large glycogen-mimicking molecules) inhibited AMPK's activity up to 90%, and as the oligosaccharides decreased in their amount of branching (i.e., smaller glycogen-mimicking molecules) there were concomitant increases in AMPK's activity as well as suppression of glycogen synthesis (77). Additionally, AMPK directly inhibits GS when activated, thus, the chronic activation of AMPK with age (128) may be a critical factor in the diminished ability of aging skeletal muscle to store glycogen (Figure 1.1).

We postulate that the low muscle glycogen content in aged muscle is an important factor contributing to the upregulation of AMPK activity and catabolic signaling/MPB and suppression of anabolic signaling/MPS and growth. However, the link(s) between glycogen content, MPS, MPB, growth, and associated signaling following chronic overload in aged skeletal muscle have not been examined. We further postulate that skeletal muscle glycogen content enhances anabolic signaling/MPS and suppresses catabolic signaling/MPB in response to leucine through AMPK in an mTORC1 manner; however, the effects of glycogen enhancement on anabolic stimuli, such as amino acids, have also never been tested in skeletal muscle. Here we propose that enhancing intramuscular glycogen content via the introduction of plasmid DNA expressing active glycogen synthase in aged rat skeletal muscle or cultured C2C12 myotubes will suppress AMPK activity, enhance anabolic signaling/MPS, suppress catabolic signaling/MPB, and enhance *in vivo* growth in response to chronic overload *in vivo* and leucine treatment *in vitro*. These studies could support the use of enhancing intramuscular glycogen content to suppress AMPK, restore the balance of MPS/MPB, and rescue growth in skeletal muscle during aging or in other conditions in which muscle mass is compromised.

1.2. Innovation

We plan to test the innovative hypothesis that enhancing glycogen content in aged rat skeletal muscle or C2C12 myotubes will suppress AMPK activity in response to both chronic overload and acute transfection with leucine treatment, resulting in similar responses (i.e., elevated MPS/anabolic signaling, elevated growth *in vivo*, suppressed catabolic [MPB] signaling). To enhance intramuscular glycogen we plan to inject and electroporate mutant GS plasmid DNA that has been mutated from serine to alanine on two key sites (2 and 3a) into old rat skeletal muscle (Figure 1.2) and transfect into C2C12 myotubes. This plasmid has been shown to enhance glycogen content in both cells (120) and rodent muscle (32, 75, 100). The innovative aspect of our study is that this method has never been tested in aged muscle, especially with respect to its potential for rescuing growth. The use of this innovative approach to enhance glycogen, instead of other known methods of manipulating muscle glycogen levels (e.g., fasting, exercise, etc.), should enable us to elucidate any physiological mechanism(s)/link(s) between muscle glycogen levels, AMPK, MPS, MPB, *in vivo* growth, and associated signaling in aged rat muscle or cultured C2C12 myotubes.

1.3 Specific Aims

Published and unpublished data from the Gordon laboratory have confirmed aged human skeletal muscle to have a significantly lower resting glycogen content vs. young adult muscle with a corresponding increase in AMPK activation in old, but not young muscle within ≤ 1-2 hours post an acute bout of RE (125). Similarly, the Gordon laboratory has found that aged rat skeletal muscle displays a significantly (3-fold) greater glycogen depletion following an acute bout of RE (via HFES), and that the lower

glycogen level in aged muscle is associated with a greater AMPK activation (126). Importantly, the Gordon laboratory has found that glycogen's influence on AMPK's activity in rats after HFES (31, 126) is a good model for similar observations in humans after RE Figures 1.3 and 1.4; (125). The Gordon laboratory has demonstrated that lower glycogen content during acute RE in human skeletal muscle is associated with higher AMPK activity (p-ACC Ser79; Figure 1.3). The same study (as Figure 1.3) also found that lower glycogen content during acute RE in human skeletal muscle was associated with a lower anabolic (MPS) signaling (data not shown) and higher catabolic (MPB) signaling (Figure 1.4), where lower FOXO3A phosphorylation leads to greater MPB.

Additionally, preliminary data (Figures 1.5-1.7) from our laboratory indicate that glycogen content increases in response to chronic overload of fast-twitch skeletal muscle (i.e., plantaris) in young adult, but not old rats (Figure

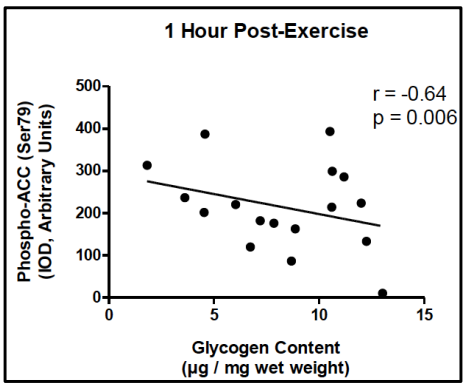

Figure 1.3. Relationship between phospho-ACC (Ser79) and glycogen content in the vastus lateralis muscles of young adult and old human subjects after an acute bout of resistance exercise.

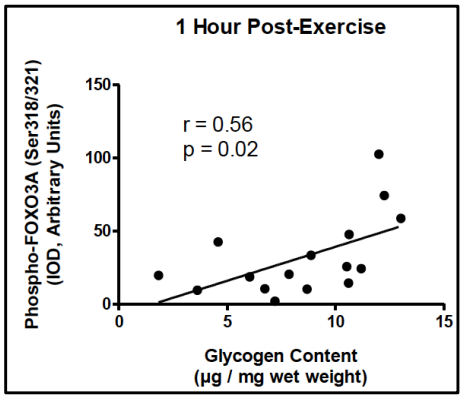

Figure 1.4. Relationship between phospho-FOXO3A (Ser318/321) and glycogen content in the vastus lateralis muscles of young adult and old human subjects after an acute bout of resistance exercise.

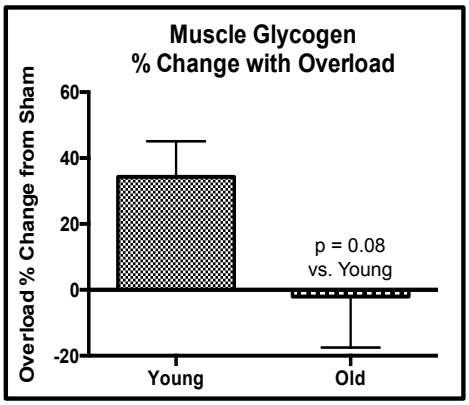

Figure 1.5: Percent (%) change in glycogen content of 7-day overloaded vs. sham-operated plantaris muscles in young adult (8 mo.) vs. old (33 mo.) rats.

1.5). Moreover, this diminished increase in glycogen content was associated with higher AMPK activity (Figure 1.6), lower protein synthesis (data not shown), and reduced muscle growth (Figure 1.7) in the old animals. We postulate that the low muscle glycogen content in aged muscle is an important factor contributing to the upregulation of AMPK activity and catabolic signaling/MPB and suppression of anabolic signaling/MPS and growth. However, the link(s) between glycogen content, MPS, MPB, growth, and associated signaling following chronic overload in aged skeletal muscle have not been examined. We further postulate that skeletal muscle glycogen content enhances anabolic signaling/MPS and suppresses catabolic signaling/MPB in response to leucine through AMPK in an mTORC1 manner; however, the effects of glycogen enhancement on anabolic stimuli, such as amino acids, have also never been tested in skeletal muscle. Therefore, the present study addressed the following aims:

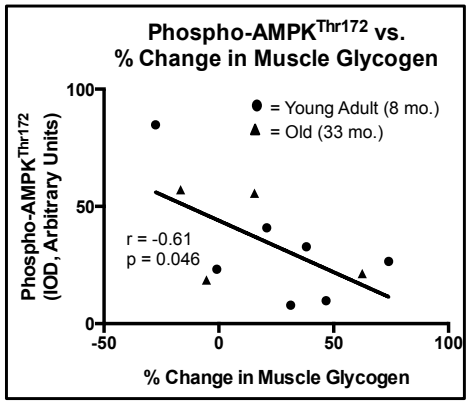

Figure 1.6: Relationship between phospho (Thr^{172}) - AMPK content in overloaded-limb and % change in muscle glycogen content with 7 days of overload in plantaris muscles of young adult (8 mo.) and old (33 mo.) rats.

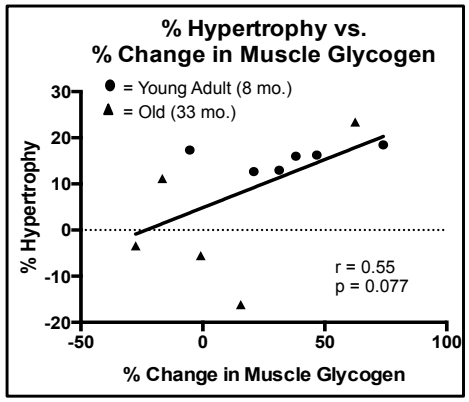

Figure 1.7: Relationship between % hypertrophy and % change in muscle glycogen content in overloaded-limb with 7 days of overload in plantaris muscles of young adult (8 mo.) and old (33 mo.) rats.

Specific Aim 1: To determine whether enhancing intramuscular glycogen content in aged rat skeletal muscle will suppress AMPK activity in response to chronic overload and thus enhance chronic anabolic signaling/MPS and suppress chronic catabolic signaling leading to a rescue in muscle growth to levels seen in young adult animals.

Hypothesis 1: Enhancing intramuscular glycogen content via the introduction of plasmid DNA expressing active glycogen synthase will suppress AMPK activity, suppress catabolic (MPB) signaling, restore anabolic signaling/MPS, and rescue overload-induced growth in aged rat skeletal muscle to levels observed in young adult muscle.

Specific Aim 2 Overall: To determine whether enhancing intracellular glycogen content can enhance anabolic signaling/MPS and decrease catabolic (MPB) signaling in response to an anabolic stimulus in skeletal myotubes.

Specific Aim 2a: To determine whether enhancing intracellular glycogen content acts through an AMPK-mTOR dependent pathway to increase anabolic signaling and muscle protein synthesis in response to leucine.

Hypothesis 2a: Glycogen enhancement via the transfection of plasmid DNA expressing active glycogen synthase in cultured C2C12 myotubes will enhance the anabolic effect of leucine by inhibiting AMPK and increasing anabolic signaling/MPS, and this effect will be eliminated by rapamycin-induced mTOR pathway blockade.

Specific Aim 2b: To determine whether enhancing intracellular glycogen content acts through an AMPK-mTOR dependent pathway to decrease catabolic signaling in response to leucine.

Hypothesis 2b: Glycogen enhancement via the transfection of plasmid DNA expressing active glycogen synthase in cultured C2C12 myotubes will enhance the anti-catabolic effect of leucine by inhibiting AMPK and decrease catabolic signaling, and the effect will be eliminated by rapamycin-induced mTOR pathway blockade.

1.4 Approach and Preliminary Data

We employed a series of experiments to test Specific Aims 1 and 2. In the first experiment (Chapter 2) we electrotransferred either the empty-vector (empty) or mutant GS vector (mutant) plasmid into the fast-twitch plantaris muscles of rats prior to a 21-day functional overload (unilateral gastrocnemius ablation). The contralateral legs received a sham-operation with no plasmid. The empty vector (pCMV4) was electrotransferred into young adult (Young empty, YE) and old (Old empty, OE), whereas, the mutant GS vector (pCMV4-M2,3a-GS) was electrotransferred into old (Old mutant, OM) only. In the second experiment (Chapter 3) we transiently transfected C2C12 myotubes to determine whether enhancing intracellular glycogen content can enhance anabolic signaling/MPS and decrease catabolic (MPB) signaling in response to leucine in skeletal myotubes. Both the *in vivo* and *in vitro* experiments were successfully employed in pilot work using the exact methodology outlined for glycogen enhancement. The preliminary experiments to enhance in vivo glycogen content led to increased protein synthesis (Figure 1.8) and growth (Figure 1.9) in overloaded plantaris muscles of young adult (8 mo.) Fischer 344 rats. Additionally, transient transfection of

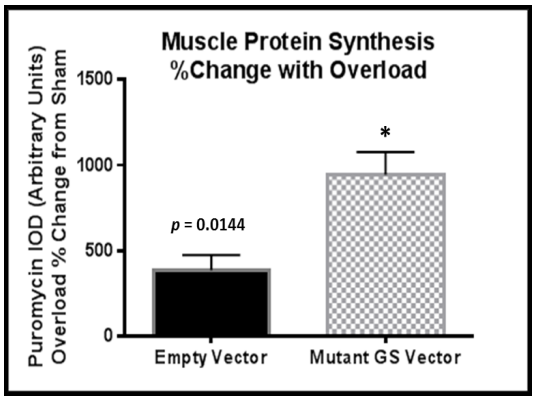

Figure 1.8: Percent (%) change in puromycin IOD protein synthesis of 21-day overloaded vs. sham-operated plantaris muscles in young adult rats with empty vs. mutant glycogen synthase (GS) plasmid treatment.

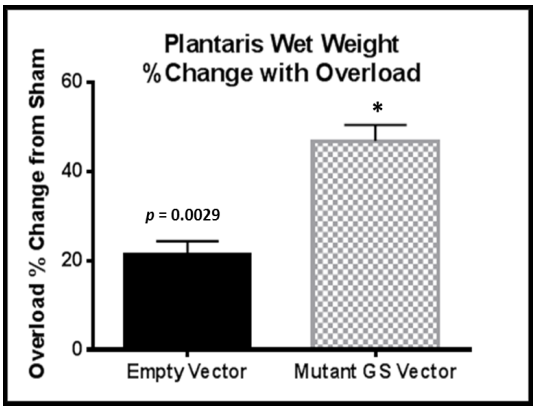

Figure 1.9: Percent (%) change in puromycin in plantaris wet weight in overloaded vs. sham-operated plantaris muscles in young adult rats with empty vs. mutant glycogen synthase (GS) plasmid treatment.

the mutant GS plasmid in cultured C2C12 myoblasts led to increases in total GS expression (Figure 1.10) with reductions in the phosphorylation status (phospho-GS/total GS) at Ser641 (Figure 1.11) compared to empty vector.

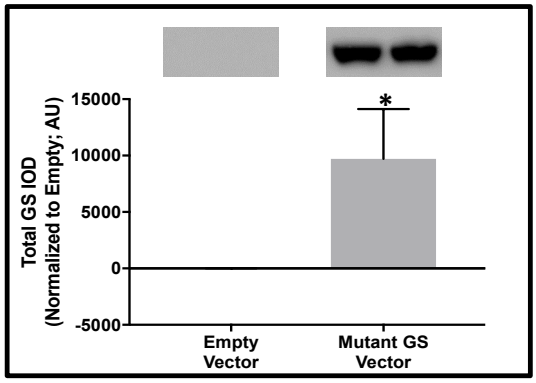

Figure 1.10: Percent (%) change in total glycogen synthase (GS) of mutant GS vector vs empty vector plasmid treated myoblasts 24 hours after transfection.

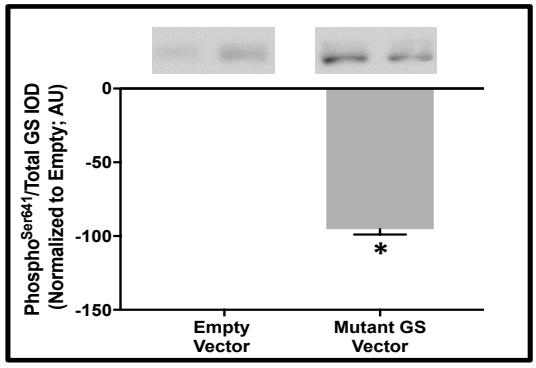

Figure 1.11: Percent (%) change in phospho-(Ser641)/total glycogen synthase (GS) of mutant GS vector vs empty vector plasmid treated myoblasts 24 hours after transfection.

CHAPTER 2: EFFECTS OF GLYCOGEN ENHANCEMENT ON CHRONIC OVERLOAD IN AGED RAT SKELETAL MUSCLE IN VIVO

2.1 Introduction

The age-related loss of muscle mass and function (i.e., sarcopenia) is a significant clinical problem and is estimated to affect 20-50% of individuals 65 years of age and older, and up to over 50% of individuals over 75 years of age and older (8). Additionally, the 65+ years of age population is estimated to double by the year 2030 (90), undoubtedly leading an increase in the prevalence and economic burden associated with sarcopenia. Therefore, research is warranted to better understand the pathophysiology of this chronic condition in order to advance the efficacy of lifestyle, therapeutic, and pharmacological treatment options.

Our laboratory (42, 126-129) has highlighted the effect of 5'-AMP-activated protein kinase (AMPK) in aged skeletal muscle. Specifically, AMPK phosphorylation status (at Thr172) and activity were chronically elevated in aged skeletal muscle (128) and this effect is highly correlated with diminished growth in response to 7-days of unilateral functional overload (128). This effect was purported to be due to AMPK's inhibition of signaling intermediates involved in regulation of protein translation (42, 129). Further, our laboratory (42) found that 5-Aminoimidazole-4-carboxamide ribonucleotide (AICAR), a pharmacological activator of AMPK, blunted the overload-induced growth of young adult muscle to the level observed in old animals. Importantly,

in the same study (42), a pharmacologic inhibitor of AMPK (Compound C) restored the overload-induced growth in aged muscle to the level seen in young adult animals. Collectively, these findings indicate that AMPK is a negative regulator of muscle protein synthesis (MPS) and growth in aged skeletal muscle and that inhibiting its activity could reduce this effect (42).

Glycogen, the stored form of glucose, serves as a critical energy reserve and is important to many metabolic processes (102, 109). Glycogen is synthesized into highly organized branched tiered granules primarily by glycogen synthase (GS) and degraded primarily by glycogen phosphorylase (GP), both working in conjunction with other enzymes and proteins (109). GS is a critical regulator of glycogen content in skeletal muscle (109). GS is phosphorylated (and thus inhibited) on nine sites (serine residues) on the N- and C-termini of the enzyme, with 4 sites (2, 2a, 3a and 3b) being identified as the most critical for glycogen synthesis (109). Glycogen content has been found to be diminished in aged skeletal muscle at rest in rats (7, 17, 23, 47) and humans (17, 82), although not consistently (53, 83, 85, 103, 108). Moreover, the contraction-induced depletion of glycogen is significantly greater in aged muscle (17, 53, 126) and there is a blunted ability to increase glycogen levels with training vs. young adult muscle in rats (17, 53, 126) and humans (17, 82).

AMPK exists in a 3-subunit complex containing 7 isoforms: α_1, α_2, β_1, β_2, γ_1, γ_2, γ_3. In addition to being activated allosterically by elevated AMP (on its γ subunit), AMPK is also activated by phosphorylation at Thr172 by upstream kinases (e.g., AMPK kinase) on its α subunit (the catalytic subunit; Figure 1.1). Moreover, AMPK can be strongly inhibited by glycogen binding to a glycogen-binding domain (GBD) on its β

subunit (50, 77, 78), although this interaction has recently been challenged (98, 122, 140). We thus postulate that the low muscle glycogen content is an important factor contributing to the upregulation of AMPK activity and catabolic signaling/muscle protein breakdown (MPB) and suppression of anabolic signaling/MPS and growth in aged muscle during overload. However, the link(s) between glycogen content, MPS, MPB, growth, and associated signaling following chronic overload has never been examined in aged humans or animals. Therefore, the goal of this investigation was to determine whether enhancing intramuscular glycogen content in aged rat skeletal muscle would suppress AMPK activity in response to chronic overload and thus enhance chronic anabolic signaling/MPS and suppress chronic catabolic signaling leading to a rescue in muscle growth to levels seen in young adult animals.

2.2 Experimental Design and Methods

2.2.1 Experimental Animals

Young adult (8 months) and old (32-34 months) male Fischer344 x Brown Norway F1 hybrid (FBN) rats (n = 9-13/group, 33 total) were obtained from the National Institutes of Aging's Aged Rodent Colony (Bethesda, MD) and were then singly housed in the vivarium at the University of North Carolina at Charlotte, an AAALAC accredited facility. The animals were kept on a 12-hr light-dark cycle and were given food and water *ad libitum*. All procedures were approved by the University of North Carolina at Charlotte Animal Care and Use Committee.

2.2.2 Surgical Procedures

Under general anesthesia (2-3% isofluorane and supplemental O_2), unilateral hindlimb surgical ablation of the gastrocnemius muscle in each animal was performed to enable

compensatory overload of the synergistic plantaris and soleus muscles for 3 weeks as described by Thomson and Gordon (128, 129). A sham (non-overload) surgery was performed on the contralateral control hindlimb.

We obtained (a kind gift from Dr. Peter Roach and Dr. Alexander Skurat, Indiana University, Bloomington, IN, USA) a pCMV4 plasmid that overexpresses a constitutively active form of glycogen synthase (pCMV4-M2,3a-GS), a rabbit skeletal muscle glycogen synthase having Ser to Ala mutations at sites 2 and 3a (120). This plasmid has been shown in COS cells (120) and rodents (32, 75, 100) to enhance skeletal muscle glycogen.

During the ablation surgery, 120 μL of plasmid DNA (either mutant GS/pCMV4-M2,3a-GS or empty vector/pCMV4) for each muscle was introduced into the plantaris muscle to be overloaded (but not the contralateral sham-operated muscle) using a 27-gauge needle and syringe following the protocol of Wu and Kandarian (139). Briefly, the needle was inserted near the distal myotendinous junction of the muscles, and slowing pushed in ~1cm rostrally to the proximal end of the muscle. 120 μL (at 1.5 μg/μL) of the plasmid DNA (in warm sterile half-saline solution) was injected evenly along the longitudinal axis of the muscles while slowly withdrawing the syringe. Following a 1-min wait period, electroporation was performed. Briefly, the surface of the muscles was moistened with sterile saline. Then, the electrodes (Tweezertrodes, Harvard Apparatus) were placed on either side of the muscle. Next, 5 square-wave electrical pulses at 75-100 V/cm, 20 ms at 1 Hz, with 200 ms interpulse intervals was applied using a BTX Electro Square Porator (Harvard Apparatus). The empty vector (pCMV4) was electrotransferred into young adult (Young empty, YE, $n = 9$) and old (Old empty, OE, $n = 11$), whereas,

the mutant GS vector (pCMV4-M2,3a-GS) was electrotransferred into old (Old mutant, OM, n = 13) only.

2.2.3 Muscle Harvesting and SUnSET Technique

Three weeks after ablation surgery, animals were fasted for 5 h to remove any potential affects on MPS due to feeding prior to being anesthetized with 2-4% inhaled isofluorane with supplemental O_2. During anesthesia, one jugular vein of the animal was exposed by incision through the skin of the neck. The vein was then slowly injected with 0.040 μmol puromycin/g BW dissolved in sterile PBS using a 25-gauge needle (61). Puromycin is incorporated into synthesizing proteins within the muscle and can be used in determining rate of protein synthesis by western blotting in harvested muscle samples (40). At 10 min after IV injection, the plantaris were very quickly harvested, trimmed of fat and connective tissue, weighed, and frozen in liquid N_2-chilled isopentane and store at -80°C until analyses were performed.

2.2.4 Glycogen Concentration Assay

Glycogen concentration was determined in the PLT muscles as previously described (99, 126), with modifications. Briefly, a portion of the PLT muscle was ground-glass homogenized in 26.67 volumes of ice-cold 0.1M NaOH. Then, in duplicate, 100 μL of homogenate was transferred to a new tube and boiled at 90°C for 20 min in a dry-block heater to remove any free glucose. After 20 min, the solution was neutralized with 100 μL of 0.2M Acetic Acid. Then 50 μL of the neutralized solution was transferred to a new tube containing 150 μL of 0.1M Sodium Acetate Buffer (0.05M Sodium Acetate, 0.05M Acetic Acid, pH 4.6-4.7) and vortexed. Glycogenolysis was then performed by adding 20 μL of amyloglucosidase (Sigma no. A7420, St. Louis, MO, USA) solution (10 μg/μL in

20 mM Tris with 0.02% BSA, pH 7.5) and incubating at 55°C for 1 h. After 1 h, the samples were centrifuged at 14,800 x *g* for 5 min and then loaded in duplicate (4 readings per sample) into cuvettes (USA Scientific no. 9090-0460, Ocala, FL, USA). The amount of free glucosyl units in each sample were then determined spectrophotometrically via a glucose assay (Sigma no. GAHK20). Glycogen content (μg/mg wet weight) of the original muscle sample was then derived from comparing the reading to a standard curve made with type III glycogen from rabbit liver (Sigma no. G8876).

2.2.5 Homogenization and Protein Concentration Assay

Homogenization was performed as previously described (128, 129). Briefly, a portion of the PLT muscle was ground-glass homogenized in 7 volumes of ice-cold homogenization buffer (50 mM HEPES (pH 7.4), 0.1% Triton X-100, 4 mM EGTA, 10 mM EDTA, 15 mM $Na_4P_2O_7 \bullet 10\ H_2O$, 100 mM β-glycerophosphate, 25 mM NaF, 50 μg/ml leupeptin, 50 μg/ml pepstatin, 33 μg/ml aprotinin, and 5 mM Na_3VO_4). Sample homogenates were then diluted 1:7 in homogenization buffer before analysis of protein concentration, which was assessed in triplicate using a modified Lowry procedure (DC Protein Assay, Bio-Rad, Hercules, CA, USA). Protein assay results were then used to calculate total protein per whole muscle as an index of muscle hypertrophy.

2.2.6 SDS-PAGE, Western Blotting, and Immunodetection

Standard western blotting protocols were used as previously described (128, 129). Briefly, total muscle protein homogenates were solubilized in sample loading buffer (50 mM Tris-HCl, pH 6.8, 10% glycerol, 2% SDS, 2% β-mercaptoethanol, 0.1% bromophenol blue) at a concentration of 1 μg/μl and boiled at 95°C for 5 min. Proteins were then separated by SDS-PAGE using either 4-15% (mTOR, p70S6K, and 4EBP1) or

7.5% (all others) Tris-HCl gels (Criterion, Bio-Rad) for 1.5 h at 100V in 4°C and then transferred for 1 h at 100V in 4°C onto a PVDF membrane (EMD Millipore, Billerica, MA, USA) in Towbin's buffer (25 mM Tris-base, 192 mM glycine, 20% methanol). To verify transfer and equal loading among lanes, membranes were then stained with Ponceau S (Sigma) and imaged. For immunodetection, membranes were blocked for 1 h at room temperature in blocking buffer (5% nonfat dry milk in TBS-T, 20 mM Tris base, 150 mM NaCl, 0.1% Tween-20, pH 7.6), briefly rinsed in TBS-T, and then incubated with primary antibody (in 2% BSA in TBS-T, with 0.02% NaN_3, pH 7.5) overnight at 4°C on a shaker. Membranes were then serially washed in TBS-T, incubated with horseradish peroxidase (HRP)-conjugated secondary in blocking buffer for 1 h, and again serially washed in TBS-T. The HRP activity was detected by enhanced chemilumenscence reagent (ECL; EMD Millipore), exposure to autoradiographic film (Alkali Scientific no. XR1570, Pompano Beach, FL, USA), and then developed (Konica Minolta no. SRX-101A). Antigen concentration was calculated by quantification of the integrated optical density (IOD) of the appropriate band and then normalized to total protein content from previous Ponceau S staining using a gel analyzer software (Image Studio Lite, Licor, Lincoln, NE, USA). Primary antibody dilutions were as follows: phospho-AMPKα^{Thr172} (Cell Signaling Technology, CST, no. 4188, Beverly, MA, USA), 1:2000; total AMPKα (CST no. 2532), 1:5000; phospho-ACC^{Ser79} (EMD Millipore no.07-303) 1:2000; total ACC (Streptavidin-HRP, GE Life Sciences no. RPN1231), 1:5000; phospho-Akt^{Thr308} (CST no. 2965), 1:1000; phosho-Akt^{S473} (CST no. 4060), 1:1000; total Akt (CST no.4691), 1:2000; phospho-eEF2^{Thr56} (CST no. 2331), 1:10,000; total eEF2 (CST no. 2332), 1:10,000; p-FOXO3A$^{Ser318/321}$ (CST no. 9465), 1:1000; total

FOXO3A (CST no. 12829), 1:2000; phospho-GS^{Ser641} (CST no. 3891), 1:5000; total GS (CST no.3893), 1:5000; phoshpo-GSK-3α/β$^{Ser21/9}$ (CST no. 8566), 1:4000; total GSK-3α/β (CST no. 5676), 1:4000; K48-linkage Specific Polyubiquitin (CST no. 8081), 1:1000; MyoD1 (CST no. 13812), 1:600; Myogenin (Santa Cruz Biotechnology no. sc-12732, Dallas, TX, USA) 1:200; phospho-mTOR^{S2448} (CST no. 5536), 1:2000; mTOR (CST no. 2983), 1:4000; phospho-p70S6K^{Thr389} (CST no. 9234), 1:750; total p70S6K (CST no. 2708), 1:2000; puromycin (EMD Millipore no. MABE343), 1:5000; total PYGM (Thermo Fisher no. PA5-11511), 1:1000; phospho-4E-BP1$^{Thr37/46}$ (CST no. 2855), 1:6000; total 4E-BP1 (CST no. 9644), 1:15,000; phospho-TSC2^{Ser1387} (CST no. 5584), 1:1500; phospho-TSC2^{Thr1462} (CST no. 3617), 1:1500; total TSC2 (CST no. 3990), 1:2000. The appropriate species-specific (goat anti-mouse or anti-rabbit) HRP secondary antibodies were from CST, except for puromycin secondary, which was from Jackson ImmunoResearch Laboratories (West Grove, PA, USA).

2.2.7 Immunofluorescent eMyHC and Laminin Staining

For immunofluorescent staining analyses, a portion of the plantaris muscle that was frozen in liquid N_2-chilled isopentane was cross-sectioned at 12-μm beginning at the mid-belly on a cryostat. To quantify embryonic myosin heavy chain (eMyHC) and total fiber number, sections were blocked in 10% normal goat serum (Vector Laboratories, Burlingame, CA, USA) in PBS for 1 h and then incubated overnight at 4°C with MyH3 anti-eMyHC IgG1 (1:25, F1.652, DSHB) and anti-laminin IgG2a (1:50, 2E8, DSHB). The following day, sections were serially washed in PBS-T and incubated with goat anti-mouse Alexa Fluor 350 IgG1 (1:250, A-21120, Thermo Fisher) and Alexa Fluor 555

IgG2a (1:500, A-21137, Thermo Fisher) for 1 h, serially washed again, and then mounted with ProLong Gold (Thermo Fisher).

2.2.8 Immunofluorescent eMyHC and Total Fiber Number Quantification

For IHC, images were captured and analyzed at the University of Kentucky Center for Muscle Biology, using previously published methods (89). Briefly, images were captured at x20 magnification at room temperature using a Zeiss upright fluorescent microscope (Zeiss AxioImager M1 Oberkochen, Germany). Whole muscle sections were obtained using the mosaic function in Zeiss Zen 2.3 imaging software. Total fiber number and eMyHC proportion were analyzed using custom software, developed by the University of Kentucky Center for Muscle Biology. This robust and highly sensitive muscle analysis software has been validated against manual human counts and is both accurate and reliable (89).

2.2.8 Statistical Analyses

A two-way analysis of variance was used (Experimental Group x Overload, with repeated measures for overload between contralateral limbs). Post-hoc comparisons were accomplished via a Fisher's LSD test, with statistical significance being set *apriori* at $p \leq 0.05$. All statistical analyses and graphs were made using Graphpad Prism 7 (GraphPad, San Diego, CA, USA). Data are presented as means ± SEM.

2.3 Results

2.3.1 Body weights and food consumption

Body weight and food consumption was measured every day throughout the 21-day overload period. There was a significantly ($p \leq 0.05$) higher body weight (BW) in OE and OM vs. YE, with no significant differences (NSD; $p > 0.05$) between OE and OM

prior to ablation surgery on Day 1 (415g ± 12.21; 492.18g ± 23.73; and 484g ± 14.35; YE, OE, and OM, respectively) and at time of sacrifice on Day 21 (393g ± 11.00; 452.91g ± 21.10; and 441g ± 10.90; YE, OE, and OM, respectively). Additionally, daily food consumption (g food/kg BW) was significantly ($p \leq 0.05$) lower across the 21-day (average of Day 0 through Day 21) procedure in OE (33.95 g/kg BW ± 1.57) and OM (34.82 g/kg BW ± 1.71) vs. YE (40.25 g/kg BW ± 1.43), with NSD ($p > 0.05$) between OE and OM.

2.3.2 Muscle glycogen synthase and glycogen contents

The phosphorylation status (phospho-GS/total GS) at Ser641 (Figure 2.5.1A) and the absolute concentration of phospho-(Ser641) GS (Figure 2.5.1C) was significantly ($p \leq 0.05$) reduced (main effect) in all overloaded muscles compared to SHAM regardless of age or plasmid treatment. This decrease was seen despite a significant ($p \leq 0.05$) increase in the absolute concentration of total GS (Figure 2.5.1B) in the overloaded muscles of OM vs. SHAM and vs. overloaded muscles of YE and OE. This plasmid (mutant GS) has been shown in both COS cells (120) and in mouse skeletal muscle (32, 75) to enhance glycogen content due to Ser to Ala mutation at two critical sites (sites 2 and 3a) for phosphorylation and, thus, decreased activity (120). Ser641 is site 3a on GS and therefore the lack of change in phosphorylation at this site despite an increase in the absolute concentration of total GS verifies that the mutant GS-vector was overexpressed in the OM overloaded muscles. As expected, glycogen content (Figure 2.5.2A) was significantly ($p \leq 0.05$) higher in the overloaded muscles of OM vs. SHAM and vs. overloaded muscles of YE and OE. There were no differences ($p > 0.05$) in overloaded YE or OE muscles vs. SHAM, although OE muscles displayed a non-significant

downward trend with overload ($p = 0.104$) vs. SHAM. The OM demonstrated a percent increase with the overload that was significantly ($p \leq 0.05$) higher than both YE and OE (Figure 2.5.2B).

2.3.3 Muscle wet weights and total protein contents

21-days of overload resulted in significant ($p \leq 0.05$) hypertrophy, as measured by wet weights and total protein content (Table 2.6.1), of the overloaded plantaris muscles vs. SHAM of both the YE and OM groups, with a significant ($p \leq 0.05$) atrophy in the OE overloaded plantaris muscles vs. SHAM. Both the overloaded and SHAM muscles of YE were significantly ($p \leq 0.05$) larger than all OE and OM muscles. Importantly, the percent hypertrophy with overload was similar between YE and OM, both of which had a percent hypertrophy significantly ($p \leq 0.05$) greater than OE.

2.3.4 Muscle protein synthesis rate

Mixed MPS rate was determined via puromycin incorporation using the SUnSET technique (40, 61). MPS rate was significantly ($p \leq 0.05$) increased in overloaded muscles (main effect) regardless of age or plasmid treatment vs. SHAM muscles (Figure 2.5.3) with NSD ($p > 0.05$) between SHAM values of any group. Further, the increase in puromycin incorporation in OM overloaded muscles was significantly ($p \leq 0.05$) higher than OE overloaded muscles with NSD ($p > 0.05$) vs. YE overloaded muscles. Moreover, the percent MPS rate was NSD ($p > 0.05$) between YE, OE, and OM (69.9%, 36.4%, and 45.9%, respectively).

2.3.5 SIGNALING INTERMEDIATES REGULATING MPS

2.3.5.1 AMPK phosphorylation and concentration

The phosphorylation status (phospho-AMPKα/totalAMPKα) at Thr172 (Figure 2.5.4A) and the absolute concentration of phospho-(Thr172) AMPKα (Figure 2.5.4C) were significantly ($p \leq 0.05$) increased (main effect) in all overloaded muscles compared to SHAM regardless of age or plasmid treatment. The phosphorylation status of AMPKα was significantly ($p \leq 0.05$) higher in overloaded muscles of OE and OM vs. overloaded muscles of YE, with NSD ($p > 0.05$) between OE and OM. Further, the absolute concentration of phospho-(Thr172) AMPKα in the overloaded muscles of OM was significantly ($p \leq 0.05$) higher than the overloaded muscles in YE. Lastly, there was a significant ($p \leq 0.05$) decrease (main effect) in the absolute concentration of total AMPKα (Figure 2.5.4B) with overload regardless of age or plasmid treatment.

2.3.5.2 ACC phosphorylation and concentration

Acetyl-CoA Carboxylase (ACC) is a well-established marker of AMPK activity *in vivo* (43). The phosphorylation status (phospho-ACC/total ACC) at Ser79 (Figure 2.5.5A) and the absolute concentration of phospho-(Ser79) ACC (Figure 2.5.5C) were significantly ($p \leq 0.05$) increased (main effect) in all overloaded muscles compared to SHAM regardless of age or plasmids treatment. The phosphorylation status of ACC was significantly ($p \leq 0.05$) higher in overloaded muscles of OE only vs. the overloaded muscles of YE. Further, regardless of plasmid treatment or loading status, the muscles of OM and OE displayed higher levels of total ACC (Figure 2.5.5B) vs. YE.

2.3.5.3 Akt phosphorylation and concentration

The phosphorylation status (phospho-Akt/total Akt) at Thr308 (Figure 2.5.6A) and at Ser473 (Figure 2.5.6B) and the absolute concentration of phospho-(Thr308) Akt (Figure 2.5.6C) and phospho-(Ser473) Akt (Figure 2.5.6D) were significantly ($p \leq 0.05$) increased (main effect) in all overloaded muscles compared to SHAM muscles regardless of age or plasmid treatment. The phosphorylation status of Akt at Thr308 was significantly ($p \leq 0.05$) lower in the overloaded muscles of OE and OM compared to YE, with NSD ($p > 0.05$) between OE and OM. The absolute concentration of total ACC was significantly ($p \leq 0.05$) increased in overloaded muscles (main effect) regardless of age or plasmid treatment. Additionally, regardless of plasmid treatment or loading status, the muscles of OM and OE displayed higher ($p \leq 0.05$) levels of total Akt (Figure 2.5.6E) vs. YE.

2.3.5.4 TSC2 phosphorylation and concentration

The phosphorylation status (phospho-TSC2/total TSC2) at Ser1387 (Figure 2.5.7A) and the absolute concentration of phospho-(Ser1387) TSC2 (Figure 2.5.7C) were significantly ($p \leq 0.05$) increased (main effect) in all overloaded muscles compared to SHAM muscles regardless of age or plasmid treatment. The absolute concentration of phospho-(Ser1387) TSC2 in overloaded muscles of OM was significantly ($p \leq 0.05$) higher than overloaded muscles of YE, with NSD ($p > 0.05$) between OE and OM. The overloaded muscles of OE also tended ($p = 0.065$) to be higher than YE overloaded muscles for phospho-(Ser1387) TSC2. The phosphorylation status (phospho-TSC2/total TSC2) at Thr1462 (Figure 2.5.7B) was significantly ($p \leq 0.05$) higher in the overloaded muscles of YE vs. SHAM and vs. the overloaded muscles of OE and OM, with NSD ($p >$

0.05) between OE and OM overloaded muscles. The absolute concentration of phospho-(Thr1462) TSC2 (Figure 2.5.7D) was significantly ($p \leq 0.05$) increased in overloaded YE muscles vs. SHAM. There was NSD ($p > 0.05$) between SHAM muscles regardless of age or plasmid treatment for any phosphorylation measure, but the SHAM muscles of OE tended ($p = 0.063$) to be higher than YE SHAM muscles for phospho-(Thr1462) TSC2. The absolute concentration of total TSC2 was significantly ($p \leq 0.05$) increased (main effect) in all overloaded muscles compared to SHAM muscles regardless of age or plasmid treatment. Additionally, regardless of loading status, the total TSC2 absolute concentration (Figure 2.5.7E) OE and OM muscles was significantly ($p \leq 0.05$) higher than YE.

2.3.5.5 mTOR phosphorylation and concentration

The phosphorylation status (phopho-mTOR/total mTOR) at Ser2448 (Figure 2.5.8A) tended ($p = 0.073$) to be higher in the overloaded muscles of OM vs. OM SHAM muscles with NSD ($p > 0.05$) between any other muscles regardless of loading status or age. The absolute concentration of phospho-(Ser2448) mTOR (Figure 2.5.8C) was significantly ($p \leq 0.05$) increased (main effect) in all overloaded muscles compared to SHAM muscles regardless of age or plasmid treatment. Moreover, the increase in OM overloaded muscles was significantly ($p \leq 0.05$) higher than YE overloaded muscles with NSD ($p > 0.05$) between OE and OM overloaded muscles or SHAM values of any group. The absolute concentration of total mTOR (Figure 2.5.8B) was significantly ($p \leq 0.05$) increased (main effect) in all overloaded muscles compared to SHAM muscles regardless of age or plasmid treatment. The total mTOR absolute concentration also tended to be higher in OE ($p = 0.083$) and OM ($p = 0.057$) overloaded muscles vs. YE overloaded

muscles, with a significantly ($p \leq 0.05$) higher concentration of total mTOR in OE and OM SHAM muscles vs. YE SHAM muscles. There was NSD ($p > 0.05$) between OE and OM regardless of loading status.

2.3.5.6 p70S6K phosphorylation and concentration

The phosphorylation status (phospho-p70S6K/total p70S6K) at Thr389 (Figure 2.5.9A) and the absolute concentration of phospho-(Thr389) p70S6K (Figure 2.5.9C) was significantly ($p \leq 0.05$) increased (main effect) in all overloaded muscles compared to SHAM muscles regardless of age or plasmid treatment with NSD ($p > 0.05$) between any groups regardless of age or plasmid treatment. The absolute concentration of total p70S6K (Figure 2.5.9B) was significantly ($p \leq 0.05$) increased (main effect) in all overloaded muscles compared to SHAM muscles regardless of age or plasmid treatment. The total p70S6K absolute concentration was also significantly ($p \leq 0.05$) higher in the overloaded muscles of OE and OM vs. YE overloaded muscles. Further, the total p70S6K concentration was significantly ($p \leq 0.05$) higher in SHAM OM muscles vs. YE SHAM muscles, and OE SHAM muscles tended ($p = 0.060$) to be higher vs. YE SHAM muscles.

2.3.5.7 4EBP1 phosphorylation and concentration

The phosphorylation status (phospho-4EBP1/total 4EBP1) at Thr37/46 (Figure 2.5.10A) only tended ($p = 0.088$) to be higher in OM overloaded muscles vs. OM SHAM muscles with NSD ($p > 0.05$) following overload regardless of loading status, age, or plasmid treatment. The absolute concentration of phospho-(Thr37/46) 4EBP1 (Figure 2.5.10C) was significantly ($p \leq 0.05$) increased (main effect) in all overloaded muscles compared to SHAM muscles regardless of age or plasmid treatment. Further, the phospho-

(Thr37/46) 4EBP1 concentration was significantly ($p \leq 0.05$) higher in OE and OM muscles vs. YE muscles, regardless of loading, with NSD ($p > 0.05$) between OE or OM. Lastly, the absolute concentration of total 4EBP1 (Figure 2.5.10B) was significantly ($p \leq 0.05$) higher in overloaded muscles of OM vs. YE, and in SHAM muscles of OE and OM vs. YE, with NSD ($p > 0.05$) between OE and OM regardless of loading status.

2.3.6 SIGNALING INTERMEDIATES REGULATING MPB

2.3.6.1 FOXO3A phosphorylation and concentration

The phosphorylation status (phospho-FOXO3A/total FOXO3A) at Ser318/321 (Figure 2.5.11A) was significantly ($p \leq 0.05$) higher in OM overloaded muscles vs. OM SHAM muscles and vs. YE overloaded muscles, with NSD ($p > 0.05$) between OE and OM regardless of overload status. Further, the phosphorylation status of FOXO3A at Ser318/321 tended ($p = 0.077$) to be higher in OE SHAM muscles vs. YE SHAM muscles, with NSD ($p > 0.05$) between OM and YE SHAM muscles. There was NSD ($p > 0.05$) in the absolute concentration of phospho-(Ser318/321) FOXO3A with overload regardless of loading status, age, or plasmid treatment (Figure 2.5.11C). The absolute concentration of total FOXO3A (Figure 2.5.11B) was significantly ($p \leq 0.05$) decreased with overload (main effect) in all overloaded muscles vs. SHAM muscles regardless of age or plasmid treatment, with NSD ($p > 0.05$) between groups regardless of loadings status, age, or plasmid treatment.

2.3.6.2 Lysine-48 Tagged Polyubiquitin concentration

K48-linked polyubiquitin is used as a marker to assess the degree of proteins being tagged for degradation by the ubiquitin-proteasome system (143). The absolute concentration of total K48-linked polyubiquitin (Figure 2.5.12) was significantly ($p \leq$

0.05) increased with overload (main effect) in all overloaded muscles vs. SHAM muscles regardless of age or plasmid treatment, with NSD ($p > 0.05$) between SHAM muscles of any group. There was a significantly ($p \leq 0.05$) higher concentration of total K48-linked polyubiquitin in overloaded muscles of OE and OM vs. YE, with NSD ($p > 0.05$) between OE and OM.

2.3.7 MARKERS OF GLYCOGEN METABOLISM

2.3.7.1 GSK3 phosphorylation and concentration

There was NSD ($p > 0.05$) between SHAM values of any group for any GSK3 measure. The phosphorylation status (phospho-GSK3α/total GSK3α) at Ser21 (Figure 2.5.13A) was significantly ($p \leq 0.05$) increased in YE overloaded muscles vs. YE SHAM muscles, with significantly ($p \leq 0.05$) lower levels detected in overloaded muscles of OE and OM vs. YE overloaded muscles. The absolute concentration of phospho-(Ser21) GSK3α (Figure 2.5.13C) was significantly ($p \leq 0.05$) higher in the overloaded muscles of OM vs. YE overloaded muscles. Further, there was a significant ($p \leq 0.05$) reduction with overload vs. SHAM muscles for absolute concentration of total GSK3α (Figure 2.5.13E) in YE, with significantly ($p \leq 0.05$) lower levels than in OE and OM overloaded muscles. The phosphorylation status (phospho-GSK3β/total GSK3β) at Ser9 (Figure 2.5.13B) displayed NSD ($p > 0.05$) between any group regardless of loading status, age, or plasmid treatment. The absolute concentration of phospho-(Ser9) GSK3β (Figure 2.5.13D) was significantly ($p \leq 0.05$) increased (main effect) in all overloaded muscles compared to SHAM muscles regardless of age or plasmid treatment. Additionally, there was a significantly ($p \leq 0.05$) higher absolute concentration of phospho-(Ser9) GSK3β in overloaded muscles of OE vs. YE overloaded muscles, and OM overloaded muscles

tended ($p = 0.065$) to be higher then YE overloaded muscles. Lastly, there was NSD ($p > 0.05$) with overload in absolute concentration of total GSK3β (Figure 2.5.13F) regardless of loading status, age, or plasmid treatment.

2.3.7.2 PYGM concentration

There was NSD ($p > 0.05$) in the absolute concentration of total muscle glycogen phosphorylase (PYGM; Figure 2.4.14) regardless of loading status, age, or plasmid treatment. However, OM overloaded muscles tended ($p = 0.077$) to be lower than YE overloaded muscles.

2.3.8 MARKERS OF MYOGENESIS AND/OR REMODELING

2.3.8.1 Myogenic regulatory factors concentrations

To assess the effect of overload and plasmid treatment on myogenic regulatory factors, we measured the total concentrations of a myogenic regulatory factor responsible for proliferation (MyoD) and terminal differentiation (myogenin). The absolute concentration of MyoD (Figure 2.5.15A) was significantly ($p \leq 0.05$) higher in overloaded OM muscles vs. OM SHAM muscles and vs. OE overloaded muscles, with NSD ($p > 0.05$) between OM and YE overloaded muscles. The absolute MyoD concentration in overloaded OE muscles tended ($p = 0.070$) to be lower than OE SHAM muscles with NSD ($p > 0.05$) between SHAM values regardless of age or plasmid treatment. The absolute concentration of myogenin (Figure 2.5.15B) was significantly ($p \leq 0.05$) increased with overload (main effect) in all overloaded muscles vs. SHAM muscles regardless of age or plasmid treatment. The myogenin concentration was significantly ($p \leq 0.05$) higher in OE and OM overloaded muscles vs. YE overloaded muscles, with OM overloaded muscles being significantly ($p \leq 0.05$) higher than OE

overloaded muscles. Additionally, OM SHAM muscles displayed significantly ($p \leq 0.05$) higher myogenin concentration than YE SHAM muscles.

2.3.8.2 Total Fiber Number & eMyHC-Stained Fibers

To quantify the regenerative response to overload, muscle fiber number and eMyHC-positive fibers were counted in whole-muscle cross-sections of YE, OE, and OM (Figure 2.5.16) muscles. There was significantly ($p \leq 0.05$) lower total fiber number (Figure 2.5.16A) in OE and OM muscles vs. YE regardless of loading status. The overloaded muscles of OM had a significant ($p \leq 0.05$) increase in total fiber vs. OM SHAM and had significantly ($p \leq 0.05$) greater fiber number than OE overloaded muscles with NSD ($p > 0.05$) between SHAM muscles in OE and OM. The percent change in total fiber number (Figure 2.5.16B) with overload in OE was significantly ($p \leq 0.05$) lower than YE, with OM displaying a significantly ($p \leq 0.05$) higher increase with overload vs. OE. The number of eMyHC-positive fibers (Figure 2.5.16C) was significantly ($p \leq 0.05$) increased with overload (main effect) in all overloaded muscles vs. SHAM muscles regardless of age or plasmid treatment. There was a significantly ($p \leq 0.05$) higher eMyHC expression in overloaded muscles of OE and OM, with the increase in OM being significantly ($p \leq 0.05$) higher than OE. The eMyHC expression was NSD ($p > 0.05$) between SHAM muscles regardless of age or plasmid treatment. OM also had a significantly ($p \leq 0.05$) higher percent increase in number of eMyHC-positive fibers with overload vs. both OE and YE (Figure 2.15D). Representative images of eMyHC/laminin stained muscle used for total fiber number and eMyHC expression can be seen in Figure 2.5.17.

2.4 Discussion and Conclusion

Aged skeletal muscle wasting (i.e., sarcopenia) is associated with elevated AMPK activity (42, 126-129), which inhibits overload-induced MPS and growth (42, 128, 129). Glycogen, an inhibitor of AMPK (77, 78), is also reduced in aged skeletal muscle (7, 16, 23, 47). However, the link(s) between glycogen content, MPS, MPB, growth, and associated signaling following chronic overload had never been examined in aged humans or animals. The novel findings of this current investigation are that enhancing glycogen content in aged skeletal muscle augmented overload-induced MPS and growth compared to aged muscle without glycogen enhancement after 21 days. The effects of glycogen enhancement may be independent of changes in AMPK signaling or intermediates regulating MPS. In contrast, glycogen enhancement may suppress factors regulating MPB during overload in aged skeletal muscle. Moreover, glycogen enhancement augments increases in MRFs, eMyHC expression, and total fiber number in response to overload in aged skeletal muscle.

Some of the most fascinating findings of the current investigation were that glycogen enhancement in aged muscle (OM) in response to overload led to significantly greater MPS and growth in fast-twitch plantaris muscle compared to aged muscle with empty vector treatment (OE). Also, the percent increase in growth and MPS with overload in glycogen enhanced aged muscle was similar to young adult muscle. Even though the increase in MPS rate with overload was significantly increased across all groups (main effect), this increase was obviously driven by the increases observed in YE and OM and not a substantial increase in OE, which actually displayed atrophy in response to overload. Our laboratory (42, 128, 129) and others (18) have found a

significant, but blunted increase in the growth response to overload of aged rat muscle compared to young adult muscle. To our knowledge, the overload procedure has never been employed in aged muscle in conjunction with the modified electroporation method utilized (139).

To examine if glycogen enhancement in aged skeletal muscle under conditions of overload potentially affected muscle protein breakdown (MPB) we chose to examine FOXO3A signaling, at a specific site (Ser318/321) indicative of inhibition of MPB (135, 142), as well as a readout of proteins being tagged for degradation by the ubiquitin proteasome system [K48-linked polyubiquitin; (143)]. When activated, FOXO3A translocates to the nucleus and increases expression of muscle-specific E3 ubiquitin ligases, MuRF1 and MAFbx (135, 142), leading to MPB through the ubiquitin proteasome system (12, 142). Glycogen enhancement in aged muscle with overload led to an augmented phosphorylation status of FOXO3A at Ser318/321 that was not seen in aged muscle with empty vector treatment, which theoretically means less stimulation of MPB pathways. However, this finding did not lead to less K48-linked polyubiquitin proteins, so it remains to be determined if there is an effect of glycogen enhancement on MPB and associated signaling.

Although glycogen enhancement augmented MPS and growth with overload in aged muscle in this investigation, the hypothesis that glycogen enhancement would elicit these effects by inhibiting AMPK was not completely supported. Although elevated with age under overload conditions, AMPK phosphorylation status was not altered by glycogen enhancement. In contrast, the overload-induced increase in ACC phosphorylation status [a well-established marker of AMPK activity *in vivo* (43)] in old

muscle with glycogen enhancement was reduced to a level not statistically different than young adult animals, an effect that was not seen in old muscle without glycogen enhancement. This finding may suggest that glycogen enhancement in aged muscle reduced the allosteric activation of AMPK and led to a decreased activity as assessed by ACC phosphorylation (51), independent of changes in overall phosphorylation status of AMPK. An increase in glycogen content is assumed to lead to an increase in inorganic phosphate as well as production of ATP (2, 44, 109), which should theoretically reduce the AMP/ATP ratio leading to reduced allosteric activation and reduced activity towards ACC (51). However, as AMP, ADP, or ATP levels were not measured in the current investigation this would need to be explored further. Nevertheless, AMPK activity was diminished with glycogen enhancement in aged muscle following 21 days of overload, but not robustly enough to detect differences compared to aged muscle with empty vector treatment.

Although AMPK activity may have been affected by glycogen enhancement in aged muscle, the overall AMPK phosphorylation status did not support this effect. In the current investigation, we confirmed previous findings from our laboratory (42, 128) following a 7-day overload procedure that AMPK phosphorylation status was significantly elevated in aged muscle compared young muscle. Even though there was no effect of glycogen enhancement on AMPK phosphorylation status, this may be due to a number of factors. Most importantly, the overall AMPK α (i.e., not separating out α_1 vs. α_2) phosphorylation status at Thr172 was measured in the current investigation. Thus, any potential differences between AMPK α_1 or α_2 phosphorylation status could not be determined. With AMPK α_1 being linked to regulating muscle growth (79, 86, 87), and

AMPK α_2 being thought to be involved in metabolic adaptations (79, 88) this may be a needed future measurement to delineate these two subunits phosphorylation status and activity in response to glycogen enhancement in aged muscle with overload. Another factor that could explain the absence of an effect of glycogen enhancement on AMPK phosphorylation status is the recent work from Stapleton and colleagues (98, 122, 140). The AMPKβ-glycogen interaction has been well supported in correlational studies *in vivo* in humans (138) and rats (123) finding an inverse relationship between AMPK activity and glycogen content. These findings were further supported *in vitro* by the use of synthesized oligosaccharides, or glycogen mimics, showing that glycogen can strongly inhibit AMPK activity (77). Collectively, these findings along with the discovery of the GBD on the AMPK β subunit (104) led to the hypothesis that AMPK was directly influenced by skeletal muscle glycogen content (78). However, Stapleton and colleagues (98, 122, 140) published work in liver (122), cells and cell-free systems (98), and skinned muscle fibers (140, 141) that refuted the direct interaction of glycogen and AMPK. The authors suggested that AMPK may interact with glycogen, but may do so indirectly through other glycogen associated proteins (140, 141). These recent findings suggest that glycogen content may affect AMPK activity *in vivo*, but that it may be through an indirect mechanism that was not measured in the current investigation and would need to be explored further.

One curious finding is that phospho-(Thr172) AMPK absolute concentration was significantly higher in OM overloaded muscles vs. YE overloaded muscles, but OE overloaded muscles were not higher than YE. AMPK has been reported to be a negative regulator of GS by phosphorylating and inhibiting the enzyme on Site 2 (109). The

mutant GS plasmid is mutated on this specific site and therefore there may have been a feedback on AMPK to constantly try to inhibit GS. However, there was no similar increase in AMPK phosphorylation status or its activity as measured via ACC, so it remains to be seen if this increase in phospho-(Thr172) AMPK has any significance. Also, this increase in the absolute concentration of phospho-(Thr172) AMPK did not lead to a similar increase, with no differences compared OE, in the absolute concentration of phospho-(Ser79) ACC and the phosphorylation status of ACC at Ser79. Therefore, the overall phosphorylation status of AMPK may be a better readout than just the absolute concentration of phospho-(Thr172) AMPK.

Another novel finding of this investigation is that glycogen enhancement in aged muscle led to augmented increases in myogenic regulator factors (MRFs), eMyHC expression, and total fiber number under conditions of overload. Even though muscle fiber cross-sectional area was not measured in the current investigation, the augmented overload-induced increase with glycogen enhancement in muscle growth that was accompanied by total fiber number increases provides insight into the degree of the growth response. While others have reported increases with synergistic ablation alone (89), to our knowledge, this is first time de novo fiber formation has been reported in aged muscle in response to overload and electroporation. It is believed that with the synergistic ablation model hyperplasia occurs as muscle fibers become too large for oxygen diffusion and therefore the fibers split to form new fibers as a protective adaptation (89). In support of the increases in total fiber number with glycogen enhancement in old muscle, there were concomitant increases in MRFs, MyoD and myogenin, and eMyHC expression. The increase in MRFs expression with aging is in

agreement with others (3, 76, 108), however, this is the first time MRF increases have been reported in aged muscle with glycogen enhancement. The increases in de novo fiber formation may be due to greater energy availability, in the form of enhanced glycogen content (2, 44, 109), throughout the 21-day overload protocol in addition to the potential regenerative response caused by the overload model with electroporation procedure.

A common finding with activities that cause muscle damage (e.g., eccentric contractions) is reductions in the amount of glycogen content, and this is seen in rodents (52, 59, 131) and humans (22, 97, 137). The reductions in glycogen content are linked to declines in contractile performance of the damaged muscle (19, 105). While some studies have linked these declines to disruption in the structural components of muscle (19, 105), others have reported metabolic factors being involved (22, 52, 59, 97, 131, 137). Interestingly, in response to damaging eccentric contractions there is an inability to replenish glycogen content in humans (97, 137), as well as, diminished glycogen content and ATP production in rats (52, 59, 131). In the current investigation, there were increases in the regenerative response when glycogen content was enhanced in old muscle after the potentially damaging stimulus (i.e., overload with electroporation). Therefore, it is possible that low glycogen may be a limiting factor in the regenerative response in aged muscle. Although it was not an overall goal of this investigation, it would be interesting for future work to test the effects of glycogen enhancement in a bona fide model of muscle injury, such as damaging eccentric contractions, to see if there is an enhancement in regeneration/myogenesis in aged or young muscle.

The decrease seen with overload in the phosphorylation status of GS at Ser641 in all groups is indicative of removal of inhibition of the enzyme, presumably due to an increase in ATP demand (i.e., a need for glycogenolysis) with overload, and occurs independent of age. The lack of differences seen in the SHAM muscles of both YE vs. OE and OM in the current investigation is in agreement with previous reports who found no differences in the phosphorylation status of GS at Ser641 in the tibialis anterior (TA) muscle of 6 mo. vs. 24 mo. fed Fischer 344 male rats (85). While we did not measure activity, some (23) have reported significant reductions in GS and GP activity in aged rat fast-twitch skeletal muscle, with some reporting no changes (85). Further, Garvey et al. (37) examined the metabolic profiles in gastrocnemius (GAST) muscles of young adult (15 mo.) and old (32 mo.) male sedentary FBN rats and found significant alterations in glycolytic intermediates responsible for glucose and glycogen metabolism in aged muscle. The authors also reported that there was an increase in specific oligosaccharides that is suggestive of initial debranching from glycogen granules, but that there was defects in the ability to catabolize the free oligosaccharides (37). The authors further postulated that the lysosomal compartment, a key site for glycogen degradation (109), contains defects that lead to the incomplete digestion of glycogen with age. This is very intriguing, as there are known deficiencies in the ability of aged skeletal muscle to process unwanted or damaged proteins, mainly via autophagy deregulation within the lysosomal compartment (111), that may also contribute to the defects found in glycogen and glucose metabolism. Collectively, these findings highlight a potential defect in glycogen metabolism in aging skeletal muscle. Importantly, in the current investigation when glycogen was enhanced in aged skeletal muscle there were increases in overload-

induced MPS and growth, suggestive of aged muscle possessing an ability to utilize this glycogen in some fashion.

Although there was no significant decrease in glycogen content of overloaded OE muscles vs. OE SHAM muscles or vs. YE SHAM or overloaded muscles, there was a trend ($p = 0.10$) towards a decline. This finding in normal aged muscle (i.e., OE SHAM) is not surprising, as the glycogen content in aged vs. young rat muscle at rest (e.g., SHAM) has been equivocal with some reporting decreases (7, 17, 23, 47) and others none (53, 83, 85, 103, 108). What has been fairly consistent in the literature is that in response to an increase in contractile activity, typically due to endurance-type exercise, there is a greater reduction in glycogen content in aged vs. young muscle in rats (17, 53, 126) and humans (17, 82), although again, this has not always been the case (108). Ribeiro et al. (108) found a significant increase in glycogen content in fast-twitch GAST muscles following resistance training (progressive loading using ladder climbing, 3 times a week for 12 weeks) in both young (3 mo.) and old (20 mo.) male Wistar rats with no differences between ages. However, our laboratory has found an increase (vs. SHAM) at 7 days of chronic overload in young adult (8 mo.) PLT glycogen content while old (33 mo.) muscle displayed a trend ($p = 0.08$) towards a decrease (unpublished data). The lack of changes in glycogen content with overload among young and old muscle with empty vector treatment in the current investigation may be due to any changes becoming normalized by the 21-day timepoint. Even though Ribiero et al. (108) found an increase in glycogen content with RE in both young and old rats, the methodological differences (e.g., timepoint, loading method, and/or strain) between the two investigations makes direct comparisons difficult.

Because AMPK has been found by our lab (42, 126-129) and others (13, 113, 114) to regulate multiple protein translational signaling intermediates we chose to examine the effect of glycogen enhancement in aged skeletal muscle on these pathways. Specifically, we measured upstream and downstream signaling related to Akt, TSC2, mTOR, and AMPK signaling (54). The current investigation found potential effects of glycogen enhancement in aged muscle on overload-induced reductions in AMPK activity (via p-ACC), and non-significant increases of phosphorylation status of mTOR and 4EBP1; however, the effects were not robust at 21 days. Despite augmented increases in MPS and growth in aged muscle with glycogen enhancement, the above-mentioned signaling intermediates largely did not support these findings after 21 days of chronic overload. Indeed, recent work (48) has found that with the synergistic ablation model of muscle growth in rats, changes that occur in AMPK and MPS signaling intermediates happen within the first 3-9 days of overload are largely lost by 12-21 days. The authors proposed this to be due to "molecular brakes" or negative regulators of mTORC1 being increased after 9 days with this supraphysiological model of muscle growth (48). In further support of the "molecular brakes" hypothesis, there were increases in total TSC2 in young adult muscle with overload after 21 days similar to what Hamilton et al. (48) found. An increase in the total amount of TSC2 is suggestive of greater mTORC1 inhibition. Even though there was a greater expression of total TSC2 with age in the current investigation, there was no attenuated effect of glycogen enhancement after 21 days of overload. Collectively, these findings suggest that any changes with glycogen enhancement in aged muscle may have been lost by 21 days.

The phosphorylation status of Akt at Thr308 in response to overload was significantly blunted with age, however this effect was not carried to the phosphorylation status of Akt at Ser473. Phosphorylation at Ser473 (in conjunction with Thr308) has been purported to be indicative of full activation of Akt (121), however any differences between ages at this site may have been lost with 21-days of overload. The lack of an age effect in phosphorylation status of Akt Ser473 does not support our labs previous finding (129). This is likely due to differences in the time frame of the overload stimulus (i.e., 7 vs. 21 days). In addition, the phosphorylation status of TSC2 at Thr1462, a marker of Akt, was also blunted in aged muscle, with NSD with glycogen enhancement. Moreover, the phosphorylation status of TSC2 at Ser1387, a marker of AMPK, was increased with overload (main effect), with glycogen enhancement not reducing this effect below old or young muscle with empty vector treatment. Again, these effects may have been lost by 21 days (48).

The elevations with age in the absolute concentrations of total Akt, mTOR, and p70S6K, with or without loading in aging muscle is interesting, but not unique (18, 72). There may be an extra need for greater amounts of protein to achieve the same anabolic response as seen in young muscle. These effects may be due, in part, to a combination of dysfunctional mechanotransduction (11) as well as deregulated autophagy (25) leading to an inability to remove non-functional proteins and therefore more protein has to be made to achieve the same effect as seen in young healthy muscle. Moreover, glycogen enhancement in aged muscle had no effect on these measurements. Although, as total protein does not indicate changes in activity, we further examined phosphorylation status of these markers. The significant increase, due to a main effect, in the absolute

concentration of phospho-(Ser2448) mTOR with overload in all groups was carried by the increases in YE and OM. However, only OM displayed a trend towards an increase in the phosphorylation status of mTOR at Ser2448 with overload, with the phosphorylation status of 4EBP1 at Thr37/46 showing the same trend. A better readout of mTOR activity than the phosphorylation status of mTOR at Ser2448 or 4EBP1 at Thr37/46 is p70S6K at Thr389 (6, 119). Indeed, in response to overload there was a significant increase, again driven by the increases in YE and OM only and not OE, in both the phosphorylation status and absolute concentration of phospho-(Thr389) p70S6K with NSD between old groups. However, as there was not a significantly accentuated effect of MPS signaling through these markers with glycogen enhancement, it remains to be determined if the augmented MPS and growth acted through this markers. With, again, the timepoint of the measurements (21 days) potentially being the biggest reason for lack of robust differences.

The electroporation method of Wu and Kandardian (139), has been optimized for use in young muscle by minimizing the known damage caused by electroporation (84) while maximizing electrotransfer of desired plasmid DNA (139). The normal hypertrophy observed in YE overloaded muscles in the current investigation strengthens this notion. However, as the OE overloaded muscles displayed atrophy, future work may be needed to optimize electrotransfer into age muscle, such as using hyaluronidase (39, 80). Regardless of the potential damage induced by the methods employed, glycogen enhancement in aged fast-twitch muscle still led to enhanced MPS, growth, and certain markers of myogenesis at 21 days of overload.

To assess the effects of our protocol on glycogen metabolism markers we chose to measure GSK3 and muscle glycogen phosphorylase (PYGM). There was NSD in total PYGM expression, regardless of overload status, age, or plasmid treatment. As total protein expression does not indicate changes in activity we cannot determine if there was any effect on this enzyme's activity. However, others using the exact mutant GS plasmid in mouse muscle (75, 100) have measured glycogenolysis and found increases in factors suggestive of enhanced glycogen catabolism such as glycogen phosphorylase (75) and glycogen debranching enzyme (100). Future work would need to explore the activity of glycogen phosphorylase with our experimental design. The NSD in the phosphorylation status of GSK3β at Ser9 even with increases in total GS expression with the mutant GS plasmid in aged skeletal muscle, as well as the NSD between aged muscle in the phosphorylation status of GSK3α at Ser21 is not surprising. Even though GSK3 has been purported to be a potent inhibitor of GS by phosphorylation on numerous sites, including Site 3a (109), others have stated that the allosteric activation of GS via glucose-6-phosphate may be more important (74). Additionally, GSK3β is inhibited (via phosphorylation) by upstream signaling pathways, namely Akt and Wnt signaling (54), and is a negative regulator of protein translation initiation (54, 66) and thus muscle growth. The current investigation supported previous findings that found no differences in phosphorylation status of GSK3α and GSK3β in young adult vs. old rats following 28 days of overload (18). However, as there were no accentuated affects of glycogen enhancement in aged muscle this again may be due to the timing of measurements.

In summary, glycogen enhancement in aged skeletal muscle led to increases in overload-induced MPS and growth. The effects of glycogen enhancement may be largely

independent of changes in AMPK signaling or intermediates regulating MPS. In contrast, glycogen enhancement may suppress factors regulating MPB during overload in aged skeletal muscle. Moreover, there was a strong and significant effect of enhancing glycogen content on myogenic regulatory factors, eMyHC expression, and total fiber number in aged skeletal muscle under conditions of overload. Thus, enhancing muscle glycogen content may lead to enhanced MPS and overload-induced growth in aged skeletal muscle. This effect may be due, in part, to enhanced myogenesis/regeneration.

2.5 Figures

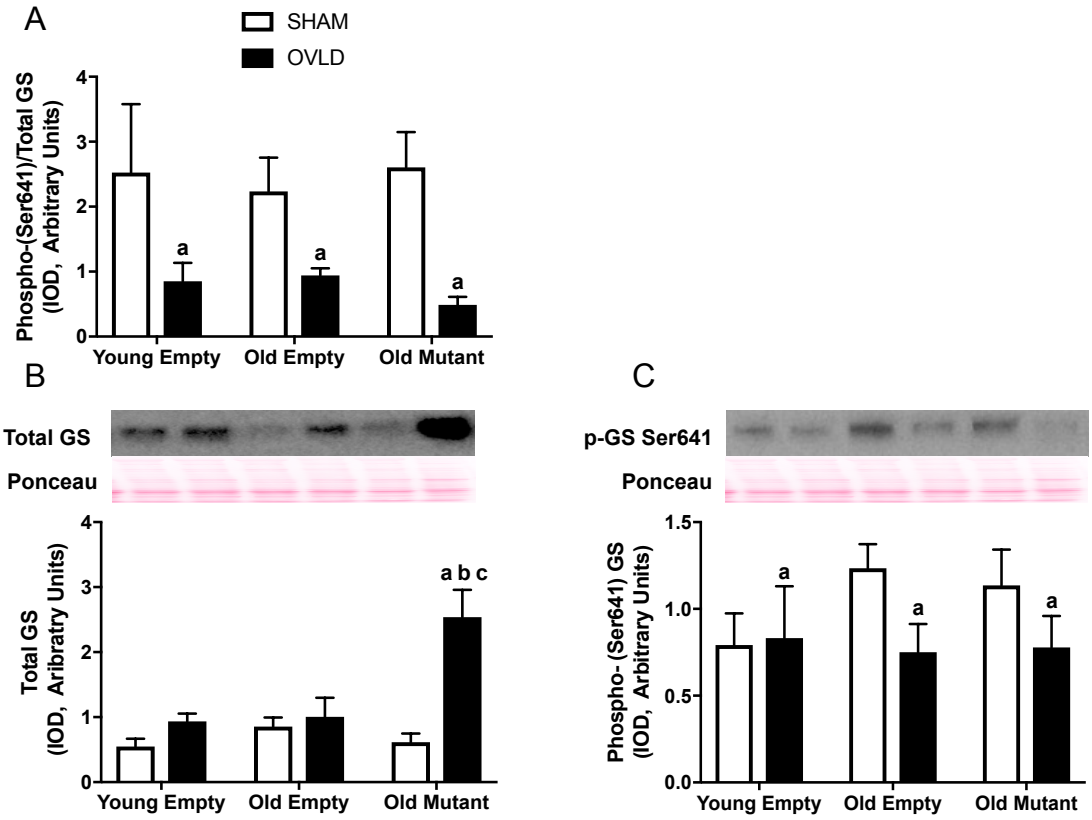

Figure 2.5.1. Total and phosphorylated GS response to overload in young adult and old skeletal muscle. A, Plantaris (PLT) phospho-(Ser641)/total glycogen synthase (GS); B, PLT absolute concentration of total GS; and C, PLT absolute concentration of phospho-(Ser641) GS (Integrated optical density, IOD) after 21 days of functional overload (OVLD; unilateral gastrocnemius ablation) compared with sham-operated (SHAM) conditions in young adult and old FBN rats. Overload muscles received electrotransfer of plasmids containing either an empty vector (empty) or mutated glycogen synthase designed to enhance glycogen content (mutant). Young empty: 8 mo., n = 9; old empty: 32-34 mo., n = 11; old mutant: 32-34 mo., n = 13. B, PLT total GS expression (IOD) and C, phospho-(Ser641) GS expression from A values. a: significantly different ($p \leq 0.05$) than respective group's SHAM value; b: significantly different from same leg in young empty; c: significantly different from same leg in old empty.

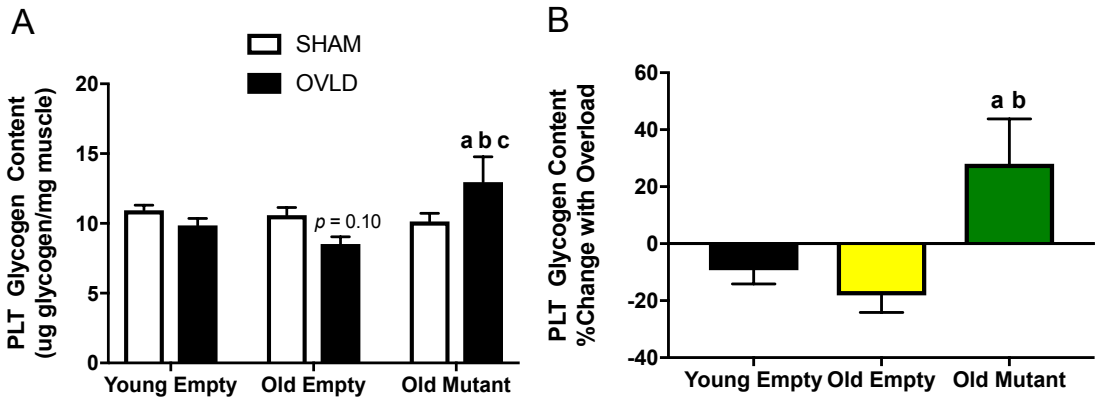

Figure 2.5.2. Plantaris glycogen content response to overload in young adult and old skeletal muscle. A, Plantaris (PLT) total glycogen content normalized to mg muscle after 21 days of functional overload (OVLD; unilateral gastrocnemius ablation) compared with sham-operated (SHAM) conditions in young adult and old FBN rats. Overload muscles received electrotransfer of plasmids containing either an empty vector (empty) or mutated glycogen synthase designed to enhance glycogen content (mutant). Young empty: 8 mo., n = 9; old empty: 32-34 mo., n = 11; old mutant: 32-34 mo., n = 13. a: significantly ($p \leq 0.05$) different than respective group's SHAM value; b: significantly different from same leg in young empty; c: significantly different from same leg in old empty. B, PLT total glycogen content percent (%) change with overload (vs. SHAM). a: significantly different from young empty; b: significantly different from old empty.

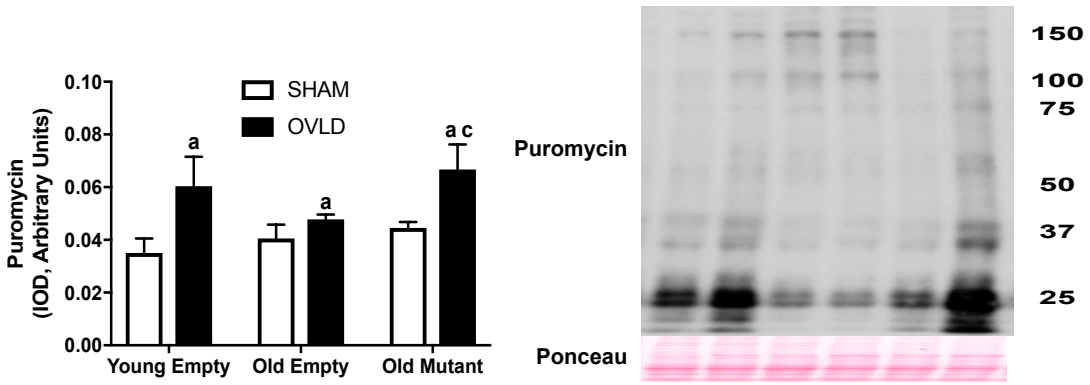

Figure 2.5.3. Plantaris mixed muscle protein synthesis rate response to overload in young adult and old skeletal muscle. Plantaris (PLT) mixed muscle protein synthesis rate measured via expression of puromycin (Integrated optical density, IOD) after 21 days of functional overload (OVLD; unilateral gastrocnemius ablation) compared with sham-operated (SHAM) conditions in young adult and old FBN rats. Overload muscles received electrotransfer of plasmids containing either an empty vector (empty) or mutated glycogen synthase designed to enhance glycogen content (mutant). Young empty: 8 mo., n = 9; old empty: 32-34 mo., n = 11; old mutant: 32-34 mo., n = 13. a: significant ($p \leq 0.05$) main effect of overload; c: significantly different than same leg in old empty.

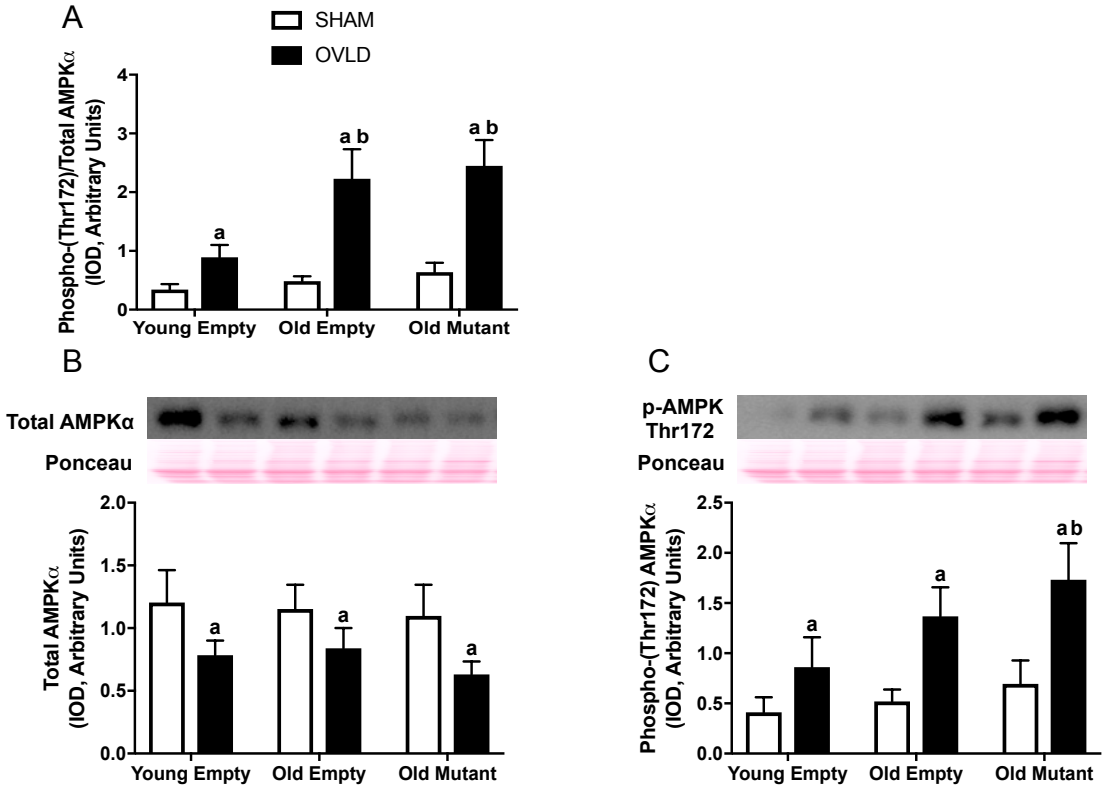

Figure 2.5.4. Total and phosphorylated AMPK response to overload in young adult and old skeletal muscle. A, Plantaris (PLT) phospho-(Thr172)/total 5'-AMP-activated protein kinase (AMPK) α expression (Integrated optical density, IOD) after 21 days of functional overload (OVLD; unilateral gastrocnemius ablation) compared with sham-operated (SHAM) conditions in young adult and old FBN rats. Overload muscles received electrotransfer of plasmids containing either an empty vector (empty) or mutated glycogen synthase designed to enhance glycogen content (mutant). Young empty: 8 mo., n = 9; old empty: 32-34 mo., n = 11; old mutant: 32-34 mo., n = 13. B, PLT total AMPKα expression (IOD) and C, phospho-(Thr172) GS expression. a: significant ($p \leq 0.05$) main effect of overload; b: significantly different from same leg in young empty.

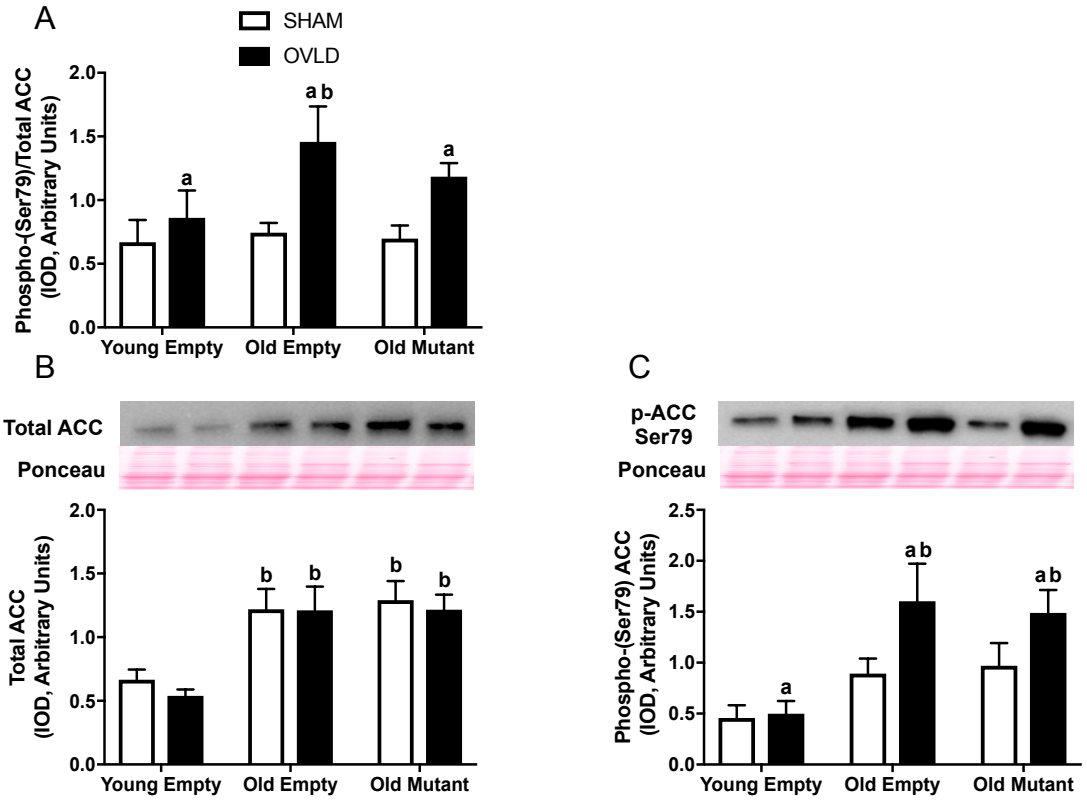

Figure 2.5.5. Total and phosphorylated ACC response to overload in young adult and old skeletal muscle. A, Plantaris (PLT) phospho-(Ser79)/total acetyl-CoA carboxylase (ACC) expression (Integrated optical density, IOD) after 21 days of functional overload (OVLD; unilateral gastrocnemius ablation) compared with sham-operated (SHAM) conditions in young adult and old FBN rats. Overload muscles received electrotransfer of plasmids containing either an empty vector (empty) or mutated glycogen synthase designed to enhance glycogen content (mutant). Young empty: 8 mo., n = 9; old empty: 32-34 mo., n = 11; old mutant: 32-34 mo., n = 13. B, PLT total ACC expression (IOD) and C, phospho-(Ser79) ACC expression. a: significant ($p \leq 0.05$) main effect of overload; b: significantly different from same leg in young empty.

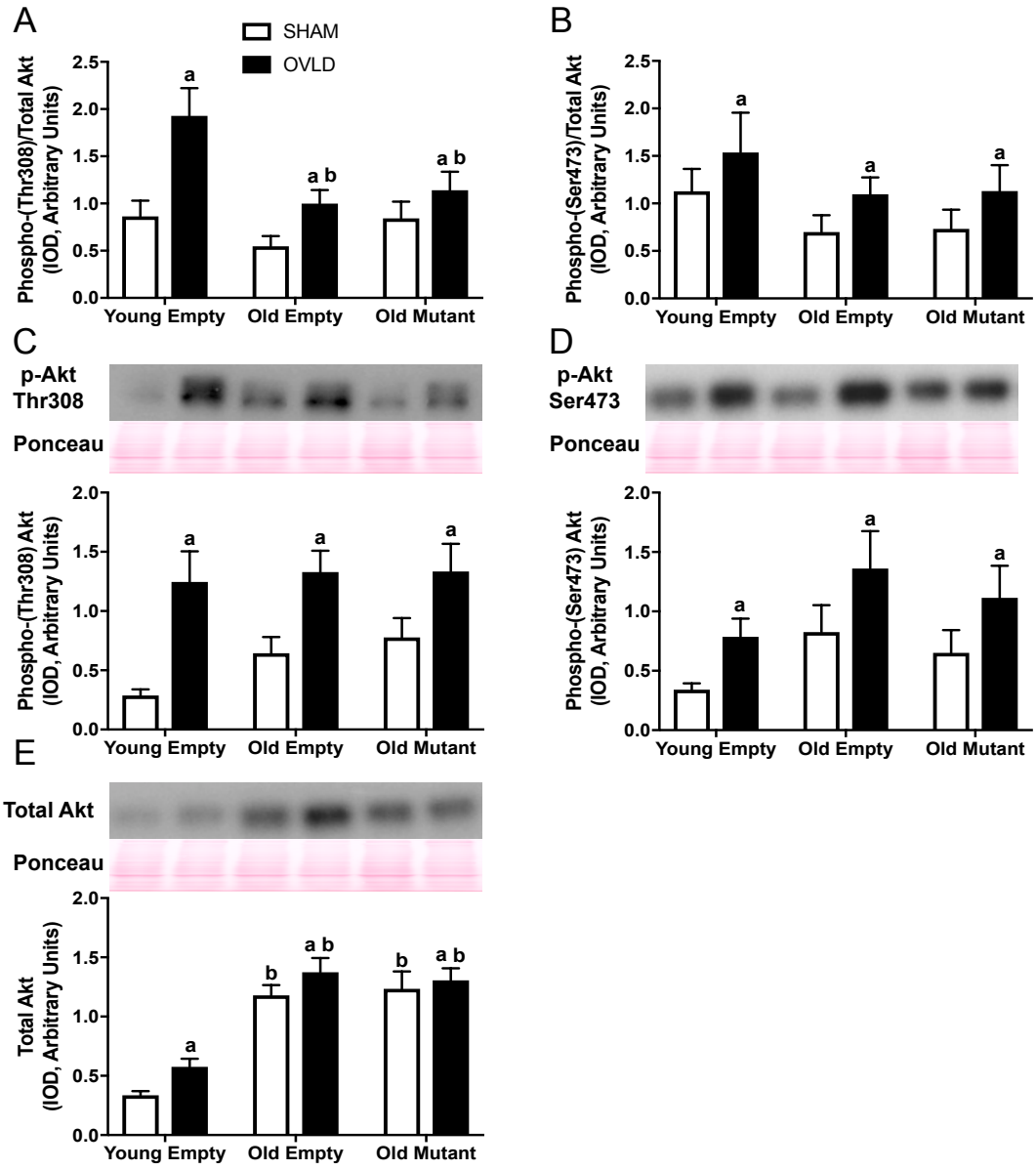

Figure 2.5.6. Total and phosphorylated Akt response to overload in young adult and old skeletal muscle. A, Plantaris (PLT) phospho-(Thr308)/total Akt expression (Integrated optical density, IOD) and B, PLT phospho-(Ser473)/total Akt expression after 21 days of functional overload (OVLD; unilateral gastrocnemius ablation) compared with sham-operated (SHAM) conditions in young adult and old FBN rats. Overload muscles received electrotransfer of plasmids containing either an empty vector (empty) or mutated glycogen synthase designed to enhance glycogen content (mutant). Young empty: 8 mo., n = 9; old empty: 32-34 mo., n = 11; old mutant: 32-34 mo., n = 13. C, phospho-(Thr308) Akt expression; D, phospho-(Ser473) Akt expression from B values; E, total Akt expression. a: significant ($p \leq 0.05$) main effect of overload; b: significantly different from same leg in young empty.

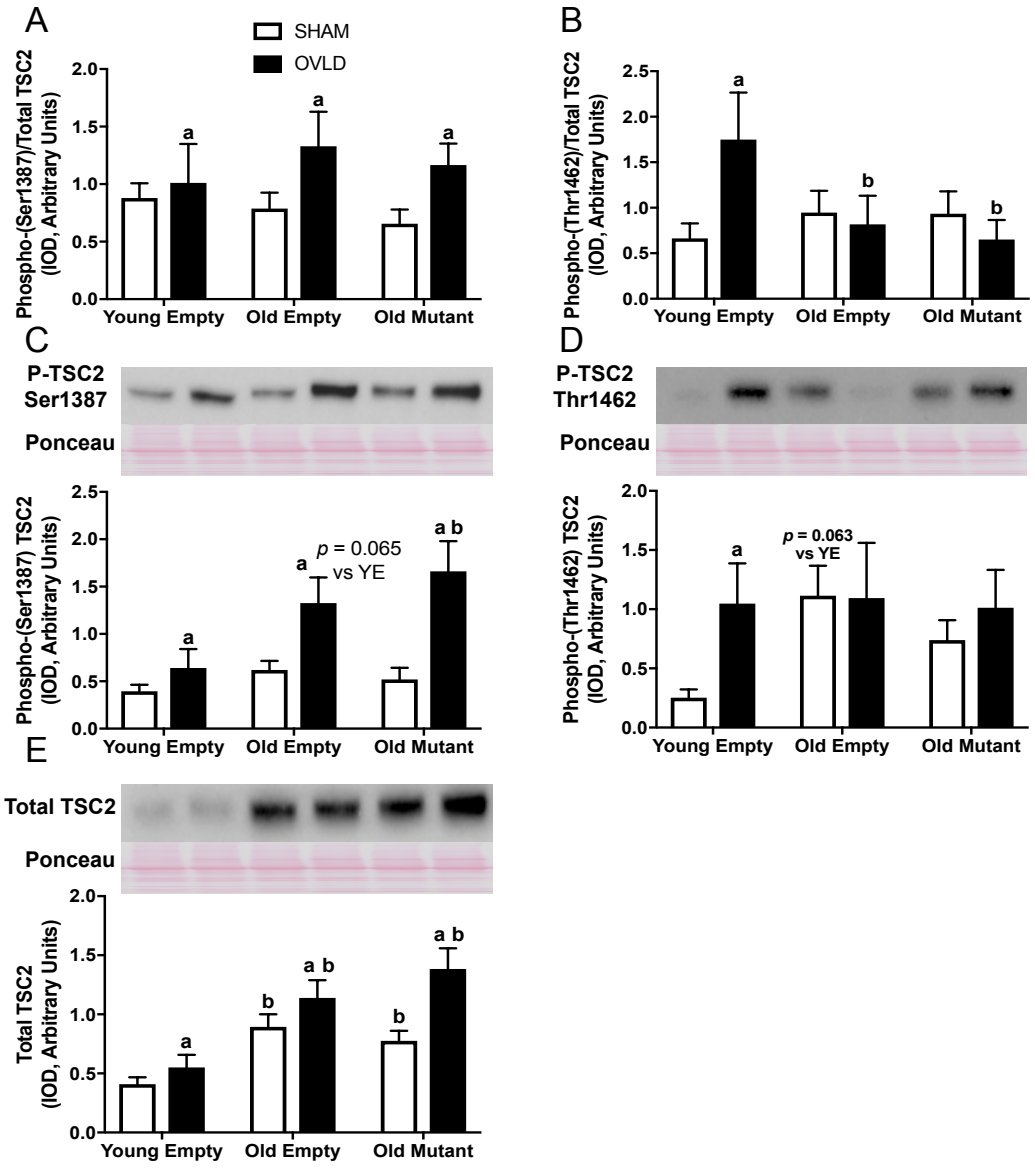

Figure 2.5.7. Total and phosphorylated TSC2 response to overload in young adult and old skeletal muscle. A, Plantaris (PLT) phospho-(Ser1387)/total TSC2 expression (Integrated optical density, IOD) and B, PLT phospho-(Thr1462)/total TSC2 expression after 21 days of functional overload (OVLD; unilateral gastrocnemius ablation) compared with sham-operated (SHAM) conditions in young adult and old FBN rats. Overload muscles received electrotransfer of plasmids containing either an empty vector (empty) or mutated glycogen synthase designed to enhance glycogen content (mutant). Young empty: 8 mo., n = 9; old empty: 32-34 mo., n = 11; old mutant: 32-34 mo., n = 13. C, phospho-(Ser1387) TSC2 expression from A values; D, phospho-(Thr1462) TSC2 expression from B values; E, total TSC2 expression. a: significant ($p \leq 0.05$) main effect of overload; b: significantly different from same leg in young empty.

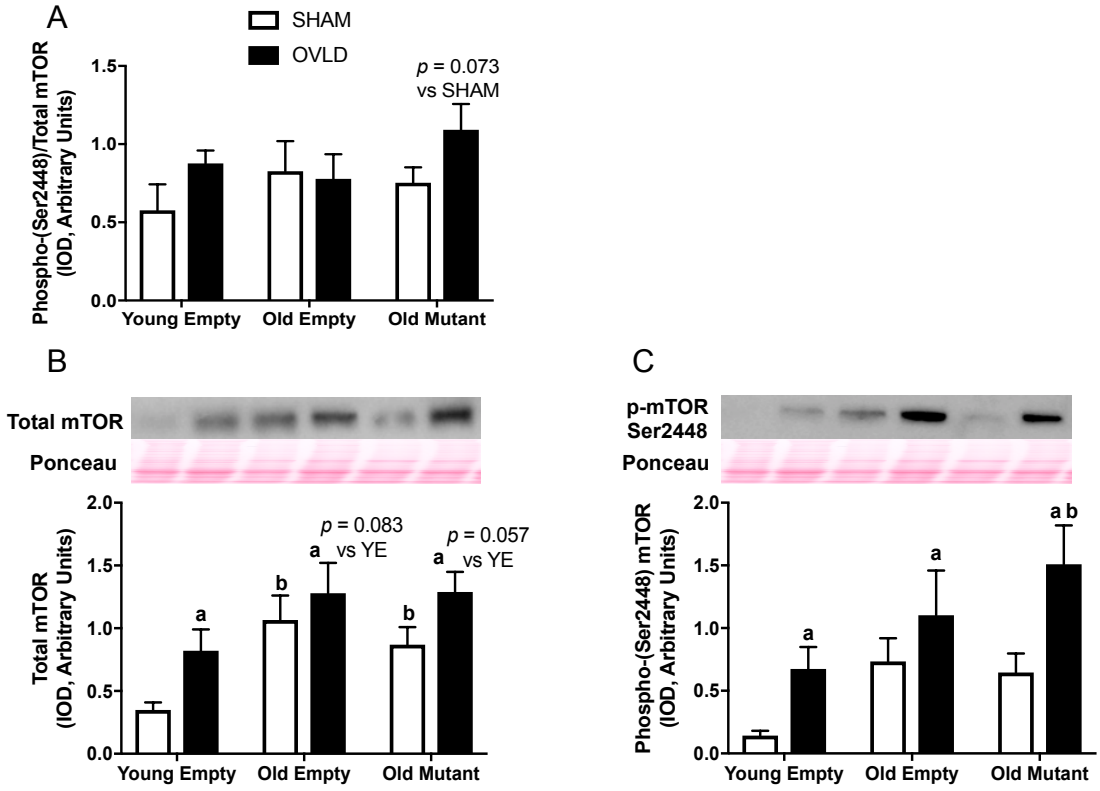

Figure 2.5.8. Total and phosphorylated mTOR response to overload in young adult and old skeletal muscle. A, Plantaris (PLT) phospho-(Ser2448)/total mechanistic target of rapamycin (mTOR) expression (Integrated optical density, IOD) after 21 days of functional overload (OVLD; unilateral gastrocnemius ablation) compared with sham-operated (SHAM) conditions in young adult and old FBN rats. Overload muscles received electrotransfer of plasmids containing either an empty vector (empty) or mutated glycogen synthase designed to enhance glycogen content (mutant). Young empty: 8 mo., n = 9; old empty: 32-34 mo., n = 11; old mutant: 32-34 mo., n = 13. B, PLT total mTOR expression (IOD) and C, phospho-(Ser2448) mTOR expression. a: significant ($p \leq 0.05$) main effect of overload; b: significantly different from same leg in young empty.

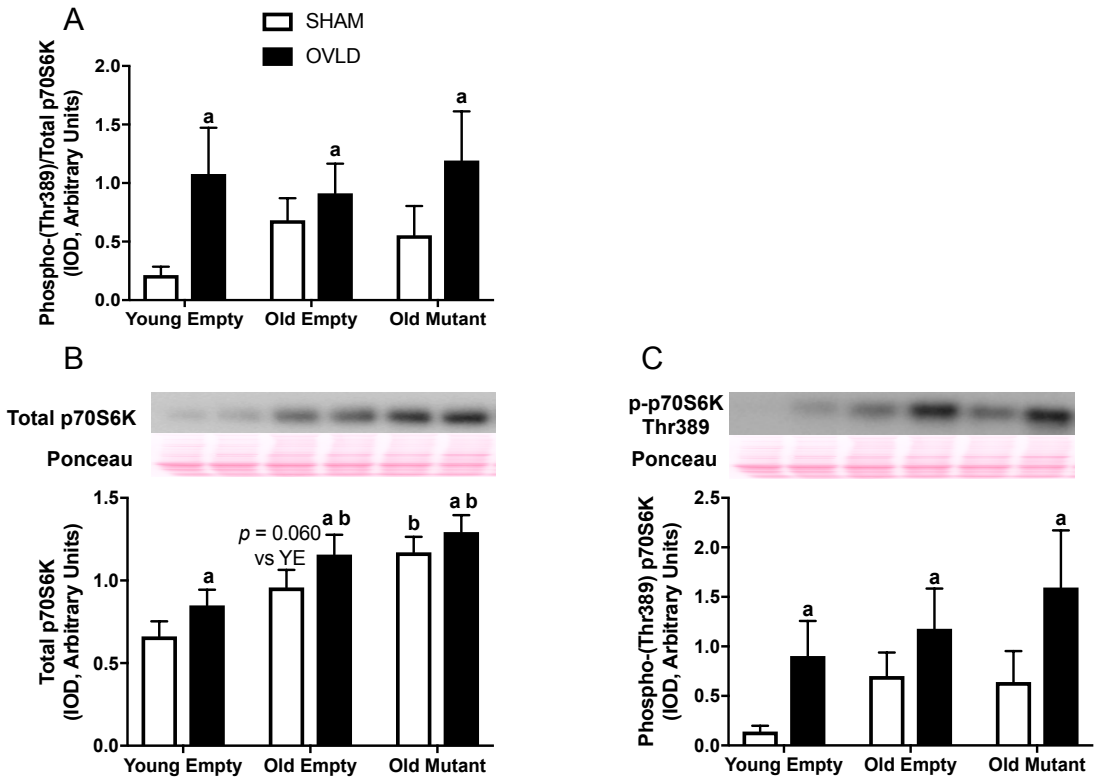

Figure 2.5.9. Total and phosphorylated p70S6K response to overload in young adult and old skeletal muscle. A, Plantaris (PLT) phospho-(Thr389)/total 70 kDa ribosomal protein S6 kinase (p70S6K) expression (Integrated optical density, IOD) after 21 days of functional overload (OVLD; unilateral gastrocnemius ablation) compared with sham-operated (SHAM) conditions in young adult and old FBN rats. Overload muscles received electrotransfer of plasmids containing either an empty vector (empty) or mutated glycogen synthase designed to enhance glycogen content (mutant). Young empty: 8 mo., n = 9; old empty: 32-34 mo., n = 11; old mutant: 32-34 mo., n = 13. B, PLT total p70S6K expression (IOD) and C, phospho-(Thr389) p70S6K expression. a: significant ($p \leq 0.05$) main effect of overload; b: significantly different from same leg in young empty.

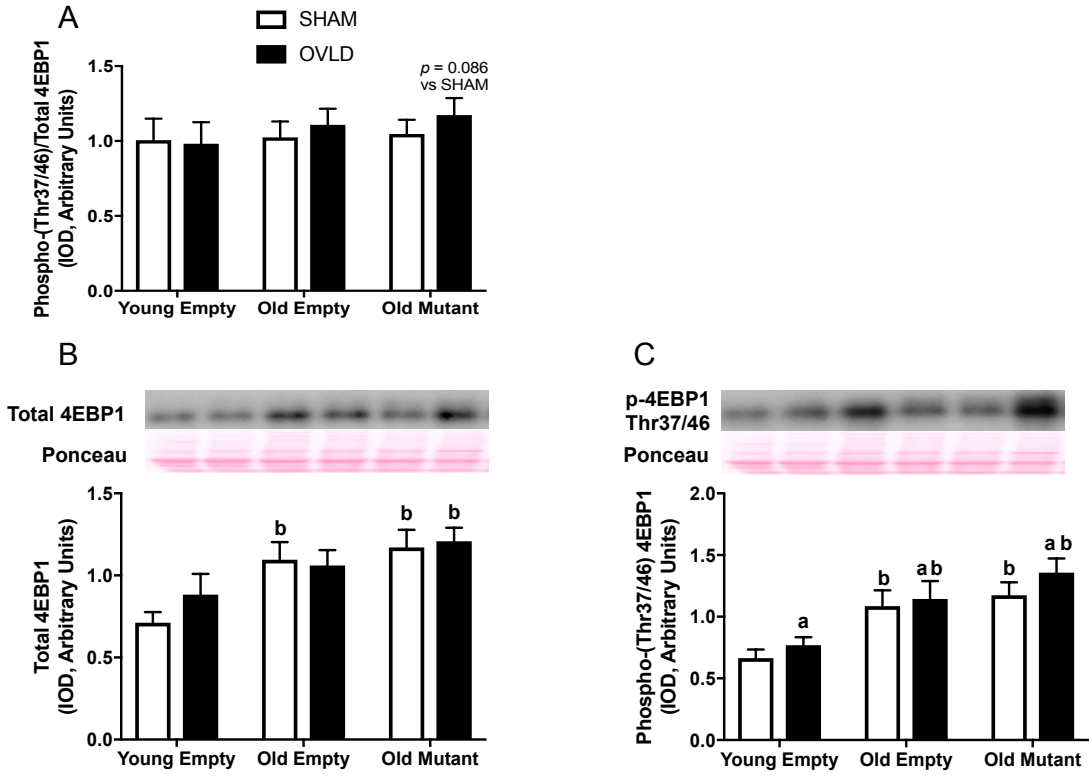

Figure 2.5.10. Total and phosphorylated 4EBP1 response to overload in young adult and old skeletal muscle. A, Plantaris (PLT) phospho-(Thr37/46)/total eIF4E binding protein (4EBP1) expression (Integrated optical density, IOD) after 21 days of functional overload (OVLD; unilateral gastrocnemius ablation) compared with sham-operated (SHAM) conditions in young adult and old FBN rats. Overload muscles received electrotransfer of plasmids containing either an empty vector (empty) or mutated glycogen synthase designed to enhance glycogen content (mutant). Young empty: 8 mo., n = 9; old empty: 32-34 mo., n = 11; old mutant: 32-34 mo., n = 13. B, PLT total 4EBP1 expression (IOD) and C, phospho-(Thr37/46) 4EBP1 expression. a: significant ($p \leq 0.05$) main effect of overload; b: significantly different from same leg in young empty.

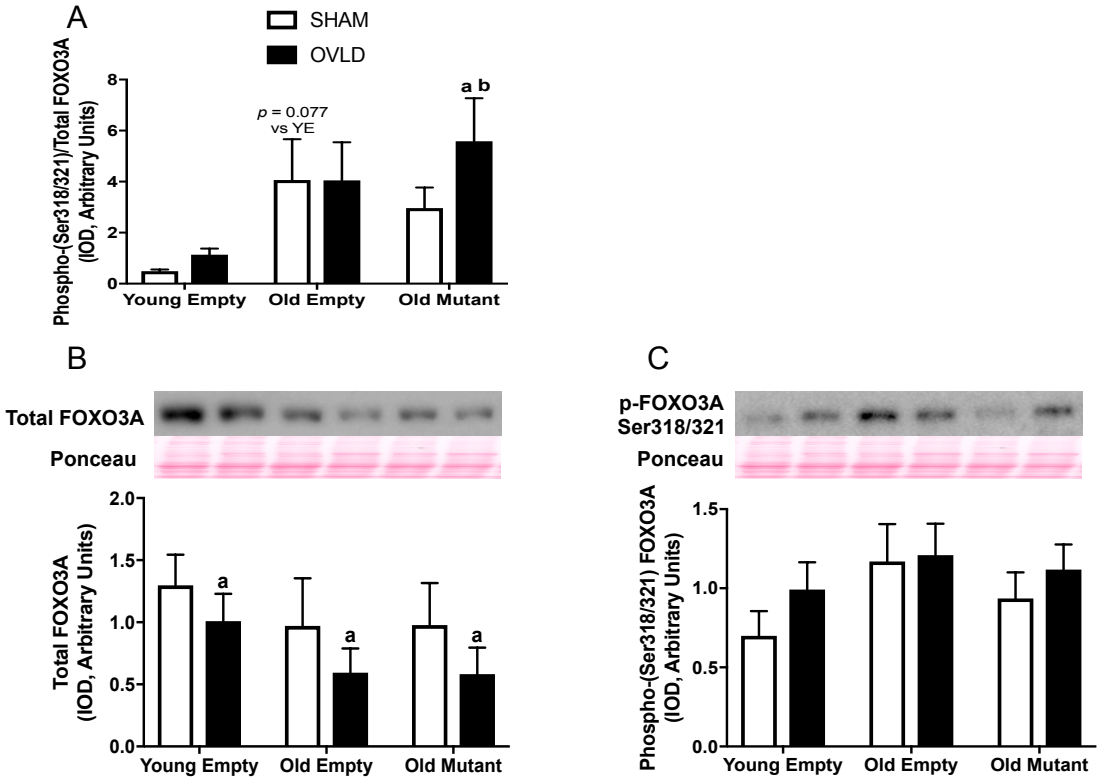

Figure 2.5.11. Total and phosphorylated FOXO3A response to overload in young adult and old skeletal muscle. A, Plantaris (PLT) phospho-(Ser318/321)/total forkhead box transcription factor 3A (FOXO3A) expression (Integrated optical density, IOD) after 21 days of functional overload (OVLD; unilateral gastrocnemius ablation) compared with sham-operated (SHAM) conditions in young adult and old FBN rats. Overload muscles received electrotransfer of plasmids containing either an empty vector (empty) or mutated glycogen synthase designed to enhance glycogen content (mutant). Young empty: 8 mo., n = 9; old empty: 32-34 mo., n = 11; old mutant: 32-34 mo., n = 13. B, PLT total FOXO3A expression (IOD) and C, phospho-(Ser318/321) FOXO3A expression. a: significant ($p \leq 0.05$) main effect of overload; b: significantly different from same leg in young empty.

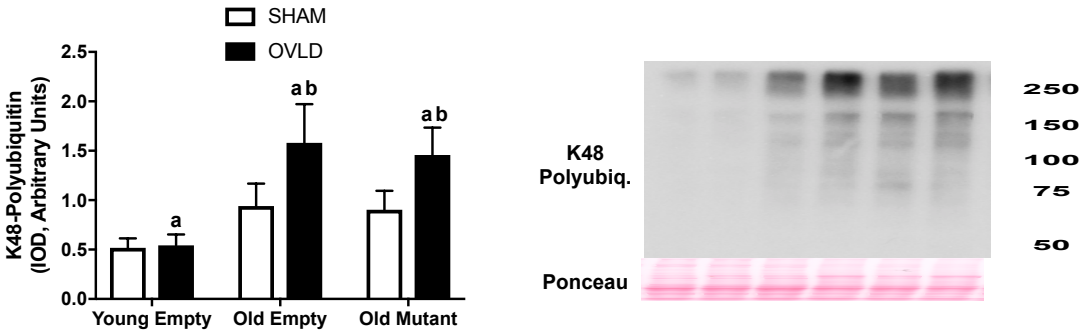

Figure 2.5.12. Plantaris K48-polyubiquitin response to overload in young adult and old skeletal muscle. Plantaris total lysine-48 (K48)-tagged polyubiquitin expression (Integrated optical density, IOD) after 21 days of functional overload (OVLD; unilateral gastrocnemius ablation) compared with sham-operated (SHAM) conditions in young adult and old FBN rats. Overload muscles received electrotransfer of plasmids containing either an empty vector (empty) or mutated glycogen synthase designed to enhance glycogen content (mutant). Young empty: 8 mo., n = 9; old empty: 32-34 mo., n = 11; old mutant: 32-34 mo., n = 13. a: significant ($p \leq 0.05$) main effect of overload; b: significantly different from same leg in young empty.

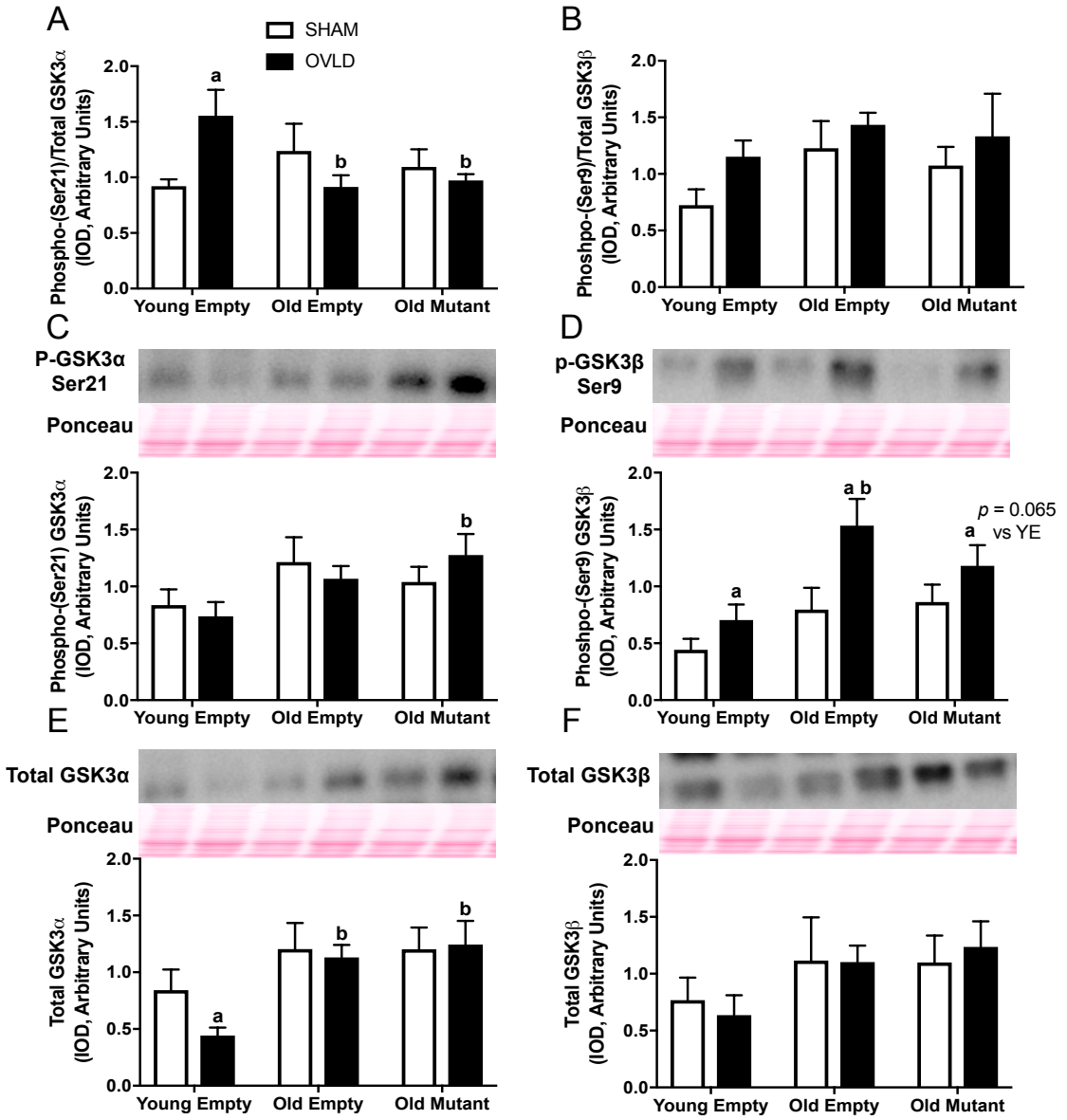

Figure 2.5.13. Total and phosphorylated GSK3α/β response to overload in young adult and old skeletal muscle. A, Plantaris (PLT) phospho-(Ser21)/total glycogen synthase kinase 3 (GSK3) α expression (Integrated optical density, IOD) and B, PLT phospho-(Ser9)/total GSK3β expression after 21 days of functional overload (OVLD; unilateral gastrocnemius ablation) compared with sham-operated (SHAM) conditions in young adult (8 mo.) and old (32-34 mo.) FBN rats. Overload muscles received electrotransfer of plasmids containing either an empty vector (empty) or mutated glycogen synthase designed to enhance glycogen content (mutant). Young empty: 8 mo., n = 9; old empty: 32-34 mo., n = 11; old mutant: 32-34 mo., n = 13. a: significant ($p \leq 0.05$) main effect of overload; b: significantly different from same leg in young empty.

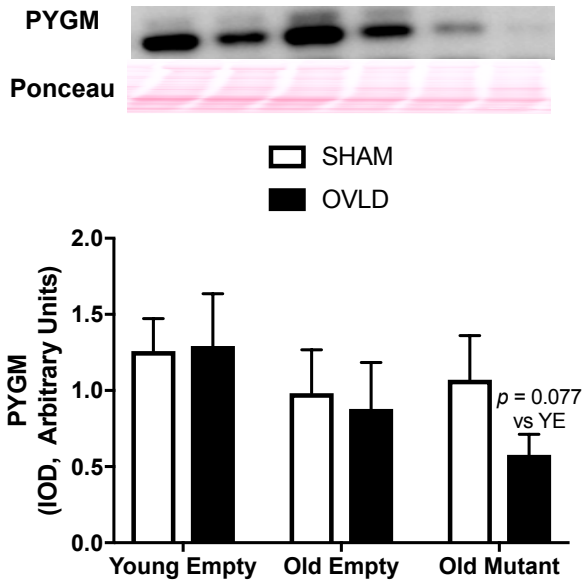

Figure 2.5.14. Plantaris PYGM response to overload in young adult and old skeletal muscle. Plantaris total muscle glycogen phosphorylase (PYGM) expression (Integrated optical density, IOD) after 21 days of functional overload (OVLD; unilateral gastrocnemius ablation) compared with sham-operated (SHAM) conditions in young adult and old FBN rats. Overload muscles received electrotransfer of plasmids containing either an empty vector (empty) or mutated glycogen synthase designed to enhance glycogen content (mutant). Young empty: 8 mo., n = 9; old empty: 32-34 mo., n = 11; old mutant: 32-34 mo., n = 13.

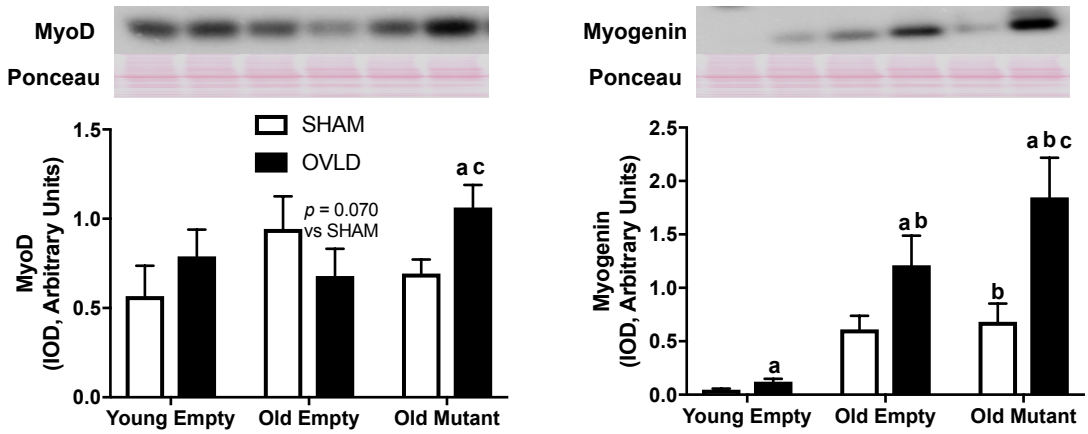

Figure 2.5.15. Plantaris MyoD and Myogenin response to overload in young adult and old skeletal muscle. A, Plantaris (PLT) MyoD and B, PLT Myogenin expression (Integrated optical density, IOD) after 21-days of functional overload (OVLD; unilateral gastrocnemius ablation) compared with sham-operated (SHAM) conditions in young adult (8 mo.) and old (32-34 mo.) FBN rats. Overload muscles received electrotransfer of plasmids containing either an empty vector (empty) or mutated glycogen synthase designed to enhance glycogen content (mutant). Young empty: 8 mo., n = 9; old empty: 32-34 mo., n = 11; old mutant: 32-34 mo., n = 13. a: significantly ($p \leq 0.05$) different than respective group's SHAM value; b: significantly different from the same leg in young empty; c: significantly different from same leg in old empty.

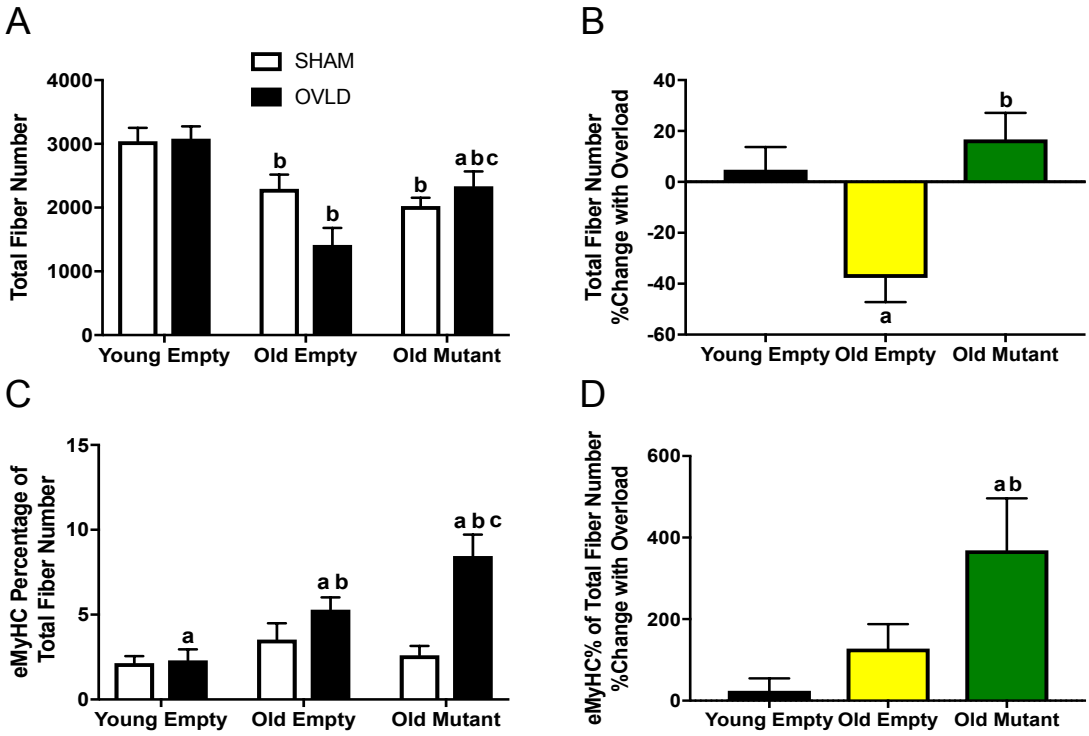

Figure 2.5.16. Plantaris Total Fiber Number and eMyHC expression response to overload in young adult and old skeletal muscle. A, Plantaris (PLT) total fiber number and C, PLT embryonic myosin heavy chain (eMyHC) percentage of total fiber number after 21-days of functional overload (OVLD; unilateral gastrocnemius ablation) compared with sham-operated (SHAM) conditions in young adult (8 mo.) and old (32-34 mo.) FBN rats. Overload muscles received electrotransfer of plasmids containing either an empty vector (empty) or mutated glycogen synthase designed to enhance glycogen content (mutant). Young empty: 8 mo., n = 9; old empty: 32-34 mo., n = 11; old mutant: 32-34 mo., n = 13. a: significantly ($p \leq 0.05$) different than respective group's SHAM value; b: significantly different from same leg in young empty; c: significantly different from same leg in old empty. B, PLT total fiber number and C, PLT eMyHC percentage of total fiber number percent (%) change with overload (vs. SHAM). a: significantly different from young empty; b: significantly different from old empty.

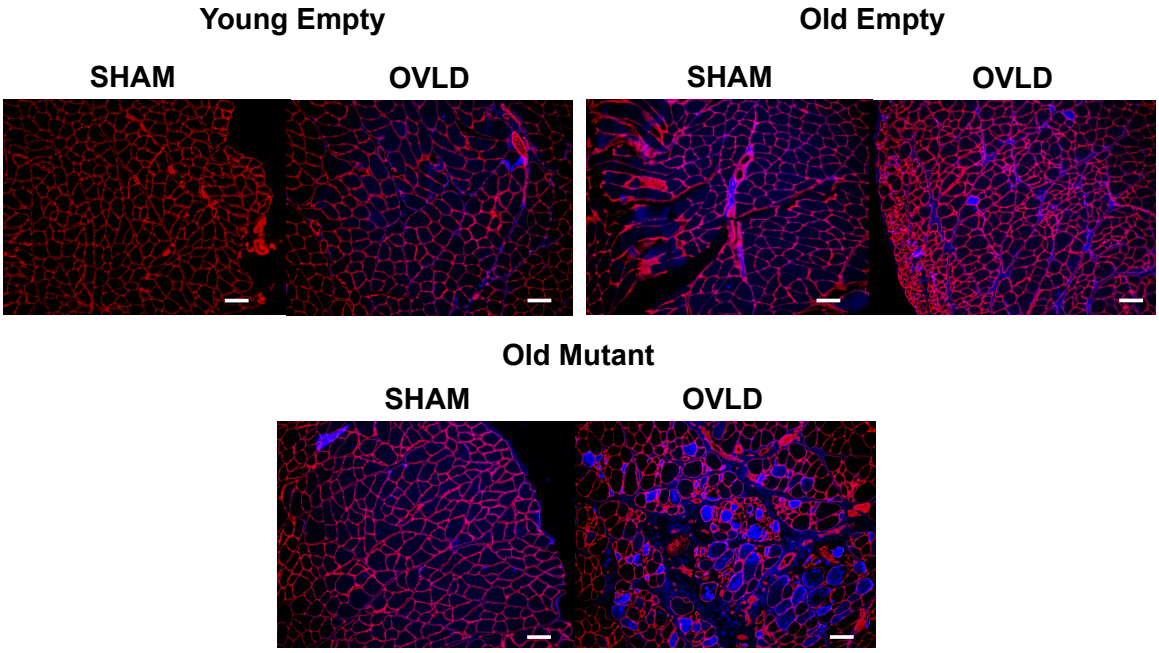

Figure 2.5.17. Plantaris representative images of Total Fiber Number and eMyHC expression response to overload in young adult and old skeletal muscle. Representative Image of Plantaris (PLT) of Young Empty, PLT of Old Empty, and PLT of Old Mutant used for determination of total fiber number and eMyHC expression (Figure 2.5.14) after 21-days of functional overload (OVLD; unilateral gastrocnemius ablation) compared with sham-operated (SHAM) conditions in young adult (8 mo.) and old (32-34 mo.) FBN rats. Overload muscles received electrotransfer of plasmids containing either an empty vector (empty) or mutated glycogen synthase designed to enhance glycogen content (mutant). Young empty: 8 mo., n = 9; old empty: 32-34 mo., n = 11; old mutant: 32-34 mo., n = 13. NOTE: Laminin staining is red (555 nm) and eMyHC staining is blue (350 nm).

Table 2.6.1 *Muscle wet weights and protein contents after the 21-day overloading protocol.*

	Young Empty (8 mo.) *n* = 9	Old Empty (32-34 mo.) *n* = 11	Old Mutant (32-34 mo.) *n* = 13
Muscle wet weight, mg/g BW			
Sham-operated	1.01 ± 0.01	0.52 ± 0.03 b	0.53 ± 0.04 b
Overloaded	1.25 ± 0.03 a	0.48 ± 0.03 a,b	0.62 ± 0.03 a,b,c
Percent Difference	24.36 ± 4.00 a	-6.08 ± 6.94 b	21.12 ± 6.34 a,c
Muscle protein content, μg/mg muscle*g BW^{-1}			
Sham-operated	196.61 ± 9.70	92.79 ± 13.39 b	94.90 ± 8.78 b
Overloaded	260.24 ± 15.54 a	80.94 ± 9.68 a,b	123.59 ± 7.27 a,b,c
Percent Difference	34.32 ± 9.17 a	-10.11 ± 7.21 b	36.81 ± 10.58 a,c

Values are means ± SE. a: significant ($p \leq 0.05$) main effect overload; b: significantly different from same leg within YE group; c: significantly different from same leg within OE group.

CHAPTER 3: EFFECTS OF GLYCOGEN ENHANCEMENT ON IN VITRO PROTEIN SYNTHESIS MANIPULATIONS IN C2C12 MYOTUBES

3.1 Introduction

Leucine, specifically L-leucine, is an essential, branched-chain amino acid (BCAA), that has been found to be a potent stimulator of muscle protein synthesis (MPS) in muscle cells *in vitro* (5, 29, 36) and *in vivo* (26, 36). Leucine has been shown to affect MPS via activation through an increase in the rapamycin-sensitive mechanistic (formerly mammalian) target of rapamycin complex 1 (mTORC1) leading to activation of downstream effectors regulating protein translation. Some of the most studied downstream markers of mTORC1 activation with leucine treatment have been p70 ribosomal protein S6 kinase (p70S6K) and eukaryotic initiation factor 4E binding protein 1 [4EBP1; (26, 36)]. In addition to MPS, leucine has also been found to affect muscle protein breakdown (MPB) by inhibiting proteolysis (15, 21, 93). The growing body of evidence for leucine affecting MPS and MPB has made it an increasingly popular nutritional supplement to potentially enhance muscle hypertrophy (26, 36).

Leucine can affect MPS and MPB by activating mTORC1 (26, 36, 62). In addition to mTORC1, another master regulator of MPS and MPB is 5'-AMP-activated protein kinase [AMPK; (30, 54, 118)]. In most instances, mTORC1 and AMPK work in direct conflict with one another (10, 54). While increases in mTORC1 activity lead to upregulation of MPS and downregulation of MPB (54, 117), AMPK activation leads to

inhibition of MPS and mTORC1 (13, 87) and increases in MPB (73, 88, 142). When activated AMPK upregulates catabolic pathways to supply energy (49), and downregulates anabolic pathways that are ATP-expensive, such as MPS, by inhibiting both directly (114) and indirectly (114) mTORC1 activation. Moreover, leucine has been found to activate MPS through increases in mTORC1, and reduce MPB, in part, by indirectly inhibiting AMPK activity *in vitro* (29) and *in vivo* (110), although not consistently (36).

AMPK is indirectly inhibited by glycogen through its β subunit containing a glycogen-binding domain [GBD; (77, 78)]. AMPK activity has been found to be inversely related with the level of glycogen content in muscle *in vivo*, with its activity being dramatically suppressed with high levels of glycogen and an increased AMPK activity with low levels of glycogen in rats (138) and humans (123). However, these findings have been recently challenged (98, 122, 140). Nevertheless, the findings of an AMPKβ-glycogen interaction have also been supported *in vitro*, where synthesized branched oligosaccharides (i.e., glycogen mimics) inhibited AMPK's activity (77).

The potential links between glycogen, leucine, AMPK, MPS, MPB, and associated signaling has never been examined in skeletal muscle *in vitro*. Therefore, the aim of this investigation was to determine whether enhancing intracellular glycogen content could enhance anabolic signaling/MPS and decrease catabolic (MPB) signaling in response to an anabolic stimulus in skeletal myotubes. We hypothesized that glycogen enhancement via the transfection of plasmid DNA expressing active glycogen synthase in cultured C2C12 myotubes would enhance the anabolic effect of leucine by inhibiting AMPK and increasing anabolic signaling/MPS, and this effect would be eliminated by

rapamycin-induced mTOR pathway blockade. We further hypothesized that glycogen enhancement via the transfection of plasmid DNA expressing active glycogen synthase in cultured C2C12 myotubes would enhance the anti-catabolic effect of leucine by inhibiting AMPK and decrease catabolic signaling, and the effect would be eliminated by rapamycin-induced mTOR pathway blockade.

3.2 Experimental Design and Methods

3.2.1 Experimental Cell Culture

3.2.2 Transient Plasmid Transfection in Myotubes

C2C12 myoblasts (ATCC) were seeded at the same density (7.5×10^4) in 12-well plates in growth media (GM; high glucose DMEM, 10% Fetal Bovine Serum) without antibiotics and grown for ~48 hours with daily media changes until ~95% confluent. At ~95% confluence, the cells were washed 2x with Dulbecco's PBS (DPBS; VWR), and then switched to differentiation media (DM; high glucose DMEM, 2% Horse Serum) without antibiotics and grown for 96 hours to achieve immature muscle fibers (i.e., myotubes). After 96 hours of differentiation, the myotubes were then transfected with 2.5 μg/well of either pCMV4/empty vector plasmid or pCMV4-M2,3a-GS/mutant GS vector plasmid, complexed with DNA transfection reagent (Lipofectamine 3000, Thermo Fisher) in Opti-MEM media (Thermo Fisher) and added to each well. The next day (~24 hours), cells were washed twice with DPBS, and switched to DM with antibiotics (1% Pen/Strep) for ~24 hours. Following ~48 hours of transfection (i.e., ~144 hours of differentiation), cells were then ready for treatments as outlined below.

3.2.3 Leucine, Rapamycin, or Leucine and Rapamycin Treatments

After 48 hours of transfection, cells were treated using a previously published protocol (5), with modifications. Briefly, cells were deprived of serum by incubation in high glucose DMEM only for 4 h followed by 1 DPBS wash, then a 1 h amino acid-deprivation period in DPBS (137 mM NaCl, 2.7 mM KCl, 10mM Na_2HPO_4, 1.8 mM KH_2PO_4, 1 mM $CaCl_2*2H_2O$, 0.5 mM $MgCl_2*6H_2O$, pH 7.4). Cells (3-wells/treatment) were then inoculated with vector (control, CT), L-leucine (LEU; Sigma no. L8912, St. Louis, MO, USA) at 10 mM (38), rapamycin (RAP; Cayman Chemicals no. 13346, Ann Arbor, MI, USA) at 100 nM, or co-treated (LEU+RAP) for 30 min in serum-free DMEM. All treatments contained 100 μM Puromycin for measuring protein synthesis using the SUnSET technique (40). Each condition (3-wells/treatment) was performed on a pair of 12-well plates transfected with pCMV4 & pCMV4-M2,3a-GS, respectively, and then replicated on a separate pair of 12-well plates for 6-wells/treatment.

3.2.4 Glycogen Concentration Assay

After 30 min treatments in both plasmid conditions were completed as described above, plates were placed on ice, media was aspirated off and cells were quickly rinsed twice in ice-cold PBS, scrapped, transferred to a new microcentrifuge tube, and spun at 8,000 x g for 8 min at 4°C. The supernatant was then removed and cell pellets were stored at -80°C until further analyses. Cell pellets were then thawed on ice before 75 μL of ice-cold 0.1M NaOH was added to the pellet prior to mechanical lysing with a 25G needle and syringe. 50 μL of the homogenate was then transferred to a new tube for glycogen concentration analyses and 10 μL of the homogenate was transferred to a separate tube containing 60 μL of 0.1M NaOH for protein content. For each cell pellet protein

concentration was determined using a 1:6 dilution, which was assessed in triplicate using a modified Lowry procedure (DC Protein Assay, Bio-Rad, Hercules, CA, USA). Glycogen concentration was determined as previously described (99, 126), with modifications. Briefly, the 50 µL homogenate was boiled at 90°C for 20 minutes in a dry-block heater to remove any free glucose. After 20 min, the solution was neutralized with 50 µL of 0.2M Acetic Acid. Then 50 µL of the neutralized solution was transferred to a new tube containing 150 µL of 0.1M Sodium Acetate Buffer (0.05M Sodium Acetate, 0.05M Acetic Acid, pH 4.6-4.7) and vortexed. Glycogenolysis was then performed by adding 15 µL of amyloglucosidase (Sigma no. A7420) solution (10 µg/µL in 20 mM Tris with 0.02% BSA, pH 7.5) and incubating at 55°C for 1 h. After 1 h, the samples were centrifuged at 14,800 x *g* for 5 min and then loaded in triplicate into cuvettes (USA Scientific no. 9090-0460, Ocala, FL, USA). The amount of free glucosyl units in each sample were then determined spectrophotometrically via a glucose assay (Sigma no. GAHK20). Glycogen content (µg/µg protein) of the original muscle sample was then derived from comparing the reading to a standard curve made with type III glycogen from rabbit liver (Sigma no. G8876).

3.2.5 SDS-PAGE, Western Blotting, and Immunodetection

After 30 min treatments in both plasmid conditions were completed as described above, plates were placed on ice, media was aspirated off and cells were quickly rinsed twice in ice-cold PBS. Then ice-cold RIPA homogenization buffer containing protease and phosphatase inhibitors (Santa Cruz Biotechnology no. sc-24948, Dallas, TX, USA) with 3% SDS and 0.1% triton X-100 was quickly added to each well and scrapped prior to transferring each wells contents to a new ice-cold microcentrifuge tube. Each tube was

then mechanically lysed using a 25G needle and syringe, followed by 10 min incubation on ice with periodic vortexing. Samples were then spun for 20 min at 21,100 x g at 4°C. The supernatant was then transferred to a new tube and were stored at -80°C until further analyses. Standard western blotting protocols were used as previously described (128, 129). Briefly, total myotube protein homogenates were solubilized in sample loading buffer (50 mM Tris-HCl, pH 6.8, 10% glycerol, 2% SDS, 2% β-mercaptoethanol, 0.1% bromophenol blue) at a concentration of 1 μg/μl and boiled at 95°C for 5 minutes. Proteins were then separated by SDS-PAGE using either 4-15% (mTOR, p70S6K, and 4EBP1) or 7.5% (all others) Tris-HCl gels (Criterion, Bio-Rad) for 1.5 h at 100V in 4°C and then transferred for 1 h at 100V in 4°C onto a PVDF membrane (EMD Millipore, Billerica, MA, USA) in Towbin's buffer (25 mM Tris-base, 192 mM glycine, 20% methanol). To verify transfer and equal loading among lanes, membranes were then stained with Ponceau S (Sigma) and imaged. For immunodetection, membranes were blocked for 1 h at room temperature in blocking buffer (5% nonfat dry milk in TBS-T, 20 mM Tris base, 150 mM NaCl, 0.1% Tween-20, pH 7.6), briefly rinsed in TBS-T, and then incubated with primary antibody (in 2% BSA in TBS-T, with 0.02% NaN_3, pH 7.5) overnight at 4°C on a shaker. Membranes were then serially washed in TBS-T, incubated with horseradish peroxidase (HRP)-conjugated secondary in blocking buffer for 1 h, and again serially washed in TBS-T. The HRP activity was detected by enhanced chemilumenscence reagent (ECL; EMD Millipore), exposure to autoradiographic film (Alkali Scientific no. XR1570, Pompano Beach, FL, USA), and then developed (Konica Minolta no. SRX-101A). Antigen concentration was calculated by quantification of the integrated optical density (IOD) of the appropriate band and then normalized to total

protein content from previous Ponceau S staining image using a gel analyzer software (Image Studio Lite, Licor, Lincoln, NE, USA). Primary antibody dilutions were as follows: phospho-AMPKα^{Thr172} (Cell Signaling Technology, CST, no. 4188, Beverly, MA, USA), 1:1000; total AMPK α (CST no. 2532), 1:2500; phospho-ACC^{Ser79} (EMD Millipore no.07-303) 1:1000; total ACC (Streptavidin-HRP, GE Life Sciences no. RPN1231), 1:4000; p-FOXO3A$^{Ser318/321}$ (CST no. 9465), 1:1000; total FOXO3A (CST no. 12829), 1:2000; phospho-GS^{Ser641} (CST no. 3891), 1:5000; total GS (CST no.3893), 1:5000; K48-linkage Specific Polyubiquitin (CST no. 8081), 1:1000; Myogenin (Santa Cruz no. sc-12732, Dallas, TX, USA) 1:200; phospho-mTOR^{S2448} (CST no. 5536), 1:2000; mTOR (CST no. 2983), 1:4000; phospho-p70S6K^{Thr389} (CST no. 9234), 1:750; total p70S6K (CST no. 2708), 1:2000; puromycin (EMD Millipore no. MABE343), 1:5000; phospho-4E-BP1$^{Thr37/46}$ (CST no. 2855), 1:6000; total 4E-BP1 (CST no. 9644), 1:15,000; phospho-TSC2^{Ser1387} (CST no. 5584), 1:1500; phospho-TSC2^{Thr1462} (CST no. 3617), 1:1500; total TSC2 (CST no. 3990), 1:2000. The appropriate species-specific (goat anti-mouse or anti-rabbit) HRP secondary antibodies were from CST except for puromycin secondary, which was from Jackson ImmunoResearch Laboratories (West Grove, PA, USA).

3.2.6 Statistical Analyses

A two-way analysis of variance was used (Treatment x Plasmid). Post-hoc comparisons were accomplished via a Fisher's LSD test, with statistical significance being set *apriori* at $p \leq 0.05$. All statistical analyses and graphs were made using Graphpad Prism 7 (GraphPad, San Diego, CA, USA). Data are presented as means ± SEM.

3.3 Results

3.3.1 Myotube glycogen content and glycogen synthase phosphorylation and concentration

The phosphorylation status (phospho-GS/total GS) at Ser641 (Figure 3.5.1A) was significantly ($p \leq 0.05$) lower (main effect) in all mutant GS-transfected myotubes regardless of treatment compared to empty-vector. This effect was seen despite NSD ($p > 0.05$) in the absolute concentration of phospho-(Ser641) GS (Figure 3.5.1B) regardless of plasmid or treatment condition. There was a concomitant significantly ($p \leq 0.05$) higher (main effect) absolute concentration of total GS (Figure 3.5.1C) in all mutant GS-transfected myotubes regardless of treatment condition compared to empty-vector. In mutant GS-transfected myotubes, LEU treatment tended ($p = 0.06$) to induce a higher total GS concentration compared to mutant GS CT, whereas RAP or LEU+RAP in mutant GS-transfected myotubes induced a significantly ($p \leq 0.05$) lower total GS concentration vs. mutant GS LEU alone. There was a significantly ($p \leq 0.05$) higher (main effect) myotube glycogen content (Figure 3.5.2) in all mutant GS-transfected myotubes, compared to empty-vector regardless of treatment. Further, in mutant GS transfected myotubes, LEU treatment had significantly ($p \leq 0.05$) higher glycogen content compared to mutant GS CT, whereas, RAP and LEU+RAP in mutant GS transfected myotubes had significantly ($p \leq 0.05$) lower glycogen content vs. mutant GS LEU. This plasmid (mutant GS) has been shown in both COS cells (120) and in mouse skeletal muscle (32, 75) to enhance glycogen content due to a Ser to Ala mutation at two critical sites (sites 2 and 3a) for phosphorylation and, thus, decreased activity (120). Ser641 is site 3a on GS and therefore the lack of change in phosphorylation at this site despite an increase in the absolute concentration of total GS verifies that the mutant GS

vector was overexpressed in the mutant GS-transfected myotubes. Moreover, the potent increase in myotube glycogen content in the mutant GS-transfected myotubes, regardless of treatment condition, compared to empty vector further confirms the correct plasmid was overexpressed.

3.3.2 Muscle protein synthesis rate

MPS rate was determined via incorporation of puromycin into synthesizing proteins using the SUnSET Technique (40). Compared to CT, regardless of plasmid condition, LEU induced significantly ($p \leq 0.05$) higher MPS (Figure 3.5.3). This effect was significantly ($p \leq 0.05$) lower with RAP and RAP+LEU treatments vs. LEU treatment regardless of plasmid condition. In mutant GS-transfected myotubes, LEU+RAP treatment displayed significantly ($p \leq 0.05$) higher MPS than RAP alone. Lastly, MPS was significantly ($p \leq 0.05$) higher (main effect) in all mutant GS-transfected myotubes regardless of treatment condition compared to empty-vector.

3.3.3 AMPK and ACC phosphorylation and concentration

There were NSD ($p > 0.05$) in phosphorylation status (phospho-AMPKα/total AMPKα) at Thr172 (Figure 3.5.4A) or absolute concentration of phospho-(Thr172) AMPKα (Figure 3.5.4B) regardless of plasmid or treatment condition. The absolute concentration of total AMPKα (Figure 3.5.4C) was significantly ($p \leq 0.05$) reduced in mutant GS-transfected myotubes treated with RAP compared to LEU treatment only. There was NSD ($p > 0.05$) between any other treatment or between plasmid conditions in total AMPKα.

Acetyl-CoA Carboxylase is a well-established marker of AMPK activity (43). There were NSD ($p > 0.05$) in phosphorylation status (phospho-ACC/total ACC) at Ser79

(Figure 3.5.5A) between any group, regardless of plasmid or treatment condition. There were NSD ($p > 0.05$) between absolute concentrations of phospho-(Ser79) ACC (Figure 3.5.5B), regardless of plasmid or treatment condition despite there being a trend towards an increase in mutant GS-transfected myotubes treated with RAP compared to mutant GS CT treatment ($p = 0.07$) and mutant GS LEU+RAP compared to mutant GS RAP treatment ($p = 0.06$). Lastly, there were NSD ($p > 0.05$) between absolute concentrations of total ACC (Figure 3.5.5C), regardless of plasmid or treatment condition.

3.3.4 SIGNALING INTERMEDIATES REGULATING MPS

3.3.4.1 mTOR, p70S6K, and 4EBP1 phosphorylation and concentration

The phosphorylation status (phoshpo-mTOR/total mTOR) at Ser2448 (Figure 3.5.6A) was significantly ($p \leq 0.05$) increased with LEU treatment compared to CT regardless of plasmid condition with NSD ($p > 0.05$) between plasmid conditions. There was significant ($p \leq 0.05$) decrease in mTOR phosphorylation status with RAP or RAP+LEU treatment compared to CT or LEU treatments regardless of plasmid condition with NSD ($p > 0.05$) between plasmid conditions. In general, the absolute concentration of phospho-(Ser2448) mTOR followed the same pattern (Figure 3.5.6B) as mTOR phosphorylation status at Ser2448. There was NSD ($p > 0.05$) between absolute concentrations of total mTOR (Figure 3.5.6C) regardless of plasmid or treatment conditions, despite there being a trend ($p = 0.07$) towards of decrease in mutant GS-transfected myotubes treated with LEU+RAP compared to empty-vector.

In empty-vector treated myotubes, the phosphorylation status (phospho-p70S6K/total p70S6K) at Thr389 (Figure 3.5.7A) was significantly ($p \leq 0.05$) increased with LEU treatment compared to CT. The same effect was evident for p70S6k Thr389

phosphorylation status in mutant GS-transfected myotubes with LEU treatment compared to mutant GS CT condition, albeit not significant (p = 0.07). Regardless of plasmid condition, both RAP and LEU+RAP treatments significantly ($p \leq 0.05$) decreased the phosphorylation status of p70S6K at Thr389 compared to CT and LEU treatments; the absolute concentration of phospho-(Thr389) p70S6K followed the exact same pattern (Figure 3.5.7B). There was NSD ($p > 0.05$) between absolute concentrations of total p70S6K (Figure 3.5.7C) regardless of plasmid or treatment condition.

The phosphorylation status (phosho-4EBP1/total 4EBP1) at Thr37/46 (Figure 3.5.8A) was significantly ($p \leq 0.05$) increased with LEU treatment compared to CT treatment regardless of plasmid condition, with NSD ($p > 0.05$) between plasmid conditions. In empty-vector transfected myotubes, RAP and LEU+RAP treatments significantly ($p \leq 0.05$) reduced the 4EBP1 phosphorylation status vs. LEU and CT treatments. In mutant GS-transfected myotubes, RAP tended ($p = 0.07$) to decrease 4EBP1 phosphorylation status compared to CT treatment, and RAP and LEU+RAP treatments were significantly ($p \leq 0.05$) decreased compared to LEU treatment. There was NSD ($p > 0.05$) between plasmid conditions for any treatment with 4EBP1 phosphorylation status at Thr37/46.

The absolute concentration of phospho-(Thr37/46) 4EBP1 (Figure 3.5.8B) was significantly ($p \leq 0.05$) increased with LEU treatment compared to CT treatment regardless of plasmid condition. In empty-vector transfected myotubes, RAP tended ($p = 0.08$) to decrease the concentration of phospho-(Thr37/46) 4EBP1 compared to empty-vector CT. Regardless of plasmid condition, RAP or LEU+RAP treatments significantly ($p \leq 0.05$) decreased the concentration of phospho-(Thr37/46) 4EBP1 compared to LEU treatments. There was a significant ($p \leq 0.05$) increase (main effect) in absolute

concentration of phospho-(Thr37/46) 4EBP1 in all mutant GS-transfected myotubes, regardless of treatment compared to empty-vector. There was NSD ($p > 0.05$) between absolute concentrations of total 4EBP1 (Figure 3.5.8C) regardless of plasmid or treatment conditions.

3.3.4.2 TSC2 phosphorylation and concentration

There were NSD ($p > 0.05$) in phosphorylation status (phospho-TSC2/total TSC2) at Ser1387 (Figure 3.5.9A) between any group regardless of plasmid or treatment condition despite a trend towards an increase in empty-vector transfected myotubes treated with LEU ($p = 0.08$), RAP ($p = 0.07$), or LEU+RAP ($p = 0.07$) compared to empty-vector CT. The absolute concentration of phospho-(Ser1387) TSC2 (Figure 3.5.9C) was significantly ($p \leq 0.05$) higher in empty-vector transfected myotubes treated with RAP or LEU+RAP compared to empty vector CT treatment. There was NSD ($p > 0.05$) between any other treatment or between plasmid condition. There were NSD ($p > 0.05$) in phosphorylation status (phospho-TSC2/total TSC2) at Thr1462 (Figure 3.5.9B), absolute concentration of phospho-(Thr1462) TSC2 (Figure 3.5.9D), or absolute concentration of total TSC2 (Figure 3.5.9E) regardless of treatment or plasmid condition.

3.3.5 SIGNALING INTERMEDIATES REGULATING MPB

3.3.5.1 FOXO3A phosphorylation and concentration

There were NSD ($p > 0.05$) in the phosphorylation status (phospho-FOXO3A/total FOXO3A) at Ser318/321(Figure 3.5.10A), the absolute concentration of phospho-(Ser318/321) FOXO3A (Figure 3.5.10B), or the absolute concentration of total FOXO3A (Figure 3.5.10C), regardless of plasmid or treatment condition.

3.3.5.2 Lysine48-Linked Polyubiquitin concentration

There was a significant ($p \leq 0.05$) decrease (main effect) in absolute concentration of total K48-linked polyubiquitin (Figure 3.5.11) in all mutant GS-transfected myotubes, regardless of treatment compared to empty-vector. Additionally, in mutant GS-transfected myotubes there was a trend ($p = 0.06$) towards an increase in the absolute concentration of total K48-linked polyubiquitin with RAP treatment compared to mutant GS CT treatment.

3.3.6 MARKERS OF MYOGENESIS AND/OR REMODELING

3.3.6.1 Myogenin concentration

As this investigation was conducted on Day 7 myotube lysates, we only assessed a myogenic regulatory factor (MRF) responsible for differentiation, myogenin. There were NSD ($p > 0.05$) in the concentration of total Myogenin regardless of plasmid or treatment condition (Figure 3.5.12). As these were fully differentiated myotubes (i.e., Day 7), the lack of changes in this specific MRF at this stage of the myogenic program is not unexpected.

3.4 Discussion and Conclusions

In most instances, mTORC1 and AMPK work in direct conflict with one another (10, 54). While increases in mTORC1 activity lead to upregulation of MPS and downregulation of MPB (54, 117), AMPK activation leads to inhibition of MPS and mTORC1 (13, 87) and increases in MPB (73, 88, 142). Leucine has been found to activate MPS through increases in mTORC1, and reduce MPB, in part, by indirectly inhibiting AMPK activity *in vitro* (29) and *in vivo* (110), although not consistently (36). Further, AMPK is directly inhibited by glycogen through its β subunit containing a GBD

(77, 78). However, the potential links between glycogen, leucine, AMPK, MPS, MPB, and associated signaling had never been examined in skeletal muscle *in vitro*. The novel findings of this investigation are that enhancing glycogen content augments basal and leucine-stimulated MPS in cultured C2C12 skeletal myotubes. Although the effect of leucine treatment on MPS is mTOR-dependent regardless of plasmid condition, glycogen enhancement augments MPS independent of changes in AMPK or mTOR signaling. In contrast, glycogen enhancement led to reductions in the amount of K48-linked polyubiquinated proteins, theoretically indicating less MPB, however, this was not carried to other MPB signaling markers assessed.

The most fascinating finding of the current investigation was that enhancing glycogen content augments basal and leucine-stimulated MPS in cultured C2C12 skeletal myotubes. We confirmed the findings of others who found a significant increase in mTORC1 signaling in either myoblasts or myotubes as measured via increases in the phosphorylation or phosphorylation status of mTOR, p70S6K, or 4EBP1 in response to leucine treatment (5, 24, 29, 45, 92) that also lead to increases in MPS (5, 29) and this effect was blocked by rapamycin treatment (5, 92, 101). We expanded upon these previous findings in showing that enhanced intracellular glycogen content in myotubes led to significant increases in MPS regardless of treatment, and this effect was augmented with leucine treatment. Although, the effect of leucine treatment is mTOR-dependent, glycogen enhancement augmented MPS independent of changes in mTOR or AMPK signaling when compared to empty vector. Therefore, other potential signaling mechanisms that were not assessed may be involved (discussed below).

To examine if intracellular glycogen enhancement in cultured myotubes had an effect on muscle protein breakdown (MPB) we chose to examine FOXO3A signaling, at a specific site (Ser318/321) indicative of inhibition of MPB (135, 142) as well as a readout of proteins being tagged for degradation by the ubiquitin proteasome system [K48-linked polyubiquitin; (143)]. When activated, FOXO3A translocates to the nucleus and increases expression of muscle-specific E3 ubiquitin ligases, MuRF1 and MAFbx (135, 142), leading to MPB through the ubiquitin proteasome system (12, 142). There was NSD regardless of treatment or plasmid condition in the phosphorylation status of FOXO3A at Ser318/321 in this investigation. This finding with glycogen enhancement may be explained by the lack of a loading stimulus (e.g., stretch or electrical stimulation) in the cultured myotubes transfected with mutant GS. In support of this, our lab found that young and old humans who had greater levels of intramuscular glycogen content displayed a higher phosphorylation status of FOXO3A at Ser318/321 following (within ≤ 1-2 h) an acute bout of resistance exercise [i.e., muscle loading; (125), unpublished data]. Therefore, the addition of a loading stimulus (e.g., stretch or electrical stimulation) to future work may be required to determine the effect of glycogen enhancement on MPB signaling. Although enhancement to intracellular glycogen content had no effect on FOXO3A signaling at the site assessed, there was a significant decrease (main effect) of the amount of K48-linked polyubiquitin proteins in the mutant GS-transfected myotubes, theoretically meaning less MPB. To our knowledge, this is the first time it has been reported that enhanced intracellular glycogen content in cultured myotubes led to reductions in a marker of MPB via the ubiquitin proteasome system. Because only one

marker (of the two assessed) of MPB was changed with glycogen enhancement more work is needed to clarify these findings.

The findings that intracellular glycogen content had no effect on AMPK phosphorylation status or activity in myotubes, even with leucine and/or rapamycin treatments, did not support our hypothesis. However, the literature has been inconsistent with some finding increases (14, 70), decreases (29), or no changes (24) with AMPK phosphorylation status and/or activity in response to leucine treatment. These inconsistencies may be due to the various doses of leucine used, the treatment time frame with leucine, myoblasts vs. myotubes, or the treatment method [i.e., starved vs. non-starved; (26, 36)]. Additionally, as this investigation measured overall AMPK α phosphorylation status at Thr172 (i.e., not separating out AMPK α_1 or α_2) we cannot isolate the effects of glycogen enhancement and/or leucine treatment on AMPK specific isoforms in cultured myotubes. AMPK α_1 is considered to control muscle growth (79) through regulating MPS (86, 87). AMPK α_1 has been found both *in vitro* (87) and *in vivo* (86) to regulate MPS through mTORC1, whereas AMPK α_2 is involved in metabolic adaptations (79, 88). Also, recent work *in vivo* (51) has found overall AMPK α phosphorylation status to reflect AMPK α_2, and not AMPK α_1 phosphorylation. Therefore, the lack of differences in the current investigation may be explained by the inability to delineate between the two AMPK α isoforms. However, as there were also no changes in AMPK activity (via p-ACC) regardless of plasmid or treatment condition, it remains to be determined if the effects seen work through AMPK at all. In addition to other potential markers needing to be assessed the lack of effects in markers measured could also be due to the starvation model employed to enhance leucine stimulation (5,

101). Future work should examine the effect of enhanced intracellular glycogen in a non-amino acid starved state, which is considered more physiologically relevant (38).

Although the effect of glycogen enhancement in cultured myotubes augmented basal and leucine-stimulated MPS, the lack of an effect on AMPK and MPS signaling markers may be explained by alternative signaling pathways or factors that were not measured. An increase in glycogen content is assumed to lead to an increase in inorganic phosphate, glucose, as well as production of ATP through glycolysis and downstream metabolic pathways (2, 44, 109). Although there was an increase in glycogen content in this investigation, glycogen degradation was not determined. However, others using the exact mutant GS plasmid in mouse muscle (75, 100) have measured glycogenolysis and found increases in factors suggestive of enhanced glycogen catabolism, such as glycogen phosphorylase (75) and glycogen debranching enzyme (100). Therefore, greater glycogen content in the current investigation should mean greater glycogenolysis, increases in glycolysis and glycolytic intermediates, and thus more ATP production (2). In addition, glycogen has been linked to providing substrates or ATP for biosynthetic pathways, such as nucleotide (115, 133) or non-essential amino acid (115, 133) synthesis. These findings may explain the increases seen in MPS with glycogen enhancement in the current investigation. Nevertheless, as none of these factors or signaling pathways were measured in this investigation more work is clearly need to elucidate the effects of glycogen enhancement on augmented MPS in cultured myotubes.

To further test the potential effects of other signaling pathways influencing AMPK and MPS, we measured TSC2 phosphorylation at a site for Akt (Thr1462) and AMPK (Ser1387). Although there was a trend for an increase in the phosphorylation

status of TSC2 at Ser1387 in leucine, rapamycin, and co-treatment in empty vector-transfected myotubes, there was NSD between any treatments regardless of plasmid condition. This falls in line with the NSD observed in AMPK phosphorylation status and activity as discussed above. Additionally, the NSD in the phosphorylation status of TSC2 at Thr1462 is in agreement with previous reports that found leucine had no effect on Akt signaling (5, 24, 38, 63, 92, 101). Although leucine (36) and glycogen content (58) can feedback to influence insulin/growth signaling (e.g., Akt), there was no effect on either pathway in the current investigation. Again, future work needs to elucidate the effect of glycogen enhancement on AMPK and MPS related signaling in a more physiologically relevant, non-starved state.

The elevation in glycogen content with leucine treatment in mutant GS-transfected myotubes was an interesting finding. As previously mentioned, leucine can influence insulin signaling (36). Specifically, leucine can enhance insulin sensitivity and glycogen synthesis (36). Moreover, as this was not anticipated in the current investigation we did not explore this phenomenon further. Although, this is not the first time that leucine has been reported to enhance glycogen content in myotubes (27), it is in response to a constitutively active GS. Although, Doi et al. (27) found increases in glycogen content with leucine treatment, there was no starvation period employed, such as the serum and amino acid starvation of the current investigation, and therefore this may be the reason for the lack of a response in the empty vector-transfected myotubes. Nevertheless, the glycogen enhancement in mutant GS-transfected myotubes regardless of treatment with the starvation period indicates that the mutant GS plasmid may have had even higher glycogen content that was lost following the starvation period.

Regardless, the mutant-GS transfected myotubes still had significantly higher glycogen content, independent of treatment, compared to empty vector at collection and allows for direct comparisons of the effects glycogen enhancement on MPS and signaling assessed.

In summary, glycogen enhancement in cultured C2C12 myotubes augments basal and leucine-stimulated MPS. Although the effect of leucine treatment on MPS is mTOR-dependent regardless of plasmid condition, glycogen enhancement augments MPS independent of changes in AMPK, mTOR, or MPS signaling markers assessed. In contrast, glycogen enhancement led to reductions in the amount proteins tagged for degradation by the ubiquitin proteasome system, theoretically indicating less MPB, however, this was not found in other MPB signaling. Future work should examine the effect of intracellular glycogen enhancement on MPS and associated signaling in a more physiologically relevant state (i.e., not amino acid starved) and in conjunction with a loading stimulus (e.g., stretch or electrical stimulation).

3.5 Figures

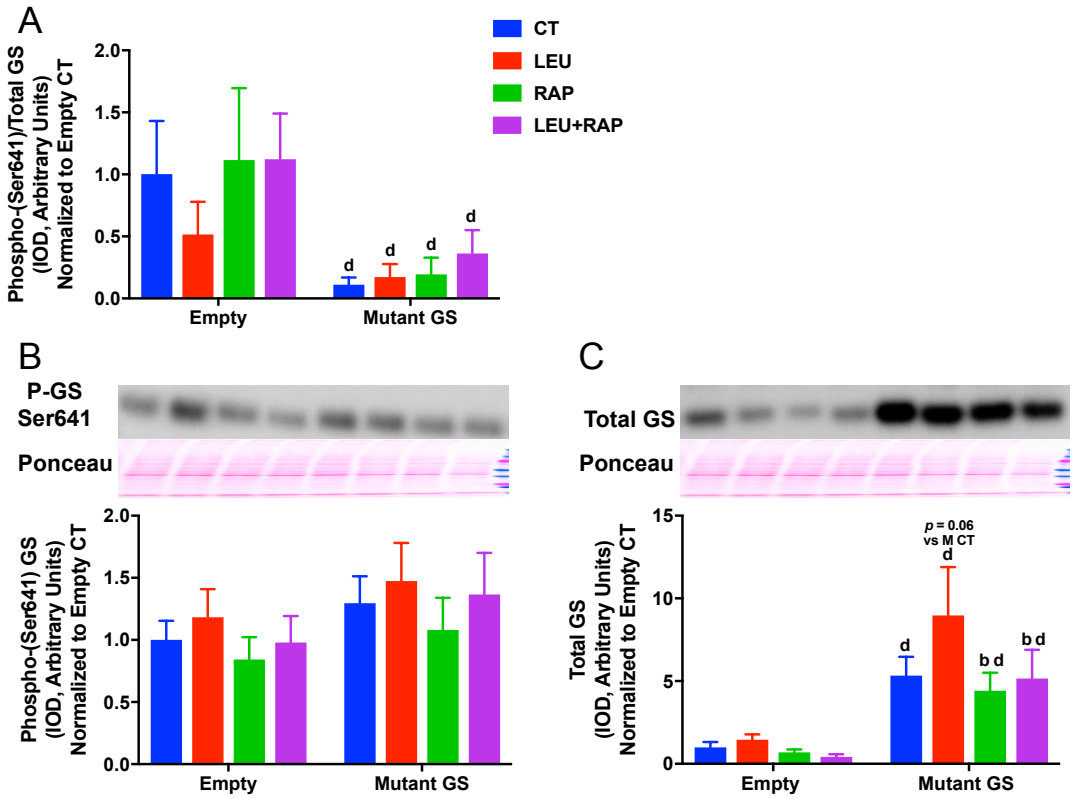

Figure 3.5.1 Glycogen Synthase in Cultured C2C12 Myotubes. A, Phospho-(Ser641)/Total Glycogen Synthase (GS); B, Phospho-(Ser641) GS; and C, Total GS expression (integrated optical density, IOD) in cultured C2C12 myotubes. At Day 4 post-differentiation, myotubes were transfected for 48 hours with plasmids containing either an empty vector (Empty) or mutated glycogen synthase vector designed to enhance glycogen content (Mutant GS). At Day 6 post-differentiation, myotubes were serum-starved for 4 hours, prior to an amino acid starvation for 1 hour. Myotubes were then treated with either a treatment control (CT), 10 mM leucine (LEU), 100 nM rapamycin (RAP), or leucine/rapamycin co-treatment (LEU+RAP) for 30 minutes. All treatments contained 100 µM puromycin. All values were normalized to Empty CT. a: significantly ($p \leq 0.05$) different than CT group within same plasmid condition; b: significantly different than LEU group within same plasmid condition; c: significantly different than RAP group within same plasmid condition; d: significant main effect of Mutant GS vector vs. Empty vector.

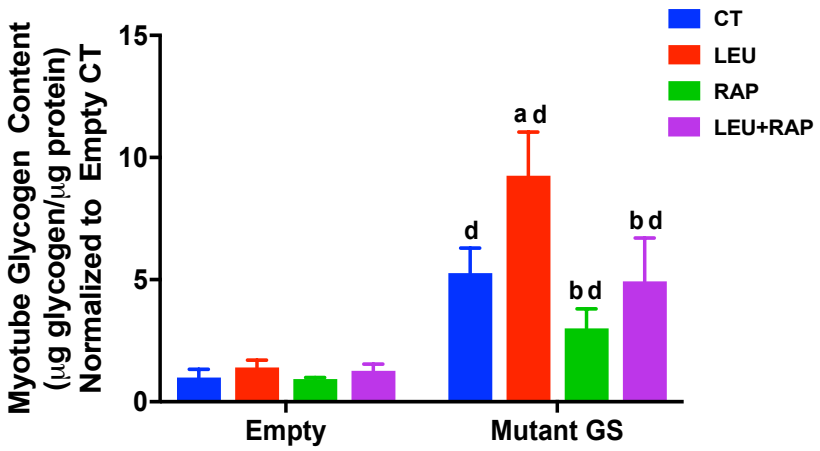

Figure 3.5.2 Glycogen Content in Cultured C2C12 Myotubes. Glycogen content normalized to total protein content cultured C2C12 myotubes. At Day 4 post-differentiation, myotubes were transfected for 48 hours with plasmids containing either an empty vector (Empty) or mutated glycogen synthase vector designed to enhance glycogen content (Mutant GS). At Day 6 post-differentiation, myotubes were serum-starved for 4 hours, prior to an amino acid starvation for 1 hour. Myotubes were then treated with either a treatment control (CT), 10 mM leucine (LEU), 100 nM rapamycin (RAP), or leucine/rapamycin co-treatment (LEU+RAP) for 30 minutes. All treatments contained 100 μM puromycin. All values were normalized to Empty CT. a: significantly ($p \leq 0.05$) different than CT group within same plasmid condition; b: significantly different than LEU group within same plasmid condition; c: significantly different than RAP group within same plasmid condition; d: significant main effect of Mutant GS vector vs. Empty vector.

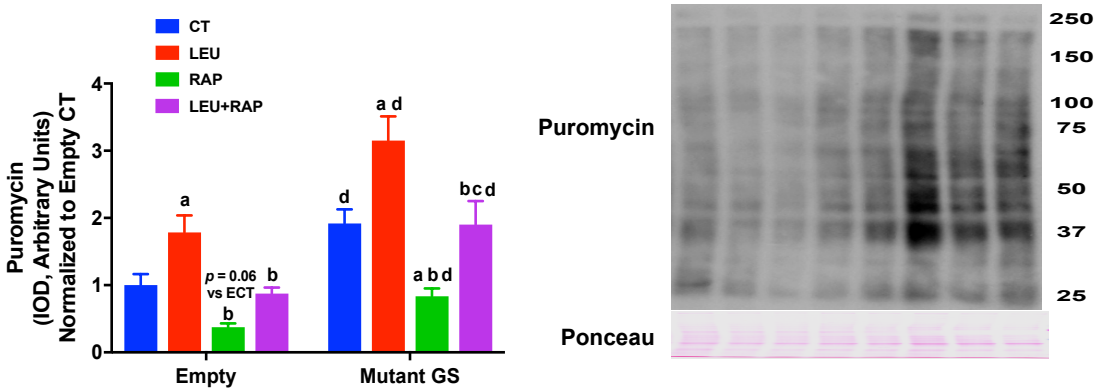

Figure 3.5.3. Muscle Protein Synthesis Rate (Puromycin) in Cultured C2C12 Myotubes. Total puromycin (integrated optical density, IOD) expression in cultured C2C12 myotubes. At Day 4 post-differentiation, myotubes were transfected for 48 hours with plasmids containing either an empty vector (Empty) or mutated glycogen synthase vector designed to enhance glycogen content (Mutant GS). At Day 6 post-differentiation, myotubes were serum-starved for 4 hours, prior to an amino acid starvation for 1 hour. Myotubes were then treated with either a treatment control (CT), 10 mM leucine (LEU), 100 nM rapamycin (RAP), or leucine/rapamycin co-treatment (LEU+RAP) for 30 minutes. All treatments contained 100 µM puromycin. All values were normalized to Empty CT. a: significantly ($p \leq 0.05$) different than CT group within same plasmid condition; b: significantly different than LEU group within same plasmid condition; c: significantly different than RAP group within same plasmid condition; d: significant main effect of Mutant GS vector vs. Empty vector.

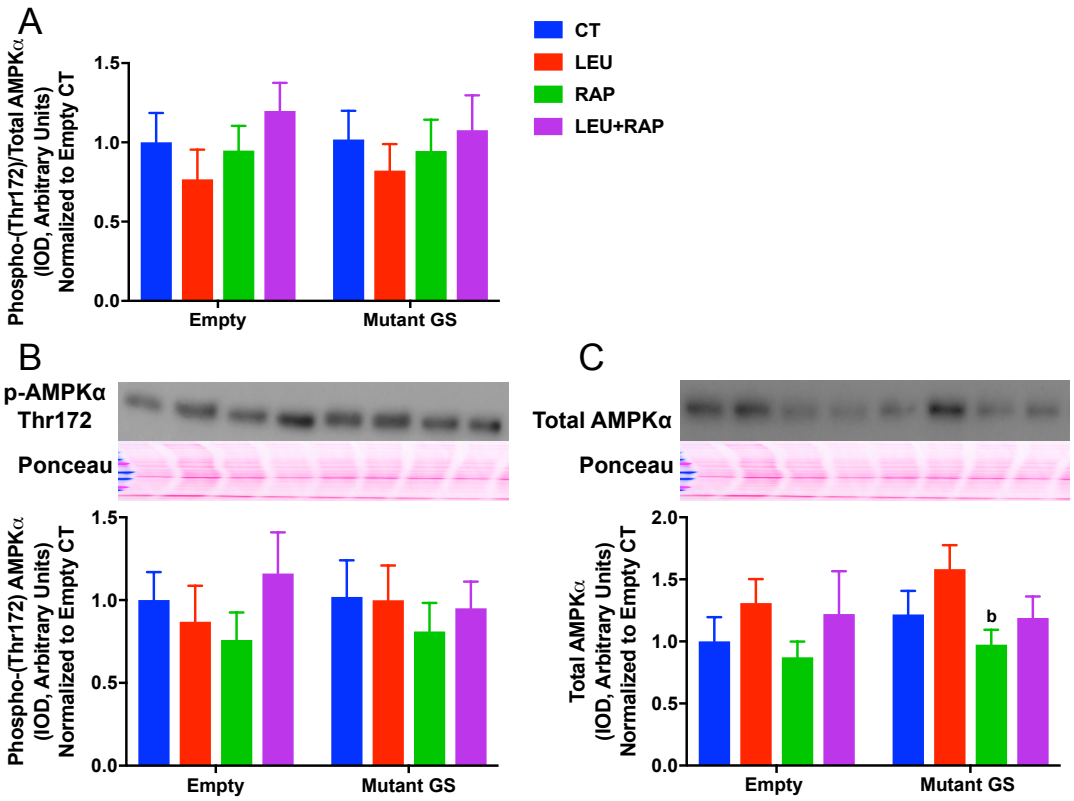

Figure 3.5.4 AMPK in Cultured C2C12 Myotubes. A, Phospho-(Thr172)/Total 5'-AMP-Activated Protein Kinase (AMPK) α; B, Phospho-(Thr172) AMPKα; C, Total AMPKα expression (integrated optical density, IOD) in cultured C2C12 myotubes. At Day 4 post-differentiation, myotubes were transfected for 48 hours with plasmids containing either an empty vector (Empty) or mutated glycogen synthase vector designed to enhance glycogen content (Mutant GS). At Day 6 post-differentiation, myotubes were serum-starved for 4 hours, prior to an amino acid starvation for 1 hour. Myotubes were then treated with either a treatment control (CT), 10 mM leucine (LEU), 100 nM rapamycin (RAP), or leucine/rapamycin co-treatment (LEU+RAP) for 30 minutes. All treatments contained 100 μM puromycin. All values were normalized to Empty CT. b: significantly ($p \leq 0.05$) different than LEU group within same plasmid condition.

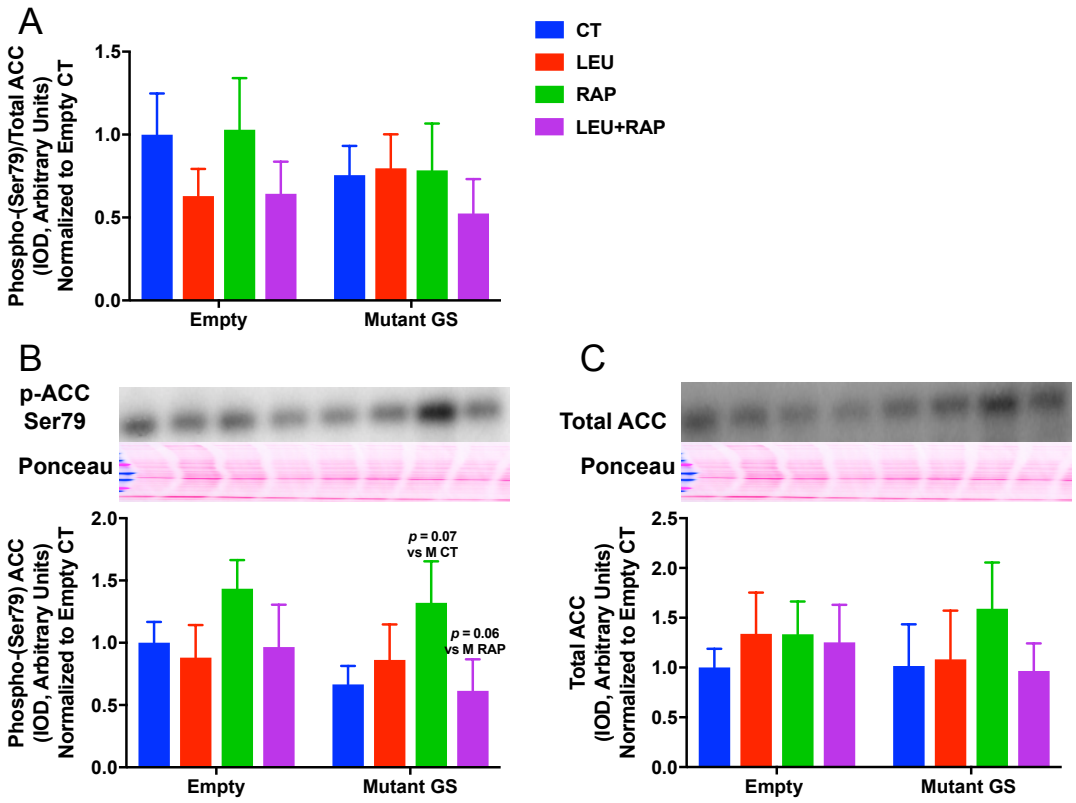

Figure 3.5.5 ACC in Cultured C2C12 Myotubes. A, Phospho-(Ser79)/Total Acetyl-CoA Carboxylase (ACC); B, Phospho-(Ser79) ACC; C, Total ACC expression (integrated optical density, IOD) in cultured C2C12 myotubes. At Day 4 post-differentiation, myotubes were transfected for 48 hours with plasmids containing either an empty vector (Empty) or mutated glycogen synthase vector designed to enhance glycogen content (Mutant GS). At Day 6 post-differentiation, myotubes were serum-starved for 4 hours, prior to an amino acid starvation for 1 hour. Myotubes were then treated with either a treatment control (CT), 10 mM leucine (LEU), 100 nM rapamycin (RAP), or leucine/rapamycin co-treatment (LEU+RAP) for 30 minutes. All treatments contained 100 µM puromycin. All values were normalized to Empty CT.

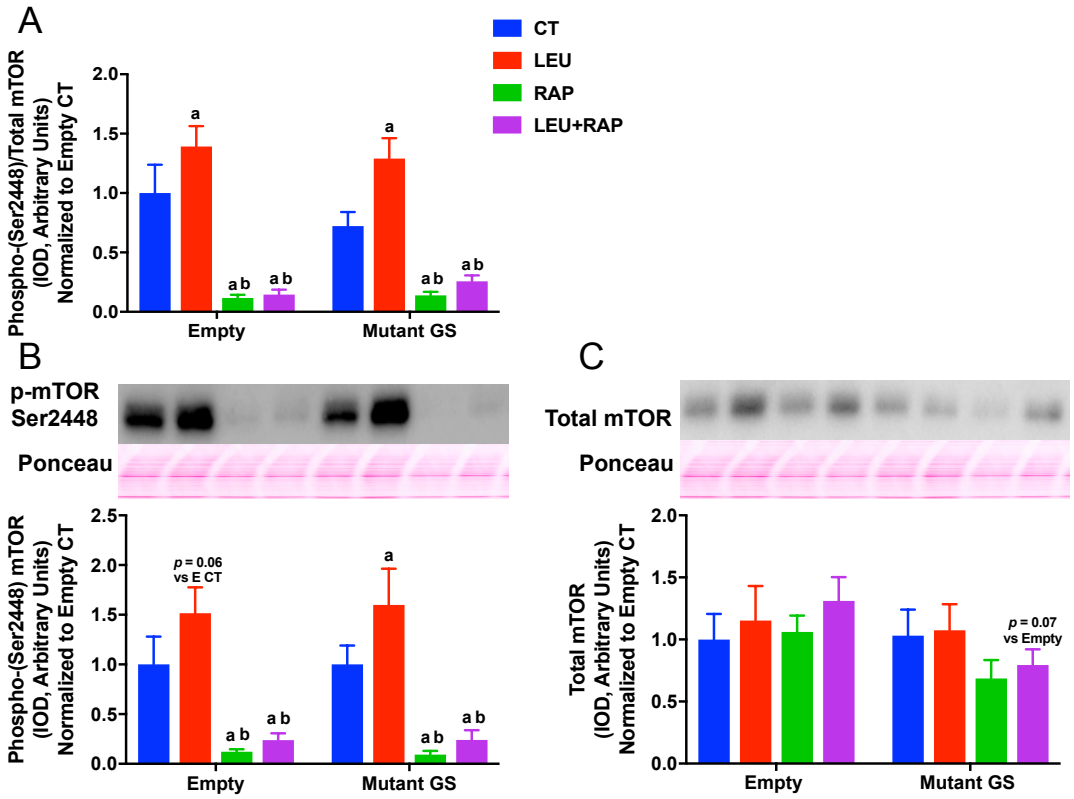

Figure 3.5.6 mTOR in Cultured C2C12 Myotubes. A, Phospho-(Ser2448)/Total mechanistic target of rapamycin (mTOR); B, Phospho-(Ser2448) mTOR; C, Total mTOR expression (integrated optical density, IOD) in cultured C2C12 myotubes. At Day 4 post-differentiation, myotubes were transfected for 48 hours with plasmids containing either an empty vector (Empty) or mutated glycogen synthase vector designed to enhance glycogen content (Mutant GS). At Day 6 post-differentiation, myotubes were serum-starved for 4 hours, prior to an amino acid starvation for 1 hour. Myotubes were then treated with either a treatment control (CT), 10 mM leucine (LEU), 100 nM rapamycin (RAP), or leucine/rapamycin co-treatment (LEU+RAP) for 30 minutes. All treatments contained 100 µM puromycin. All values were normalized to Empty CT. a: significantly ($p \leq 0.05$) different than CT group within same plasmid condition; b: significantly different than LEU group within same plasmid condition.

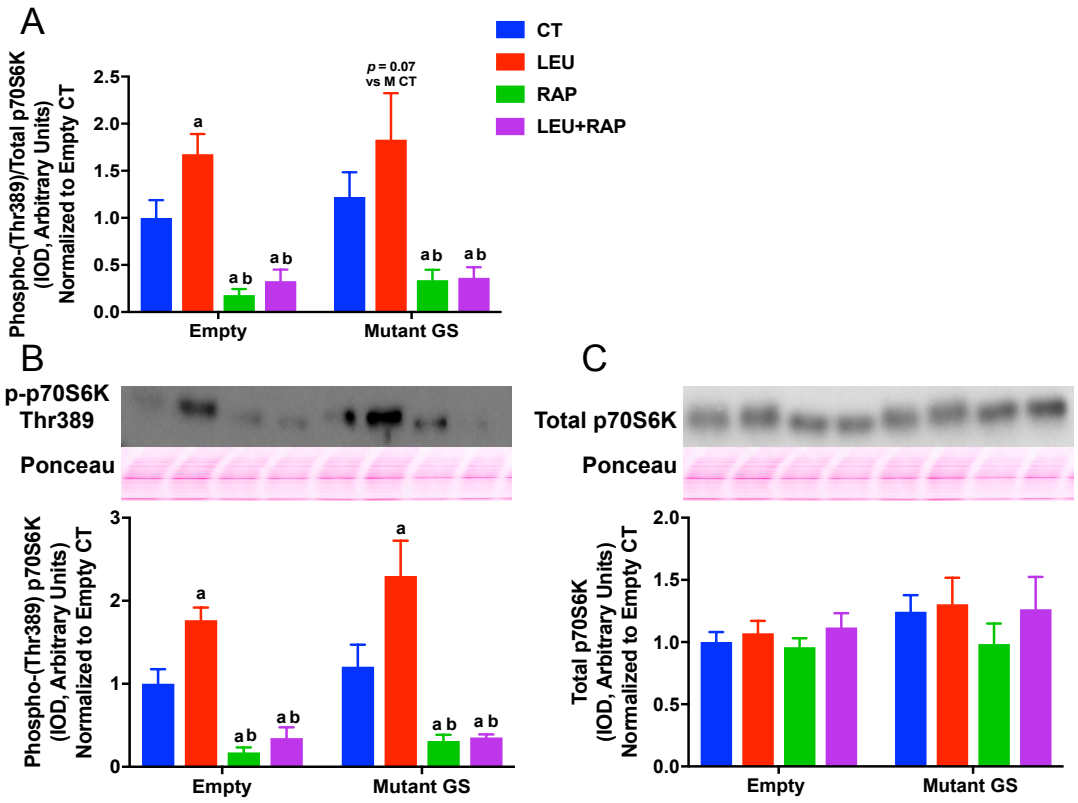

Figure 3.5.7 p70S6K in Cultured C2C12 Myotubes. A, Phospho-(Thr389)/Total 70 kDa ribosomal protein S6 kinase (p70S6K); B, Phospho-(Thr389) p70S6K; C, Total p70S6K expression (integrated optical density, IOD) in cultured C2C12 myotubes. At Day 4 post-differentiation, myotubes were transfected for 48 hours with plasmids containing either an empty vector (Empty) or mutated glycogen synthase vector designed to enhance glycogen content (Mutant GS). At Day 6 post-differentiation, myotubes were serum-starved for 4 hours, prior to an amino acid starvation for 1 hour. Myotubes were then treated with either a treatment control (CT), 10 mM leucine (LEU), 100 nM rapamycin (RAP), or leucine/rapamycin co-treatment (LEU+RAP) for 30 minutes. All treatments contained 100 µM puromycin. All values were normalized to Empty CT. a: significantly ($p \leq 0.05$) different than CT group within same plasmid condition; b: significantly different than LEU group within same plasmid condition.

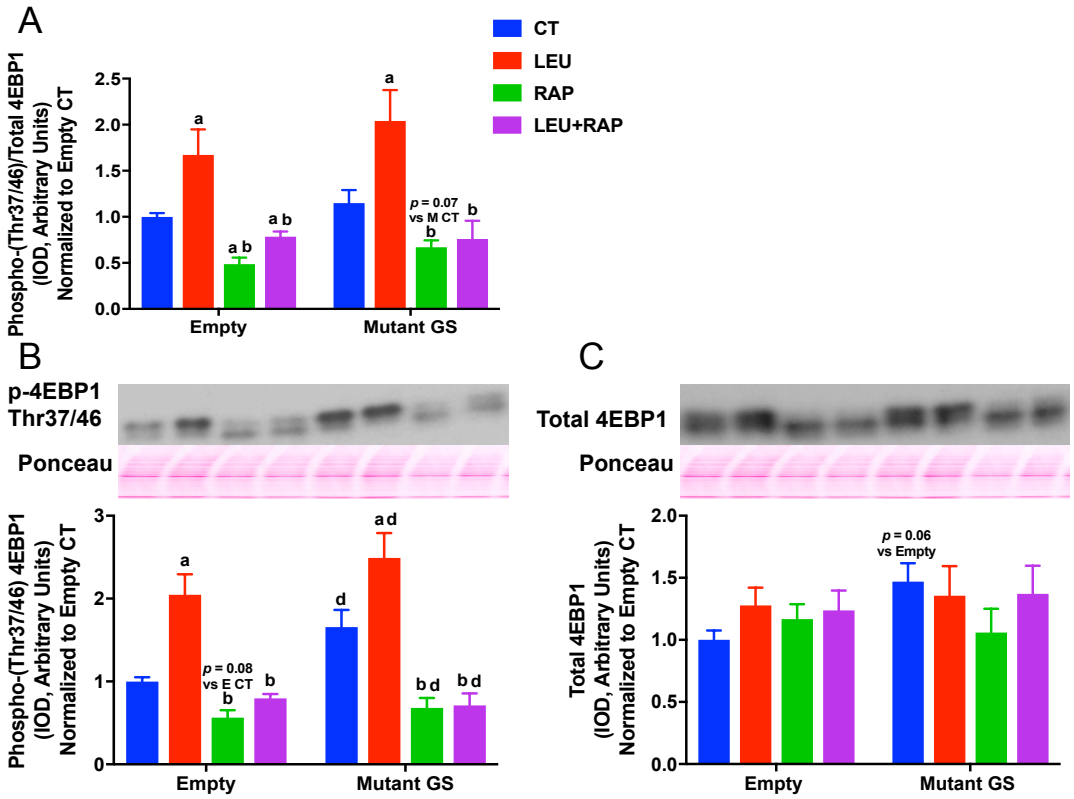

Figure 3.5.8 4EBP1 in Cultured C2C12 Myotubes. A, Phospho-(Thr37/46)/Total eukaryotic initiation factor 4E binding protein (4EBP1); B, Phospho-(Thr37/46) 4EBP1; C, Total 4EBP1 expression (integrated optical density, IOD) in cultured C2C12 myotubes. At Day 4 post-differentiation, myotubes were transfected for 48 hours with plasmids containing either an empty vector (Empty) or mutated glycogen synthase vector designed to enhance glycogen content (Mutant GS). At Day 6 post-differentiation, myotubes were serum-starved for 4 hours, prior to an amino acid starvation for 1 hour. Myotubes were then treated with either a treatment control (CT), 10 mM leucine (LEU), 100 nM rapamycin (RAP), or leucine/rapamycin co-treatment (LEU+RAP) for 30 minutes. All treatments contained 100 μM puromycin. All values were normalized to Empty CT. a: significantly ($p \leq 0.05$) different than CT group within same plasmid condition; b: significantly different than LEU group within same plasmid condition; d: significant main effect of Mutant GS vector vs. Empty vector.

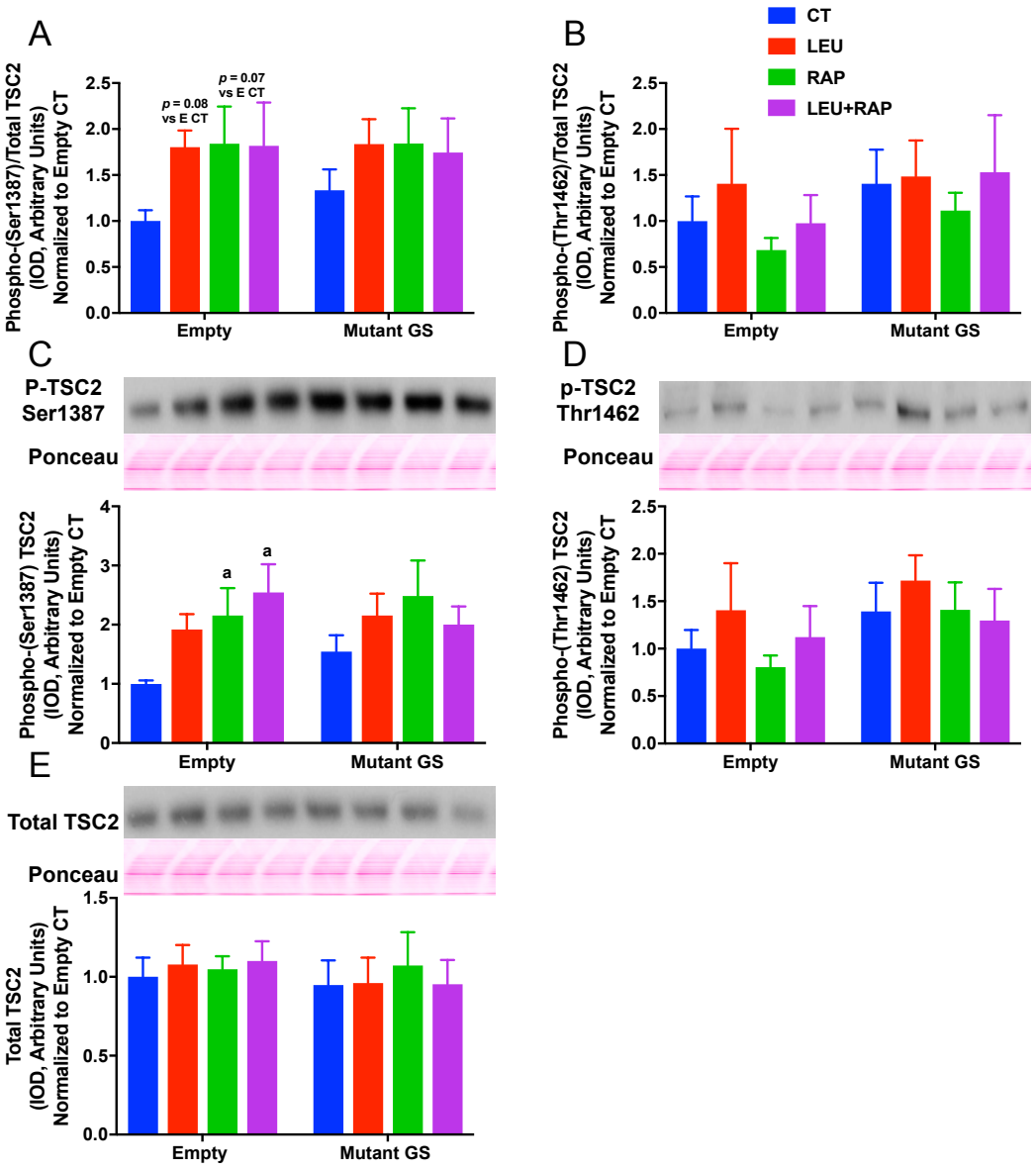

Figure 3.5.9 TSC2 in Cultured C2C12 Myotubes. A, Phospho-(Ser1387)/Total tuberous sclerosis complex 2 (TSC2); B, Phospho-(Thr1462)/Total TSC2; C, Phospho-(Ser1387) TSC2; D, Phospho-(Thr1462) TSC2; E, Total TSC2 expression (integrated optical density, IOD) in cultured C2C12 myotubes. At Day 4 post-differentiation, myotubes were transfected for 48 hours with plasmids containing either an empty vector (Empty) or mutated glycogen synthase vector designed to enhance glycogen content (Mutant GS). At Day 6 post-differentiation, myotubes were serum-starved for 4 hours, prior to an amino acid starvation for 1 hour. Myotubes were then treated with either a treatment control (CT), 10 mM leucine (LEU), 100 nM rapamycin (RAP), or leucine/rapamycin co-treatment (LEU+RAP) for 30 minutes. All treatments contained 100 µM puromycin. All values were normalized to Empty CT. a: significantly ($p \leq 0.05$) different than CT group within same plasmid condition.

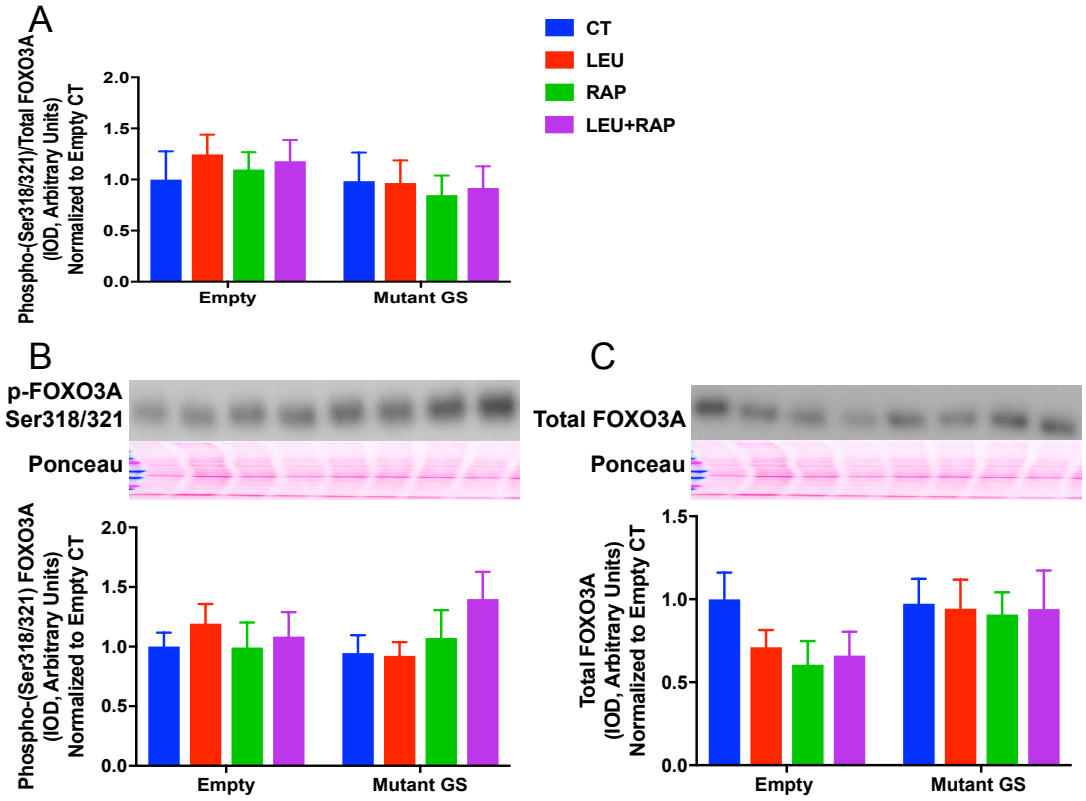

Figure 3.5.10 FOXO3A in Cultured C2C12 Myotubes. A, Phospho-(Ser318/321)/Total Forkhead box Transcription Factor 3A (FOXO3A); B, Phospho-(Ser318/321) FOXO3A; C, Total FOXO3A expression (integrated optical density, IOD) in cultured C2C12 myotubes. At Day 4 post-differentiation, myotubes were transfected for 48 hours with plasmids containing either an empty vector (Empty) or mutated glycogen synthase vector designed to enhance glycogen content (Mutant GS). At Day 6 post-differentiation, myotubes were serum-starved for 4 hours, prior to an amino acid starvation for 1 hour. Myotubes were then treated with either a treatment control (CT), 10 mM leucine (LEU), 100 nM rapamycin (RAP), or leucine/rapamycin co-treatment (LEU+RAP) for 30 minutes. All treatments contained 100 µM puromycin. All values were normalized to Empty CT.

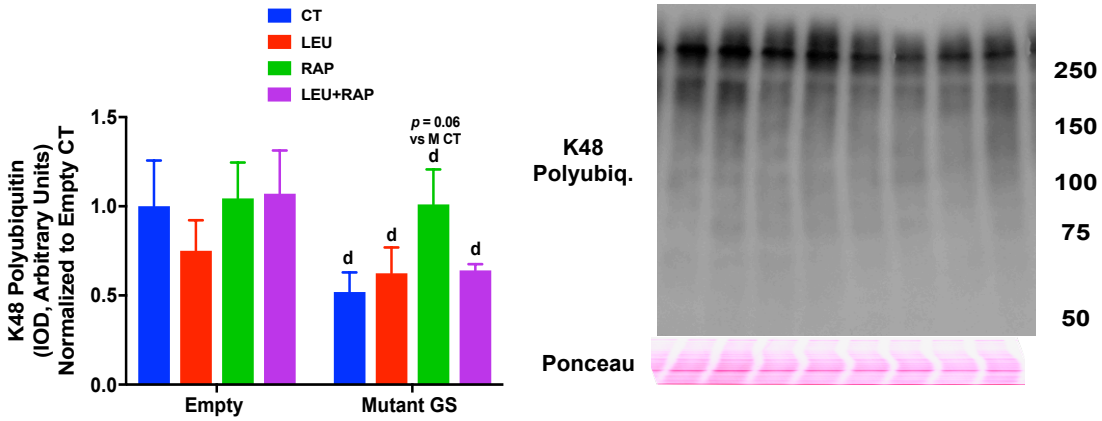

Figure 3.5.11 K48 Polyubiquitin in Cultured C2C12 Myotubes. Total Lysine -48 (K48) tagged polyubiquitin expression (integrated optical density, IOD) in cultured C2C12 myotubes. At Day 4 post-differentiation, myotubes were transfected for 48 hours with plasmids containing either an empty vector (Empty) or mutated glycogen synthase vector designed to enhance glycogen content (Mutant GS). At Day 6 post-differentiation, myotubes were serum-starved for 4 hours, prior to an amino acid starvation for 1 hour. Myotubes were then treated with either a treatment control (CT), 10 mM leucine (LEU), 100 nM rapamycin (RAP), or leucine/rapamycin co-treatment (LEU+RAP) for 30 minutes. All treatments contained 100 µM puromycin. All values were normalized to Empty CT. d: significant ($p \leq 0.05$) main effect of Mutant GS vector vs. Empty vector.

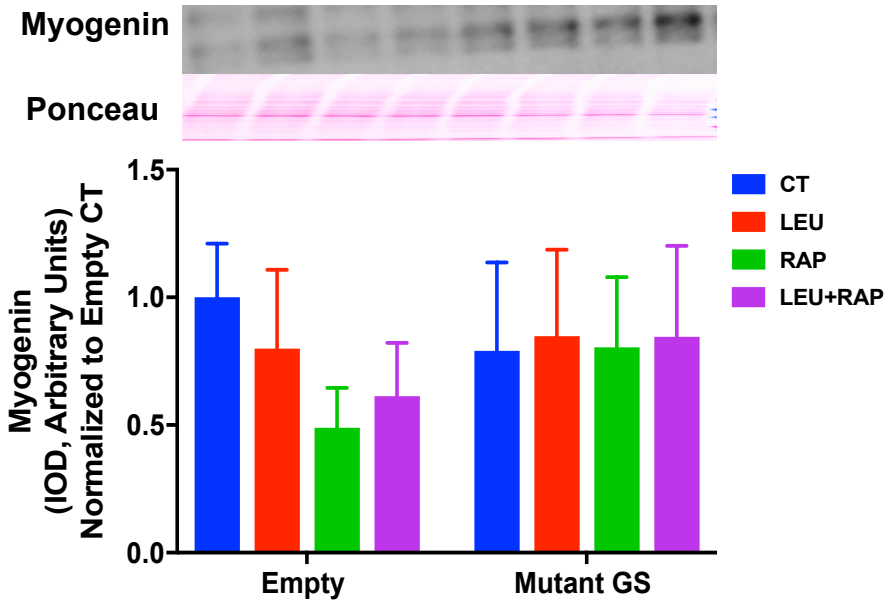

Figure 3.5.12 Myogenin in Cultured C2C12 Myotubes. Total Myogenin expression (integrated optical density, IOD) in cultured C2C12 myotubes. At Day 4 post-differentiation, myotubes were transfected for 48 hours with plasmids containing either an empty vector (Empty) or mutated glycogen synthase vector designed to enhance glycogen content (Mutant GS). At Day 6 post-differentiation, myotubes were serum-starved for 4 hours, prior to an amino acid starvation for 1 hour. Myotubes were then treated with either a treatment control (CT), 10 mM leucine (LEU), 100 nM rapamycin (RAP), or leucine/rapamycin co-treatment (LEU+RAP) for 30 minutes. All treatments contained 100 µM puromycin. All values were normalized to Empty CT.

CHAPTER 4: DISSERTATION SUMMARY

Aging is associated with a progressive loss of skeletal muscle mass and function (sarcopenia), particularly in fast-twitch (i.e., type II) skeletal muscle fibers, and leads to an inability to perform activities of daily living, reduction in overall quality of life, and significantly increases the risk for all-cause mortality (94). Additionally, in response to anabolic stimuli (i.e., RE, amino acids, growth factors, etc.) aged muscle has a blunted ability to hypertrophy (42, 65). This diminished ability to maintain or increase muscle fiber size/mass occurs both in aged humans (65, 107) and in rats (11, 42). Importantly, the Gordon laboratory found that an enzyme within skeletal muscle fibers called AMPK plays a major role in the suppression of acute (31, 126) and chronic MPS/anabolic signaling (42, 128, 129) and thus, impaired growth in aged muscle (42, 128, 129). Therefore, any mechanism than can inhibit AMPK in aged skeletal muscle, may be able to rescue MPS and growth. One such mechanism is glycogen. Glycogen content has been found to be diminished in aged skeletal muscle at rest in both rats (7, 17, 23, 47) and humans (17, 82), although not consistently (53, 83, 85, 103, 108). Moreover, the contraction-induced depletion of glycogen is significantly greater in aged muscle (17, 53, 126) and there is a blunted ability to increase glycogen levels with training vs. young adult muscle in both rats (17, 53, 126) and humans (17, 82).

We postulated that the low muscle glycogen content in aged muscle is an important factor contributing to the upregulation of AMPK activity and catabolic

signaling/MPB and suppression of anabolic signaling/MPS and growth. However, the link(s) between glycogen content, MPS, MPB, growth, and associated signaling following chronic overload in aged skeletal muscle had not been examined. We further postulated that skeletal muscle glycogen content enhances anabolic signaling/MPS and suppresses catabolic signaling/MPB in response to leucine through AMPK in an mTORC1 manner; however, the effects of glycogen enhancement on anabolic stimuli, such as amino acids, had also never been tested in skeletal muscle. We performed a series of experiments to test whether enhancing intramuscular glycogen content via the introduction of plasmid DNA expressing active glycogen synthase in aged rat skeletal muscle or cultured C2C12 myotubes would suppress AMPK activity, enhance anabolic signaling/MPS, suppress catabolic signaling/MPB, and enhance *in vivo* growth in response to chronic overload *in vivo* and leucine treatment *in vitro*.

The main findings from these experiments (summarized in Table 4.1) were that glycogen enhancement in aged skeletal muscle *in vivo* augmented overload-induced growth compared to aged skeletal muscle without glycogen manipulation (Chapter 2). Associated with this effect was an increase in MPS, an effect that was also confirmed with intracellular glycogen enhancement in cultured myotubes (Chapter 3). However, these increases occurred mostly independent of changes in AMPK signaling, and other signaling intermediates affecting MPS were also largely unaltered with glycogen enhancement. In contrast, glycogen enhancement may suppress factors regulating MPB during overload in aged skeletal muscle and in cultured myotubes, even though all MPB markers measured did not support this finding. The discrepancies between *in vivo* and *in vitro* MPB markers affected may have been due to an absence of a loading stimulus in the

cultured C2C12 myotubes. Hence, more work is needed utilizing a loading stimulus (i.e., stretch or electrical stimulation) with glycogen enhancement in cultured myotubes. Further, we found glycogen enhancement augments basal and leucine-stimulated MPS in cultured C2C12 myotubes (Chapter 3). Although the effect of leucine treatment on MPS was mTOR-dependent regardless of plasmid condition, glycogen enhancement augmented MPS independent of changes in AMPK or mTOR signaling in cultured myotubes.

Further exploration of the effects of glycogen enhancement in aged skeletal muscle *in vivo* led us to discover increases in markers of myogenesis and regeneration in response to overload. Even though muscle fiber cross-sectional area was not measured in the current work, the augmented overload-induced increase with glycogen enhancement in muscle growth that was accompanied by increases in total fiber number and may provide some insight into the degree of the growth response. While others have reported increases with synergistic ablation alone (89), to our knowledge, this is first time de novo fiber formation has been reported in aged muscle in response to overload and electroporation. It is believed that with the synergistic ablation model hyperplasia occurs as muscle fibers become too large for oxygen diffusion and therefore the fibers split to form new fibers as a protective adaptation (89). In support of the increases in total fiber number with glycogen enhancement in old muscle, there were concomitant increases in MRFs, MyoD and myogenin, and eMyHC expression. The increase in MRF expression with aging is in agreement with others (3, 76, 108), however, this is the first time MRF increases have been reported in aged muscle with glycogen enhancement. The increases in de novo fiber formation may be due to greater energy availability, in the form of

enhanced glycogen content (2, 44, 109), throughout the 21-day overload protocol in addition to the potential regenerative response caused by the overload model with electroporation procedure.

A common finding with activities that cause muscle damage (e.g., eccentric contractions) is reductions in the amount of glycogen content, and this is seen in both rodents (52, 59, 131) and humans (22, 97, 137). The reductions in glycogen content are linked to declines in contractile performance of the damaged muscle (19, 105). While some studies have linked these declines to disruptions in the structural components of muscle (19, 105), others have reported metabolic factors being involved (22, 52, 59, 97, 131, 137). Interestingly, in response to damaging eccentric contractions there is an inability to replenish glycogen content in humans (97, 137) as well as diminished glycogen content and ATP production in rats (52, 59, 131). In the current investigation when glycogen content was enhanced in aged muscle, in potentially a damaging stimulus (i.e., overload with electroporation), there was a greater regenerative response. Although it was not an overall goal of this investigation, it would be interesting for future work to test the effects of glycogen enhancement in a bona fide model of muscle injury, such as damaging eccentric contractions, to see if there is an enhancement in regeneration/myogenesis in aged or young muscle. While we did not observe enhanced markers of myogenesis with glycogen enhancement *in vitro*, this was likely due to the fact that we transfected (and thus enhanced intracellular glycogen) in myotubes that were already fully differentiated. Given that myogenesis was stimulated by enhanced glycogen levels in aged muscle with overload *in vivo*, future experiments elucidating the effects of glycogen enhancement at the onset of differentiation or during more

proliferative stages of myogenesis *in vitro* will be important to delineate this phenomenon.

Although we found strong and significant effects of augmented MPS (*in vivo* and *in vitro*), growth (*in vivo*), and myogenesis markers (*in vivo*) with glycogen enhancement in skeletal muscle, the assessed signaling intermediates regulating MPS and AMPK activity were largely unaltered. There are a number of possible alternative mechanisms or limitations that may explain these findings. For instance, other signaling pathways or markers that were not assessed may have been altered. We hypothesized that enhancing glycogen content in skeletal muscle either *in vivo* or *in vitro* would suppress AMPK signaling, and thus restore MPS signaling intermediates, leading to the enhanced MPS and *in vivo* growth. While we measured upstream and downstream signaling related to Akt, TSC2, mTOR, AMPK signaling, we were unable to detect robust differences in these pathways with glycogen enhancement follow 21 days of chronic overload *in vivo* or with acute transfection *in vitro*. Although we assessed very well established markers regulating MPS translational signaling (30, 54, 119), there are numerous other potential pathways that could have been affected.

A number of alternative mechanisms could relate to the fact that overload and/or leucine treatment can be influenced by Insulin/Insulin-like Growth Factor 1 (IGF-1)-related signaling, G-Protein Coupled Receptor (GPCR)-mediated signaling, Mitogen Activated Protein Kinase (MAPK)-signaling, TGFβ superfamily-related signaling (namely myostatin and activin), Glucocorticoid-mediated signaling, transcriptional coactivator peroxisome proliferator-activated receptor-γ coactivator-1α (PGC-1α)-related signaling, nuclear factor kappa B (NF-kB)-related signaling, as well as many others (30,

41, 54, 62). Moreover, many of these pathways have been found to affect aged skeletal muscle (111, 116). Also, several aforementioned pathways are associated with glycogen metabolism (64, 102). For instance, the amount of glycogen in muscle is known to influence PGC-1α-related signaling and can affect mitochondrial biogenesis (64, 102), which is considered a major factor affecting aged skeletal muscle's ability to maintain protein turnover (91). Additionally, myostatin, a negative regulator of muscle growth, has been found to affect glycogen storage and glucose uptake in skeletal muscle (20). Myostatin expression increases in differing states of muscles atrophy (111, 112, 136) and downstream signaling of myostatin is suggested to contribute to sarcopenia (111). Insulin/IGF-1-related signaling is also implicated in glycogen metabolism (58, 64, 132) and is influenced by leucine (26, 36) and aging muscle (111, 116). Moreover, high glucocorticoid expression in skeletal muscle influences glycogenolysis and insulin-stimulated glycogen synthesis (67). High glucocorticoid expression is also connected to upregulation of MuRF1 and MAFbx leading to MPB and thus muscle atrophy (30). Lastly, many of the aforementioned pathways can also interact with one another (30, 36, 58, 62, 64, 102, 118), further adding to the complexity of glycogen metabolism and skeletal muscle plasticity.

There are numerous other factors involved with aging of all physiological systems, not just the muscular system (71). The nine common factors affecting aging have been named the "hallmarks of aging" and include genomic instability, telomere attrition, epigenetic alterations, loss of proteostasis, deregulated nutrient sensing, mitochondrial dysfunction, cellular senescence, stem cell exhaustion, and altered intracellular communication (71). While the current work investigated some aspects of

these hallmarks of aging, such as loss of proteostasis, deregulated nutrient sensing, and altered intracellular communication, there are numerous others that could have been influenced by glycogen enhancement. Additionally, there are other factors known to affect skeletal muscle that also fall under one of the nine hallmarks. For example, there are reductions in sex hormones (testosterone and estradiol) with age (68, 124) and these reductions contribute to processes involved with sarcopenia (68) and can influence many of the hallmarks of aging (95). Testosterone and estradiol levels can also impact glycogen metabolism in muscle (106, 130). Aged skeletal muscle also displays high levels of factors responsible for chronic inflammation (e.g., cytokines) and oxidative damage [e.g. reactive oxygen and nitrogen species (56, 81)] that contribute to sarcopenia (25, 94) and effect different hallmarks of aging (95). Additionally, circulating cytokines (46, 96) and reactive oxygen species (60) have been found to influence glycogen metabolism. Collectively, even though we largely found no affect of glycogen enhancement on MPS and AMPK related signaling intermediates assessed in aged skeletal muscle under conditions of overload and cultured C2C12 myotubes with leucine treatment, the potential signaling pathways or factors that could be affected are vast. Clearly, more work is needed to further examine the above-mentioned factors with regards to glycogen enhancement.

Our hypothesis that glycogen enhancement would inhibit AMPK activity was based on previous findings *in vivo* (123) and *in vitro* (138) that found glycogen interacting with AMPK, which is thought to work through its GBD within the β subunit (77, 78). However, the AMPKβ-glycogen interaction has been challenged (98, 122, 140). Using a proteomics approach, Stapleton and colleagues (122) first found that highly

purified glycogen had no interaction with AMPK *in vivo*. This group then discovered a novel phosphorylation site at Thr148 on the AMPK β subunit that regulates glycogen binding (98). Thr148 is found in the GBD of the β subunit and was found to autophosphorylate itself and this led to an inability of AMPK to interact with glycogen *in vitro* (98). Also, this inhibitory autophosphorylation at Thr148 on the β subunit was found to occur independent of changes in phosphorylation at Thr172 on the catalytic α subunit (98). Lastly, this group (140) found in skinned rat skeletal muscle fibers, that β_2-AMPK was not associated with glycogen and that activation of AMPK at Thr172 via stimulation did not dephosphorylate Thr148 on the β subunit. The authors concluded that any regulation of AMPK via glycogen most likely occurs in an indirect way through other glycogen associated proteins (140, 141). As we did not measure Thr148 on the β subunit in the current work we cannot determine if the AMPKβ-glycogen was affected at this site and if this could explain our largely unaffected AMPK signaling. Additionally, as there are numerous other glycogen associated proteins (109, 141) that could potentially mediate the glycogen-AMPK interaction more work is needed in this regard.

Another aspect that was not explored in the current investigation is the emerging role of AMPK structure, specifically the heterotrimer composition, in skeletal muscle plasticity (88). In mammals, AMPK exists as an obligatory 3-subunit heterotrimer containing 7 isoforms that are encoded by separate genes, enabling the formation of a diverse collection of the αβγ heterotrimer (88). In human fast-twitch skeletal muscle, only three heterotrimer complexes have been found: (in order of most to least abundant) $\alpha_2\beta_2\gamma_1$, $\alpha_2\beta_2\gamma_3$, and $\alpha_1\beta_2\gamma_1$ (9, 88). Whereas, in rodent fast-twitch skeletal muscle, up to 5 heterotrimer complexes have been found: (again, in order of most to least abundant)

$\alpha_2\beta_2\gamma_1$, $\alpha_2\beta_2\gamma_3$, $\alpha_1\beta_1\gamma_1$, $\alpha_2\beta_1\gamma_1$, and $\alpha_1\beta_1\gamma_1$ (88). While there is still much to be discovered about AMPK heterotrimer composition in various physiological states in skeletal muscle, Hardman et al. (51) found that there was age-related differences in expression of heterotrimer subunits in young adult vs. old rat fast-twitch muscle. The same study also found age-related differences in specific subunits that associated with (using immunoprecipitation) AMPK α_1 or α_2, as well as differences in AMPK α_1 or α_2 activity with age in response to endurance type *ex vivo* stimulation (51). Specifically, there was depressed AMPK α_2 activity and enhanced AMPK α_1 in old vs. young adult muscle following stimulation (51). The authors postulated that the enhanced AMPK α_1 activity in old fast-twitch skeletal muscle may underlie the depressed MPS seen through mTORC1, contributing to sarcopenia (51). In support of this notion, Mounier and colleagues (86, 87) found that AMPK α_1, but not α_2, inhibited MPS through mTORC1 both *in vitro* (87) and *in vivo* (86). In addition, Baar and colleagues (79) found that overload-induced hypertrophy was regulated by AMPK α_1, but not α_2. The authors of this study therefore postulated that AMPK α_1 regulates growth, and AMPK α_2 is necessary for metabolic adaptations (79). As the current investigation measured overall AMPK α phosphorylation at Thr172 (i.e., not separating out α_1 vs. α_2), any differences between the two with glycogen enhancement could not be delineated either *in vivo* or *in vitro*. Also, Hardman et al. (51) found that the overall AMPK α phosphorylation at Thr172 reflected AMPK α_2 activity and not α_1 in both young and old rat muscle after stimulation, which they postulated to be due AMPK α_2 being the predominant isoform in skeletal muscle. Therefore, any differences that could have occurred in AMPK α_1 activity with glycogen enhancement could have been washed out by AMPK α_2 changes

due to the measurement of overall AMPK α phosphorylation at Thr172. Future work should determine if glycogen enhancement differentially affects AMPK α_1 and α_2 activity, as well as heterotrimer composition.

A limitation of our *in vivo* experimental design was that we measured the effects of glycogen enhancement in aged muscle after 21 days of overload. Although MPS and growth were different at that timepoint, potential AMPK or MPS signaling differences may have normalized by this timepoint. An overload period of 21 days was chosen based on pilot work from our laboratory (Figure 1.8 and 1.9) as well as the reported reductions in the inflammatory response associated with this procedure by ~10-14 days (1, 4). Our findings that there were largely NSD with overload in young adult vs. old rat muscle in mTORC1 signaling intermediates support previous literature after 28 days of overload (18). In fact, recent work using the synergistic ablation model of muscle growth in rats (48) found that AMPK and MPS signaling changes occur within the first 3-9 days of overload and are largely lost by 12-21 days. The authors proposed this to be due to "molecular brakes" or negative regulators of mTORC1 being increased after 9 days with this supraphysiological model of muscle hypertrophy. Interestingly, the authors also reported that AMPK α_1 activity changes occurred within the first 3-9 days of overload and were lost by days 12-21. Therefore, although overall AMPK phosphorylation and activity (as assessed by ACC phosphorylation) were elevated at 21 days in all groups, any changes in AMPK α_1-specific activity *in vivo* in the current investigation may have been lost by day 21 of overload. However, again, as we did not delineate between AMPK α_1 and α_2 we cannot determine if differences did exist at this timepoint.

In summary, glycogen enhancement in aged skeletal muscle augmented overload-induced growth. The greater growth with glycogen enhancement was accompanied by greater MPS response in aged muscle, an effect that was further confirmed in response to enhanced intracellular glycogen content in cultured myotubes. Moreover, enhancing glycogen content augments not only basal, but leucine-stimulated MPS in cultured myotubes. Although the effect of leucine treatment on MPS is mTOR-dependent in all cultured myotubes (regardless of plasmid condition/glycogen manipulation), glycogen enhancement augments MPS *in vivo* and *in vitro* largely independent of changes in AMPK or mTOR signaling. In contrast, glycogen enhancement led to reductions in markers of MPB both *in vivo* and *in vitro*, although this effect was not seen in all markers assessed. Further, there was a strong and significant effect of enhancing glycogen content on markers of myogenesis and regeneration in aged muscle under conditions of overload *in vivo*. These findings may support the need to enhance glycogen content in aged skeletal muscle of humans to augment MPS and growth under conditions of overload (i.e., resistance exercise training). Because of the potential impact of glycogen enhancement on growth in aging muscle, more exploration is thus warranted regarding more applied methods (namely diet) to enhance glycogen in young and old muscle with or without loading. Lastly, these findings also indicate the need for further research to examine the effect(s) of glycogen enhancement in rat and human muscle in: conditions requiring regeneration or myogenesis; young muscle with or without loading; and old muscle under normal conditions (i.e., without loading).

Table 4.1 Comparison of Effects of Glycogen Enhancement In Aged Skeletal Muscle (*In Vivo*) & Cultured C2C12 Myotubes (*In Vitro*)

Marker Assessed:	21-day Chronic Overload in Aged Skeletal Muscle Main Findings (*In Vivo*)	Transfection in C2C12 Myotubes Treated with Luecine Main Findings (*In Vitro*)	**Summary of Findings from *In Vivo* and *In Vitro* Results**
Total GS & Glycogen Content	Total GS and glycogen content ↑ (vs SHAM) in OM overloaded muscle and was higher than all muscles (SHAM or OVLD) of YE and OE.	Total GS and glycogen content was higher in all mutant GS-transfected myotubes vs. empty vector regardless of treatment & w/ LEU treatment ↑ compared to CT treatment in mutant GS condition.	**Mutant GS plasmid led to increased total GS expression and glycogen content both *in vivo* and *in vitro*.**
Muscle Protein Synthesis (MPS) rate and Hypertrophy (In Vivo ONLY)	MPS rate and hypertrophy (vs SHAM) ↑ in all groups, with OM overloaded muscles being higher than OE overloaded muscles. Also, the percent change increase in OM was NSD than YE.	In both plasmid conditons, LEU treatment ↑ MPS rate vs. CT, and reduced with RAP or RAP+LEU vs. LEU. Further, MPS rate was higher in all mutant GS-trasnfected mytoubes vs. empty vector regardless of treatment.	**MPS rate (*in vivo* and *in vitro*) and hypertrophy (*in vivo* only) were augmented with glycogen enhancement.**
AMPK Signaling: Phospho Status of AMPK (Thr172), ACC (Ser79), TSC2 (Ser1387)	Phospho status of AMPK (Thr172), ACC (Ser79), and TSC2 (Ser1387) all ↑ with OVLD in all groups. AMPK and ACC were higher in old OVLD muscles vs. YE, with NSD between OE and OM.	Phospho status of AMPK (Thr172), ACC (Ser79), and TSC2 (Ser1387) were NSD regardless of plasmid or treatment conditions.	**Markers of AMPK signaling assessed were largely (except p-ACC *in vivo*) not affected with glycogen enhancement both *in vivo* and *in vitro*.**
MPS Signaling: Phospho Status of mTOR (Ser2448), p70S6K (Thr389), 4EBP1 (Thr37/46)	Phospho status of p70S6K (Thr389) was ↑ with OVLD in all groups, with NSD between groups. mTOR and 4EBP1 were NSD regardless of group or loading status.	Phospho status of mTOR (Ser2448), p70S6K (Thr389), and 4EBP1 (Thr37/46) were ↑ with LEU vs. CT, and reduced with RAP or RAP+LEU vs. LEU, with NSD between plasmid conditios.	**Markers of MPS signaling assessed were not affected with glycogen enhancement both *in vivo* and *in vitro*.**
MPB Signaling: Phospho Status of FOXO3A (Ser318/321) & Total K48-Linked Polyubiquitin)	Phospho status of FOXO3A (Ser318/321) was ↑ with OVLD in OM, with NSD between OVLD muscles vs. OE or YE. K48-linked was higher in old OVLD muscles with NSD between OE and OM.	Phospho status of FOXO3A (Ser318/321) was NSD regardless of plasmid or treatment condition. K48-linked polyubiqutin was ↓ in all mutant GS-transfected myotubes vs. empty vector.	**FOXO3A was affected *in vivo*, but not *in vitro*, whereas, K48-linked polyubiquitin was affected *in vitro*, but not *in vivo*.**
Misc. Signaling (Phospho Status of Akt (Thr308;Ser473), TSC2 (Thr1462), GSK3α/β (Ser21/9), and total PYGM.	Phospho status of Akt (Thr308;Ser473) and TSC2 (Thr1462) was ↑ with OVLD in all groups, with NSD between OE and OM. GSK3α/β (Ser21/9) was NSD between OE and OM. NSD in PYGM regardless of loading status or plasmid.	Phospho status of TSC2 (Thr1462) and total PYGM was NSD regardless of plasmid or treatment conditions.	**Akt signaling (Akt, TSC2) and glycogen metabolism (GSK3α/β, PYGM) signaling markers assessed were not affected with glycogen enhancement *in vivo* and *in vitro*.**
Myogenesis Markers: Total MyoD and Myogenin, eMyHC percentage (*In Vivo*), Total Fiber Number (*In Vivo*).	Total MyoD & myogenin, eMyHC percentage, and total fiber number (vs SHAM) in OM overloaded muscles and was ↑ vs. OE overloaded muscles	MyoD was non-existent at this time point. Myogenin was NSD regardless of plasmid or treatment condition.	**Markers of myogenesis assessed were strongly augmented by glycogen enhancement *in vivo*, with NSD *in vitro*.**

In vivo chronic overload: 21-days of functional overload (OVLD; unilateral gastrocnemius ablation) compared with sham-operated (SHAM) conditions in young adult (8 mo.) and old (32-34 mo.) FBN rats. Overload muscles received electrotransfer of plasmids containing either an empty vector (empty) or mutated glycogen synthase designed to enhance glycogen content (mutant). Young empty: 8 mo., n = 9; old empty: 32-34 mo., n = 11; old mutant: 32-34 mo., n = 13. *In vitro transfection*: At Day 4 post-differentiation, myotubes were transfected for 48 hours with plasmids containing either an empty vector (Empty) or mutated glycogen synthase vector designed to enhance glycogen content (Mutant GS). At Day 6 post-differentiation, myotubes were serum-starved for 4 hours, prior to an amino acid starvation for 1 hour. Myotubes were then treated with either a treatment control (CT), 10 mM leucine (LEU), 100 nM rapamycin (RAP), or leucine/rapamycin co-treatment (LEU+RAP) for 30 minutes. All treatments contained 100 μM puromycin.

REFERENCES

1. Adams GR, Bamman MM. Characterization and regulation of mechanical loading-induced compensatory muscle hypertrophy. *Compr Physiol*. 2012;2(4):2829-70.

2. Adeva-Andany MM, Gonzalez-Lucan M, Donapetry-Garcia C et al. Glycogen metabolism in humans. *BBA Clin*. 2016;5:85-100.

3. Alway SE, Lowe DA, Chen KD. The effects of age and hindlimb supension on the levels of expression of the myogenic regulatory factors MyoD and myogenin in rat fast and slow skeletal muscles. *Exp Physiol*. 2001;86(4):509-17.

4. Armstrong RB, Marum P, Tullson P et al. Acute hypertrophic response of skeletal muscle to removal of synergists. *J Appl Physiol Respir Environ Exerc Physiol*. 1979;46(4):835-42.

5. Atherton PJ, Smith K, Etheridge T et al. Distinct anabolic signalling responses to amino acids in C2C12 skeletal muscle cells. *Amino Acids*. 2010;38(5):1533-9.

6. Baar K, Esser K. Phosphorylation of p70(S6k) correlates with increased skeletal muscle mass following resistance exercise. *Am J Physiol*. 1999;276(1 Pt 1):C120-7.

7. Bastien C, Sanchez J. Phosphagens and glycogen content in skeletal muscle after treadmill training in young and old rats. *Eur J Appl Physiol Occup Physiol*. 1984;52(3):291-5.

8. Berger MJ, Doherty TJ. Sarcopenia: prevalence, mechanisms, and functional consequences. *Interdiscip Top Gerontol*. 2010;37:94-114.

9. Birk JB, Wojtaszewski JF. Predominant alpha2/beta2/gamma3 AMPK activation during exercise in human skeletal muscle. *J Physiol*. 2006;577(Pt 3):1021-32.

10. Blaauw B, Schiaffino S, Reggiani C. Mechanisms modulating skeletal muscle phenotype. *Compr Physiol.* 2013;3(4):1645-87.

11. Blough ER, Linderman JK. Lack of skeletal muscle hypertrophy in very aged male Fischer 344 x Brown Norway rats. *J Appl Physiol*. 2000;88(4):1265-70.

12. Bodine SC, Latres E, Baumhueter S et al. Identification of ubiquitin ligases required for skeletal muscle atrophy. *Science*. 2001;294(5547):1704-8.

13. Bolster DR, Crozier SJ, Kimball SR et al. AMP-activated protein kinase suppresses protein synthesis in rat skeletal muscle through down-regulated mammalian target of rapamycin (mTOR) signaling. *J Biol Chem*. 2002;277(27):23977-80.

14. Bruckbauer A, Zemel MB. Synergistic effects of polyphenols and methylxanthines with Leucine on AMPK/Sirtuin-mediated metabolism in muscle cells and adipocytes. *PLoS One*. 2014;9(2):e89166.

15. Busquets S, Alvarez B, Llovera M et al. Branched-chain amino acids inhibit proteolysis in rat skeletal muscle: mechanisms involved. *J Cell Physiol*. 2000;184(3):380-4.

16. Cartee GD. Aging skeletal muscle: response to exercise. *Exerc Sport Sci Rev*. 1994;22:91-120.

17. Cartee GD. Influence of age on skeletal muscle glucose transport and glycogen metabolism. *Med Sci Sport Exerc.* 1994;26(5):577-85.

18. Chale-Rush A, Morris EP, Kendall TL et al. Effects of chronic overload on muscle hypertrophy and mTOR signaling in young adult and aged rats. *J Gerontol A Biol Sci Med Sci*. 2009;64(12):1232-9.

19. Cleak MJ, Eston RG. Delayed onset muscle soreness: mechanisms and management. *J Sports Sci*. 1992;10(4):325-41.

20. Cleasby ME, Jarmin S, Eilers W et al. Local overexpression of the myostatin propeptide increases glucose transporter expression and enhances skeletal muscle glucose disposal. *Am J Physiol Endocrinol Metab*. 2014;306(7):E814-23.

21. Combaret L, Dardevet D, Rieu I et al. A leucine-supplemented diet restores the defective postprandial inhibition of proteasome-dependent proteolysis in aged rat skeletal muscle. *J Physiol*. 2005;569(Pt 2):489-99.

22. Costill DL, Pascoe DD, Fink WJ et al. Impaired muscle glycogen resynthesis after eccentric exercise. *J Appl Physiol*. 1990;69(1):46-50.

23. Dall'Aglio E, Chang H, Reaven GM et al. Age-related changes in rat muscle glycogen synthase activity. *J Gerontol*. 1987;42(2):168-72.

24. Deldicque L, Sanchez Canedo C, Horman S et al. Antagonistic effects of leucine and glutamine on the mTOR pathway in myogenic C2C12 cells. *Amino Acids*. 2008;35(1):147-55.

25. Demontis F, Piccirillo R, Goldberg AL et al. Mechanisms of skeletal muscle aging: insights from Drosophila and mammalian models. *Dis Model Mech*. 2013;6(6):1339-52.

26. Dodd KM, Tee AR. Leucine and mTORC1: a complex relationship. *Am J Physiol Endocrinol Metab*. 2012;302(11):E1329-42.

27. Doi M, Yamaoka I, Fukunaga T et al. Isoleucine, a potent plasma glucose-lowering amino acid, stimulates glucose uptake in C2C12 myotubes. *Biochem Biophys Res Commun*. 2003;312(4):1111-7.

28. Drummond MJ, Dreyer HC, Pennings B et al. Skeletal muscle protein anabolic response to resistance exercise and essential amino acids is delayed with aging. *J Appl Physiol*. 2008;104(5):1452-61.

29. Du M, Shen QW, Zhu MJ et al. Leucine stimulates mammalian target of rapamycin signaling in C2C12 myoblasts in part through inhibition of adenosine monophosphate-activated protein kinase. *J Anim Sci*. 2007;85(4):919-27.

30. Egerman MA, Glass DJ. Signaling pathways controlling skeletal muscle mass. *Crit Rev Biochem Mol Biol*. 2014;49(1):59-68.

31. Fick CA. Regulation of protein synthesis: singular and combined effects of age, AMPK, and resisted contractions on control of protein synthesis and elongation factors in skeletal muscle (Doctoral Disseration). Greenville, NC: East Carolina University, 2007.

32. Fogt DL, Pan S, Lee S et al. Effect of glycogen synthase overexpression on insulin-stimulated muscle glucose uptake and storage. *Am J Physiol Endocrinol Metab*. 2004;286(3):E363-9.

33. Francaux M, Demeulder B, Naslain D et al. Aging Reduces the Activation of the mTORC1 Pathway after Resistance Exercise and Protein Intake in Human Skeletal Muscle: Potential Role of REDD1 and Impaired Anabolic Sensitivity. *Nutrients*. 2016;8(1).

34. Fry CS, Drummond MJ, Glynn EL et al. Aging impairs contraction-induced human skeletal muscle mTORC1 signaling and protein synthesis. *Skeletal Muscle*. 2011;1(1):11.

35. Fry CS, Rasmussen BB. Skeletal muscle protein balance and metabolism in the elderly. *Curr Aging Sci*. 2011;4(3):260-8.

36. Gannon NP, Vaughan RA. Leucineinduced anaboliccatabolism: two sides of the same coin. *Amino Acids*. 2016;48(2):321-36.

37. Garvey SM, Dugle JE, Kennedy AD et al. Metabolomic profiling reveals severe skeletal muscle group-specific perturbations of metabolism in aged FBN rats. *Biogerontology*. 2014;15(3):217-32.

38. Giron MD, Vilchez JD, Salto R et al. Conversion of leucine to beta-hydroxy-beta-methylbutyrate by alpha-keto isocaproate dioxygenase is required for a potent stimulation of protein synthesis in L6 rat myotubes. *J Cachexia Sarcopenia Muscle*. 2016;7(1):68-78.

39. Gollins H, McMahon J, Wells KE et al. High-efficiency plasmid gene transfer into dystrophic muscle. *Gene Ther*. 2003;10(6):504-12.

40. Goodman CA, Mabrey DM, Frey JW et al. Novel insights into the regulation of skeletal muscle protein synthesis as revealed by a new nonradioactive in vivo technique. *FASEB J*. 2011;25(3):1028-39.

41. Goodman CA, Mayhew DL, Hornberger TA. Recent progress toward understanding the molecular mechanisms that regulate skeletal muscle mass. *Cellular Signal*. 2011;23(12):1896-906.

42. Gordon SE, Lake JA, Westerkamp CM et al. Does AMP-activated protein kinase negatively mediate aged fast-twitch skeletal muscle mass? *Exerc Sport Sci Rev*. 2008;36(4):179-86.

43. Gowans GJ, Hawley SA, Ross FA et al. AMP is a true physiological regulator of AMP-activated protein kinase by both allosteric activation and enhancing net phosphorylation. *Cell Metab*. 2013;18(4):556-66.

44. Graham TE, Yuan Z, Hill AK et al. The regulation of muscle glycogen: the granule and its proteins. *Acta Physiol (Oxf)*. 2010;199(4):489-98.

45. Gran P, Cameron-Smith D. The actions of exogenous leucine on mTOR signalling and amino acid transporters in human myotubes. *BMC Physiol*. 2011;11:10.

46. Gudiksen A, Schwartz CL, Bertholdt L et al. Lack of Skeletal Muscle IL-6 Affects Pyruvate Dehydrogenase Activity at Rest and during Prolonged Exercise. *PLoS One*. 2016;11(6):e0156460.

47. Gupta G, She L, Ma XH et al. Aging does not contribute to the decline in insulin action on storage of muscle glycogen in rats. *Am J Physiol Regul Integr Comp Physiol*. 2000;278(1):R111-7.

48. Hamilton DL, Philp A, MacKenzie MG et al. Molecular brakes regulating mTORC1 activation in skeletal muscle following synergist ablation. *Am J Physiol Endocrinol Metab*. 2014;307(4):E365-73.

49. Hardie DG. Sensing of energy and nutrients by AMP-activated protein kinase. *Am J Clin Nutr*. 2011;93(4):891S-6.

50. Hardie DG, Ross FA, Hawley SA. AMPK: a nutrient and energy sensor that maintains energy homeostasis. *Nat Rev Mol Cell Biol*. 2012;13(4):251-62.

51. Hardman SE, Hall DE, Cabrera AJ et al. The effects of age and muscle contraction on AMPK activity and heterotrimer composition. *Exp Gerontol*. 2014;55:120-8.

52. Hesselink MK, Kuipers H, Keizer HA et al. Acute and sustained effects of isometric and lengthening muscle contractions on high-energy phosphates and glycogen metabolism in rat tibialis anterior muscle. *J Muscle Res Cell Motil*. 1998;19(4):373-80.

53. Hopp JF. Anaerobic metabolism during electrical stimulation of aged rat skeletal muscle. *Phys Ther*. 1996;76(3):260-7.

54. Hoppeler H, Baum O, Lurman G et al. Molecular mechanisms of muscle plasticity with exercise. *Compr Physiol*. 2011;1(3):1383-412.

55. Hornberger TA. Mechanotransduction and the regulation of mTORC1 signaling in skeletal muscle. *Int J Biochem Cell Biol*. 2011;43(9):1267-76.

56. Jackson MJ. Reactive oxygen species in sarcopenia: Should we focus on excess oxidative damage or defective redox signalling? *Mol Aspects Med*. 2016;50:33-40.

57. Jacobs BL, Goodman CA, Hornberger TA. The mechanical activation of mTOR signaling: an emerging role for late endosome/lysosomal targeting. *J Muscle Res Cell Motil*. 2014;35(1):11-21.

58. Jensen J, Rustad PI, Kolnes AJ et al. The role of skeletal muscle glycogen breakdown for regulation of insulin sensitivity by exercise. *Front Physiol*. 2011;2:112.

59. Kato H, Miura K, Suzuki K et al. Leucine-Enriched Essential Amino Acids Augment Muscle Glycogen Content in Rats Seven Days after Eccentric Contraction. *Nutrients*. 2017;9(10).

60. Katz A. Role of reactive oxygen species in regulation of glucose transport in skeletal muscle during exercise. *J Physiol*. 2016;594(11):2787-94.

61. Kelleher AR, Kimball SR, Dennis MD et al. The mTORC1 signaling repressors REDD1/2 are rapidly induced and activation of p70S6K1 by leucine is defective in skeletal muscle of an immobilized rat hindlimb. *Am J Physiol Endocrinol Metab*. 2013;304(2):E229-36.

62. Kimball SR. Integration of signals generated by nutrients, hormones, and exercise in skeletal muscle. *Am J Clin Nutr*. 2014;99(1):237S-42S.

63. Kimball SR, Shantz LM, Horetsky RL et al. Leucine regulates translation of specific mRNAs in L6 myoblasts through mTOR-mediated changes in availability of eIF4E and phosphorylation of ribosomal protein S6. *J Biol Chem*. 1999;274(17):11647-52.

64. Knuiman P, Hopman MT, Mensink M. Glycogen availability and skeletal muscle adaptations with endurance and resistance exercise. *Nutr Metab (Lond)*. 2015;12:59.

65. Kosek DJ, Kim JS, Petrella JK et al. Efficacy of 3 days/wk resistance training on myofiber hypertrophy and myogenic mechanisms in young vs. older adults. *J Appl Physiol*. 2006;101(2):531-44.

66. Kubica N, Bolster DR, Farrell PA et al. Resistance exercise increases muscle protein synthesis and translation of eukaryotic initiation factor 2Bepsilon mRNA in a mammalian target of rapamycin-dependent manner. *J Biol Chem*. 2005;280(9):7570-80.

67. Kuo T, McQueen A, Chen TC et al. Regulation of Glucose Homeostasis by Glucocorticoids. *Adv Exp Med Biol*. 2015;872:99-126.

68. La Colla A, Pronsato L, Milanesi L et al. 17beta-Estradiol and testosterone in sarcopenia: Role of satellite cells. *Ageing Res Rev*. 2015;24(Pt B):166-77.

69. Lexell J. Human aging, muscle mass, and fiber type composition. *J Gerontol A Biol Sci Med Sci*. 1995;50 Spec No:11-6.

70. Liang C, Curry BJ, Brown PL et al. Leucine Modulates Mitochondrial Biogenesis and SIRT1-AMPK Signaling in C2C12 Myotubes. *J Nutr Metab*. 2014;2014:239750.

71. Lopez-Otin C, Blasco MA, Partridge L et al. The hallmarks of aging. *Cell*. 2013;153(6):1194-217.

72. Lushaj EB, Johnson JK, McKenzie D et al. Sarcopenia accelerates at advanced ages in Fisher 344xBrown Norway rats. *J Gerontol A Biol Sci Med Sci*. 2008;63(9):921-7.

73. Mammucari C, Milan G, Romanello V et al. FoxO3 controls autophagy in skeletal muscle in vivo. *Cell Metab*. 2007;6(6):458-71.

74. Manabe Y, Gollisch KS, Holton L et al. Exercise training-induced adaptations associated with increases in skeletal muscle glycogen content. *FEBS J*. 2013;280(3):916-26.

75. Manchester J, Skurat AV, Roach P et al. Increased glycogen accumulation in transgenic mice overexpressing glycogen synthase in skeletal muscle. *Proc Natl Acad Sci U S A*. 1996;93(20):10707-11.

76. Marsh DR, Criswell DS, Carson JA et al. Myogenic regulatory factors during regeneration of skeletal muscle in young, adult, and old rats. *J Appl Physiol*. 1997;83(4):1270-5.

77. McBride A, Ghilagaber S, Nikolaev A et al. The glycogen-binding domain on the AMPK beta subunit allows the kinase to act as a glycogen sensor. *Cell Metab*. 2009;9(1):23-34.

78. McBride A, Hardie DG. AMP-activated protein kinase--a sensor of glycogen as well as AMP and ATP? *Acta Phys (Oxf)*. 2009;196(1):99-113.

79. McGee SL, Mustard KJ, Hardie DG et al. Normal hypertrophy accompanied by phosphoryation and activation of AMP-activated protein kinase alpha1 following overload in LKB1 knockout mice. *J Physiol*. 2008;586(6):1731-41.

80. McMahon JM, Signori E, Wells KE et al. Optimisation of electrotransfer of plasmid into skeletal muscle by pretreatment with hyaluronidase -- increased expression with reduced muscle damage. *Gene Ther*. 2001;8(16):1264-70.

81. Meng SJ, Yu LJ. Oxidative stress, molecular inflammation and sarcopenia. *Int J Mol Sci*. 2010;11(4):1509-26.

82. Meredith CN, Frontera WR, Fisher EC et al. Peripheral effects of endurance training in young and old subjects. *J Appl Physiol*. 1989;66(6):2844-9.

83. Meynial-Denis D, Miri A et al. Insulin-dependent glycogen synthesis is delayed in onset in the skeletal muscle of food-deprived aged rats. *J Nutr Biochem*. 2005;16(3):150-4.

84. Mir LM. Application of electroporation gene therapy: past, current, and future. *Method Mol Biol*. 2008;423:3-17.

85. Montori-Grau M, Minor R, Lerin C et al. Effects of aging and calorie restriction on rat skeletal muscle glycogen synthase and glycogen phosphorylase. *Exp Gerontol*. 2009;44(6-7):426-33.

86. Mounier R, Lantier L, Leclerc J et al. Antagonistic control of muscle cell size by AMPK and mTORC1. *Cell Cycle*. 2011;10(16):2640-6.

87. Mounier R, Lantier L, Leclerc J et al. Important role for AMPKalpha1 in limiting skeletal muscle cell hypertrophy. *FASEB J*. 2009;23(7):2264-73.

88. Mounier R, Theret M, Lantier L et al. Expanding roles for AMPK in skeletal muscle plasticity. *Trends Endocrinol Metab*. 2015;26(6):275-86.

89. Murach KA, White SH, Wen Y et al. Differential requirement for satellite cells during overload-induced muscle hypertrophy in growing versus mature mice. *Skeletal Muscle*. 2017;7(1):14.

90. N.A. Projections of the Population by Age and Sex for the United States: 2010 to 2050 (NP2008-T12), Population Division, U.S. Census Bureau; Release Date: August 14, 2008. Retrieved from http://www.aoa.gov/Aging_Statistics/Profile/2011/4.aspx, on April 28, 2014.

91. Nair KS. Aging muscle. *Am J Clin Nutr*. 2005;81(5):953-63.

92. Nakai N, Kawano F, Terada M et al. Effects of peroxisome proliferator-activated receptor alpha (PPARalpha) agonists on leucine-induced phosphorylation of translational targets in C2C12 cells. *Biochim Biophys Acta*. 2008;1780(10):1101-5.

93. Nakashima K, Ishida A, Yamazaki M et al. Leucine suppresses myofibrillar proteolysis by down-regulating ubiquitin-proteasome pathway in chick skeletal muscles. *Biochem Biophys Res Commun*. 2005;336(2):660-6.

94. Narici MV, Maffulli N. Sarcopenia: characteristics, mechanisms and functional significance. *Br Med Bull*. 2010;95:139-59.

95. Navas-Enamorado I, Bernier M, Brea-Calvo G et al. Influence of anaerobic and aerobic exercise on age-related pathways in skeletal muscle. *Ageing Res Rev*. 2017;37:39-52.

96. Nieman DC, Zwetsloot KA, Meaney MP et al. Post-Exercise Skeletal Muscle Glycogen Related to Plasma Cytokines and Muscle IL-6 Protein Content, but not Muscle Cytokine mRNA Expression. *Front Nutr*. 2015;2:27.

97. O'Reilly KP, Warhol MJ, Fielding RA et al. Eccentric exercise-induced muscle damage impairs muscle glycogen repletion. *J Appl Physiol*. 1987;63(1):252-6.

98. Oligschlaeger Y, Miglianico M, Chanda D et al. The recruitment of AMP-activated protein kinase to glycogen is regulated by autophosphorylation. *J Biol Chem*. 2015;290(18):11715-28.

99. Passonneau JV, Lauderdale VR. A comparison of three methods of glycogen measurement in tissues. *Anal Biochem*. 1974;60(2):405-12.

100. Pederson BA, Csitkovits AG, Simon R et al. Overexpression of glycogen synthase in mouse muscle results in less branched glycogen. *Biochem Biophys Res Commun*. 2003;305(4):826-30.

101. Peyrollier K, Hajduch E, Blair AS et al. L-leucine availability regulates phosphatidylinositol 3-kinase, p70 S6 kinase and glycogen synthase kinase-3 activity in L6 muscle cells: evidence for the involvement of the mammalian target of rapamycin (mTOR) pathway in the L-leucine-induced up-regulation of system A amino acid transport. *Biochem J*. 2000;350 Pt 2:361-8.

102. Philp A, Hargreaves M, Baar K. More than a store: regulatory roles for glycogen in skeletal muscle adaptation to exercise. *Am J Physiol Endocrinol Metab*. 2012;302(11):E1343-51.

103. Poland JL, Poland JW, Honey RN. Substrate changes during fasting and refeeding contrasted in old and young rats. *Gerontology*. 1982;28(2):99-103.

104. Polekhina G, Gupta A, van Denderen BJ et al. Structural basis for glycogen recognition by AMP-activated protein kinase. *Structure*. 2005;13(10):1453-62.

105. Raastad T, Owe SG, Paulsen G et al. Changes in calpain activity, muscle structure, and function after eccentric exercise. *Med Sci Sports Exerc*. 2010;42(1):86-95.

106. Ramamani A, Aruldhas MM, Govindarajulu P. Differential response of rat skeletal muscle glycogen metabolism to testosterone and estradiol. *Can J Physiol Pharmacol*. 1999;77(4):300-4.

107. Raue U, Slivka D, Jemiolo B et al. Proteolytic gene expression differs at rest and after resistance exercise between young and old women. *J Gerontol A Biol Sci Med Sci*. 2007;62(12):1407-12.

108. Ribeiro MBT, Guzzoni V, Hord JM et al. Resistance training regulates gene expression of molecules associated with intramyocellular lipids, glucose signaling and fiber size in old rats. *Sci Rep*. 2017;7(1):8593.

109. Roach PJ, Depaoli-Roach AA, Hurley TD et al. Glycogen and its metabolism: some new developments and old themes. *Biochem J*. 2012;441(3):763-87.

110. Saha AK, Xu XJ, Lawson E et al. Downregulation of AMPK accompanies leucine- and glucose-induced increases in protein synthesis and insulin resistance in rat skeletal muscle. *Diabetes*. 2010;59(10):2426-34.

111. Sakuma K, Aoi W, Yamaguchi A. Current understanding of sarcopenia: possible candidates modulating muscle mass. *Pflugers Arch*. 2015;467(2):213-29.

112. Sakuma K, Watanabe K, Hotta N et al. The adaptive responses in several mediators linked with hypertrophy and atrophy of skeletal muscle after lower limb unloading in humans. *Acta Physiol (Oxf)*. 2009;197(2):151-9.

113. Salminen A, Kaarniranta K. AMP-activated protein kinase (AMPK) controls the aging process via an integrated signaling network. *Ageing Res Rev*. 2012;11(2):230-41.

114. Salminen A, Kaarniranta K, Kauppinen A. Age-related changes in AMPK activation: Role for AMPK phosphatases and inhibitory phosphorylation by upstream signaling pathways. *Ageing Res Rev*. 2016;28:15-26.

115. Salway JG. *Metabolism at a Glance*. Third ed.: Blackwell Publishing; 2004.

116. Sandri M, Barberi L, Bijlsma AY et al. Signalling pathways regulating muscle mass in ageing skeletal muscle: the role of the IGF1-Akt-mTOR-FoxO pathway. *Biogerontology*. 2013;14(3):303-23.

117. Saxton RA, Sabatini DM. mTOR Signaling in Growth, Metabolism, and Disease. *Cell*. 2017;168(6):960-76.

118. Schiaffino S, Dyar KA, Ciciliot S et al. Mechanisms regulating skeletal muscle growth and atrophy. *FEBS J*. 2013;280(17):4294-314.

119. Schiaffino S, Mammucari C. Regulation of skeletal muscle growth by the IGF1-Akt/PKB pathway: insights from genetic models. *Skeletal Muscle*. 2011;1(1):4.

120. Skurat AV, Wang Y, Roach PJ. Rabbit skeletal muscle glycogen synthase expressed in COS cells. Identification of regulatory phosphorylation sites. *J Biol Chem*. 1994;269(41):25534-42.

121. Song G, Ouyang G, Bao S. The activation of Akt/PKB signaling pathway and cell survival. *J Cell Mol Med*. 2005;9(1):59-71.

122. Stapleton D, Nelson C, Parsawar K et al. Analysis of hepatic glycogen-associated proteins. *Proteomics*. 2010;10(12):2320-9.

123. Steinberg GR, Watt MJ, McGee SL et al. Reduced glycogen availability is associated with increased AMPKalpha2 activity, nuclear AMPKalpha2 protein abundance, and GLUT4 mRNA expression in contracting human skeletal muscle. *Appl Physiol Nutr Metab*. 2006;31(3):302-12.

124. Szulc P, Duboeuf F, Marchand F et al. Hormonal and lifestyle determinants of appendicular skeletal muscle mass in men: the MINOS study. *Am J Clin Nutr*. 2004;80(2):496-503.

125. Tharrington IH. Skeletal Muscle Forkhead Box 3A (FOXO3A) Response to Acute Resistance Exercise in Young and Old Men and Women: Relationship to Muscle Glycogen Content and 5'-AMP-Activated Protein Kinase (AMPK) Activity (Master's Thesis). Greenville, NC: East Carolina University, 2010.

126. Thomson DM, Brown JD, Fillmore N et al. AMP-activated protein kinase response to contractions and treatment with the AMPK activator AICAR in young adult and old skeletal muscle. *J Physiol*. 2009;587(Pt 9):2077-86.

127. Thomson DM, Fick CA, Gordon SE. AMPK activation attenuates S6K1, 4E-BP1, and eEF2 signaling responses to high-frequency electrically stimulated skeletal muscle contractions. *J Appl Physiol*. 2008;104(3):625-32.

128. Thomson DM, Gordon SE. Diminished overload-induced hypertrophy in aged fast-twitch skeletal muscle is associated with AMPK hyperphosphorylation. *J Appl Physiol*. 2005;98(2):557-64.

129. Thomson DM, Gordon SE. Impaired overload-induced muscle growth is associated with diminished translational signalling in aged rat fast-twitch skeletal muscle. *J Physiol*. 2006;574(Pt 1):291-305.

130. van Breda E, Keizer H, Kuipers H et al. Effect of testosterone and endurance training on glycogen metabolism in skeletal muscle of chronic hyperglycaemic female rats. *Br J Sports Med*. 2003;37(4):345-50.

131. van der Meulen JH, Kuipers H, Stassen FR et al. High energy phosphates and related compounds, glycogen levels and histology in the rat tibialis anterior muscle after forced lengthening and isometric exercise. *Pflugers Arch*. 1992;420(3-4):354-8.

132. Vestergaard H. Studies of gene expression and activity of hexokinase, phosphofructokinase and glycogen synthase in human skeletal muscle in states of altered insulin-stimulated glucose metabolism. *Dan Med Bull*. 1999;46(1):13-34.

133. Voet D, Voet JG. *Biochemistry*. Fourth ed.: John Wiley & Sons, Inc.; 2011.

134. Walker DK, Dickinson JM, Timmerman KL et al. Exercise, amino acids, and aging in the control of human muscle protein synthesis. *Med Sci Sports Exerc*. 2011;43(12):2249-58.

135. Wang X, Hu S, Liu L. Phosphorylation and acetylation modifications of FOXO3a: Independently or synergistically? *Oncol Lett*. 2017;13(5):2867-72.

136. Wehling M, Cai B, Tidball JG. Modulation of myostatin expression during modified muscle use. *FASEB J*. 2000;14(1):103-10.

137. Widrick JJ, Costill DL, McConell GK et al. Time course of glycogen accumulation after eccentric exercise. *J Appl Physiol*. 1992;72(5):1999-2004.

138. Wojtaszewski JF, Jorgensen SB, Hellsten Y et al. Glycogen-dependent effects of 5-aminoimidazole-4-carboxamide (AICA)-riboside on AMP-activated protein kinase and glycogen synthase activities in rat skeletal muscle. *Diabetes*. 2002;51(2):284-92.

139. Wu CL, Kandarian SC. Protein overexpression in skeletal muscle using plasmid-based gene transfer to elucidate mechanisms controlling fiber size. *Methods Mol Biol*. 2012;798:231-43.

140. Xu H, Frankenberg NT, Lamb GD et al. When phosphorylated at Thr148, the beta2-subunit of AMP-activated kinase does not associate with glycogen in skeletal muscle. *Am J Physiol Cell Physiol*. 2016;311(1):C35-42.

141. Xu H, Stapleton D, Murphy RM. Rat skeletal muscle glycogen degradation pathways reveal differential association of glycogen-related proteins with glycogen granules. *J Physiol Biochem*. 2015;71(2):267-80.

142. Zhao J, Brault JJ, Schild A et al. FoxO3 coordinately activates protein degradation by the autophagic/lysosomal and proteasomal pathways in atrophying muscle cells. *Cell Metab*. 2007;6(6):472-83.

143. Zhao J, Zhai B, Gygi SP et al. mTOR inhibition activates overall protein degradation by the ubiquitin proteasome system as well as by autophagy. *Proc Natl Acad Sci U S A*. 2015;112(52):15790-7.

APPENDIX 1: INSTITUTIONAL ANIMAL CARE AND USE COMMITTEE APPROVAL LETTER

UNC CHARLOTTE

Research and Economic Development

Office of Research Compliance

9201 University City Boulevard, Charlotte, NC 28223-0001
t/ 704.687.1876 | f/ 704.687.0980 | http://research.uncc.edu/compliance-ethics

Notice of Initial Protocol Approval

To:	**Dr. Scott Gordon** **Department of Kinesiology**
From:	**Dr. Yvette Huet** **IACUC Chair**
Subject:	**Approval of Protocol**
Protocol #:	**16-005**
Title:	**Glycogen Content, Protein Synthesis, and Overload-Induced Growth of Skeletal Muscle**
Approval Date:	**04/12/2016**

The Institutional Animal Care and Use Committee (IACUC) approved the protocol entitled **"Glycogen Content, Protein Synthesis, and Overload-Induced Growth of Skeletal Muscle."** Approvals are valid for one year and may be renewed before the anniversary of the original approval date for a total of three years. After three years, a new protocol application must be submitted to continue the study. Please note the following information:

Initial Approval date:	**04/12/2016**
Renewal 1 – due and approved before:	**04/12/2017**
Renewal 2 – due and approved before:	**04/12/2018**
Expiration date:	**04/12/2019**

Please note that it is the investigator's responsibility to promptly inform the committee of any changes in the proposed research, as well as any unanticipated problems that may occur involving care and use of animals. All changes (e.g. personnel additions, change in animal strain, change in procedures, etc.) must be submitted to the IACUC via an Amendment. All forms (e.g. amendments, annual renewal, etc.) can be found at: http://research.uncc.edu/departments/office-research-compliance-orc/animal-care-use/protocol-application-forms

Before starting any protocol involving survival surgery, tumor and/or disease induction, and any other painful animal procedure, a meeting with the Attending Veterinarian, Vivarium Director, and Vivarium staff is required. If the research involves surgical procedures, it is also the investigator's responsibility to maintain detailed surgical records. These records must be approved by the Vivarium Director and the Attending Veterinarian and a copy must be kept with the animals at all times.

To better help you and your research team, please inform Vivarium personnel which phase/specific aim of your protocol is being conducted at any given time. It is helpful for the staff to know which endpoints are required for the phase/specific aim being investigated.

A renewal/status report is due annually for IACUC protocols. The annual renewal application can be accessed via the above-listed website. If you do not plan to continue your study at the time of your renewal anniversary date, please contact the Office of Research Compliance before the anniversary date to terminate your study.

If you need additional assistance, please contact Cindy Stone in the Office of Research Compliance at (704) 687-1872 or via email at C.Stone@uncc.edu.

APPENDIX 2: INSTITUTIONAL BIOSAFETY COMMITTEE EXEMPTION LETTER

UNC CHARLOTTE
Research & Economic Development
Office of Research Compliance
9201 University City Blvd., Charlotte, NC 28223
t/ 704.687.1825 | f/ 704.687.0980 | http://research.uncc.edu/compliance-ethics

Notice of Exemption

To:	**Dr. Scott E. Gordon** **Mr. Marcus Lawrence** **Department of Kinesiology**
Title of Protocol:	**"Effect of Glycogen Content, Protein Synthesis, and Overload-Induced Growth in Skeletal Muscle"**
Classification:	**BSL-1/RG-1; rDNA work – exempt from *NIH Guidelines* *(III-F-8/Appendix C-II)***
Date:	**August 28, 2014**

Thank you for submitting your experiments to the University of North Carolina Charlotte's Institutional Biosafety Committee (IBC) for review. An administrative review was conducted in accordance with the *NIH Guidelines for Research Involving Recombinant or Synthetic Nucleic Acid Molecules*. It has been determined that your proposed research entitled "Glycogen Content, Protein Synthesis, and Overload Induced Growth in Skeletal Muscle" is exempt under section III-F-8 of the NIH Guidelines. As outlined in your protocol, this work can be safely conducted at Biosafety Level I (BSL-1). Please keep a copy of this letter for your records.

If the scope of the research changes it may be necessary to submit another registration form to the IBC. Substantive changes include, but are not limited to, using a microorganism or genetic tool other than what is listed in the experiments described, changes in procedures that may influence exposure potential or changes in equipment, facilities or personnel.

Thank you for your commitment to conducting your experiments in a safe manner. I wish you success in achieving your ultimate research goals.

Sincerely,

Gina Ramoz
Biosafety Program Director

cc: Todd Steck
Dixie Airey
Cindy Stone

APPENDIX 3: AMERICAN COLLEGE OF SPORTS MEDICINE FOUNDATION DOCTORAL STUDENT RESEARCH GRANT

A3.1 PART A:

A3.1.1 Lay Summary

Age-related muscle wasting (i.e., sarcopenia) results in a loss of independence, and current interventions are relatively ineffective in restoring muscle mass in elderly. A major factor underlying sarcopenia is the inability of aged skeletal muscle (SkM) cells to synthesize new proteins. Our lab has established that a molecule within muscle cells called 5'-AMP-activated kinase (AMPK) as one main cause of this. AMPK activity is elevated in muscle with age, and is a major factor suppressing muscle protein synthesis (MPS) and growth in aged SkM. Therefore, an intervention than can inhibit AMPK and thus restore MPS and growth could potentially be important for reducing or reversing sarcopenia in aged SkM.
Glycogen, the stored form of glucose (sugar) in SkM, is a suppressor of AMPK. Importantly, glycogen content is reduced in aged SkM and this may underlie the increased AMPK activity in older muscle. However, the link between glycogen content and muscle growth during overload (i.e., muscle loading) has not been previously examined in aged humans or animals. Therefore, the aim of the current project is to determine whether enhancing intramuscular glycogen content in aged rat SkM during overload will rescue growth to levels seen in young adult rats. We hypothesize that enhancing intramuscular glycogen content in aged rat skeletal muscle via the plasmid DNA expression of active glycogen synthase will rescue overload-induced muscle growth to levels observed in young adult muscle and to levels significantly greater than age-matched controls lacking glycogen enhancement. We further hypothesize that the mechanisms underlying this effect in the glycogen-enhanced, overloaded muscles of aged animals will be suppressed AMPK activity, enhanced anabolic protein translational signaling and MPS rates, and suppressed catabolic signaling compared to the age-matched controls.

A3.1.2 Biographical Sketch of Principal Investigator/Student Investigator

Part A

9. Biographical Sketch of Principal Investigator/Student Investigator

Name: Marcus Michael Lawrence Position/Title: Ph.D. Candidate

If this is a student award:
a. Date entered graduate program (state degree): August 2012, Ph.D. in Biology
b. Date passed comprehensive exam equivalent: September 2014
c. Date expected to receive graduate or equivalent degree (state degree): August 2017, Ph.D. in Biology
(Advisor, please initial after each date listed)

Education *(Baccalaureate through postdoctoral training)*

Institution	Degree	Years	Field
California State University Monterey Bay	B.S.	2006-2010	Kinesiology
Appalachian State University	M.S.	2010-2012	Exercise Science
University of North Carolina at Charlotte	Ph.D.	2012-present	Biology

Professional Experience *(in chronological order)*

Institution	Position	Years
California State University Monterey Bay	Undergraduate Research Assistant	2009-2010
Appalachian State University	Graduate Research Assistant	2010-2012
North Carolina Research Campus (N.C. State)	USDA Research Fellow (N.C. State)	2011-2012
University of North Carolina at Charlotte	Graduate Research Assistant	2012-present

Memberships and Honors

Memberships:

2009-present	American College of Sports Medicine (ACSM)
2009-2010	Southwest Chapter of ACSM
2010-present	Southeast Chapter of ACSM
2010-present	American Physiological Society
2009-present	National Strength and Conditioning Association* (NSCA); *NSCA Certified Strength and Conditioning Specialist

Honors:

2010	Distinction in the Major, CSU Monterey Bay Department of Kinesiology
2010-2012	Out-of-State Tuition Scholarship, Appalachian State University
2011-2012	USDA Transdisciplinary Training Program in Functional Foods Kannapolis Scholars Fellowship, North Carolina Research Campus (USDA funding to N.C. State University)
2012-2013	Out-of-State Tuition Scholarship, University of North Carolina at Charlotte
2013-present	In-state Tuition Scholarship, University of North Carolina at Charlotte
2014-present	Peer-Reviewer, NSCA's *Journal of Strength and Conditioning Research*

Other Support:

No current support.

A3.1.3 Biographical Sketch of Student Advisor

Part A

10. Biographical Sketch of Student Advisor

Name: Scott Edward Gordon Position/Title: Professor and Chairperson

A. Personal Statement: Research in the Gordon laboratory in humans and animal models is attempting to identify molecular mechanisms of skeletal muscle remodeling with aging, disuse, and overloading/resistance exercise, especially with respect to the muscle protein synthesis and degradation. Significant skeletal muscle wasting with age can result in lost functional independence, and interventions such as resistance exercise training are not fully effective in restoring muscle mass in elderly individuals. Current and past projects (supported in part by grants from the NIH and the American Federation for Aging Research) are specifically examining the mechanisms by which deficits in cellular energy balance may underlie the atrophy and/or the diminished capacity for growth that both occur predominantly in fast-twitch muscle fibers with age. This research is also attempting to determine if protein synthesis and growth in aging skeletal muscle can be rescued by interventions such as exercise, nutrition, or other factors that either restore, or bypass the deficit in, energy balance.

Education

Institution	Degree	Years	Field
Bowdoin College, Brunswick, ME	B.A.	1982-1986	Biology
Pennsylvania State Univ., University Park, PA	M.S.	1989-1992	Exercise Physiology
Pennsylvania State Univ., University Park, PA	Ph.D.	1992-1997	Physiology
University of Texas Medical School, Houston, TX	Post-Doctoral	1997-1999	Physiology/Molecular Biology
University of Missouri, Columbia, MO	Post-Doctoral	1999-2001	Physiology/Molecular Biology

B. Positions and Honors

Positions and Employment:

1986-1989 Biological Science Assistant, U. S. Army Research Inst. of Environmental Medicine, Natick, MA.
1989-1994 Graduate Research Asst., Center for Sports Med., Penn State University, University Park, PA.
1994-1997 National Institute on Aging Predoctoral Fellow, The Gerontology Center/Center for Sports Medicine, Penn State University, University Park, PA.
1997-1999 NASA Postdoctoral Research Associate in Space Biology, Dept. of Integrative Biology, Pharmacology, and Physiology, Univ. of Texas Medical School, Houston, TX.
1999-2001 NIH Postdoctoral Fellow, Dept. of Veterinary Biomedical Sciences, University of Missouri, Columbia, MO.
2001-2007 Assistant Professor, Department of Exercise and Sport Science and Department of Physiology, East Carolina University, Greenville, NC.
2007-2012 Associate Professor, Department of Exercise and Sport Science and Department of Physiology, East Carolina University, Greenville, NC.
2012-present Professor and Chairperson, Department of Kinesiology, The University of North Carolina at Charlotte, Charlotte, NC.

Other Experience and Professional Memberships:

NASA Review Panel Study Section: "NASA Research Announcement (NRA) NNH04ZUU003N for Ground-Based Studies for Human Health in Space", December 2004.
NIH Minority Biomedical Research Support (MBRS) ad hoc review panel (NIGMS), February 2006.
NASA Postdoctoral Program (NPP) Grant Review Panel, September 2006.
Scientific Committee of the Association Française contre les Myopathies (France) Review Panel, 2007-2010.
Canada Foundation for Innovation - Leaders Opportunity Infrastructure Grant Review Panel, June 2009.
American Federation for Aging Research Research Grant Review Panel, 2010 - present.
NIH Skeletal Muscle Biology and Exercise Physiology (SMEP) Study Section, Ad hoc Reviewer, June 2010-present.
Member and Fellow, American College of Sports Medicine
Member, American Physiological Society
Member, American Society for Gravitational and Space Biology

Other Experience and Professional Memberships (Continued):
Member, Gerontological Society of America
Member, National Strength and Conditioning Association
Member, Sigma Xi
Member, Southeast Regional Chapter, American College of Sports Medicine

Honors:

1993	National Institute on Aging Predoctoral Trainee Fellowship in Adult Development and Aging.
1994	American Association of Retired Persons Scholarship Grant.
2005-2006	Outstanding Researcher Award, East Carolina Univ. College of Health and Human Performance.
2006-2007	Scholar-Teacher Award, East Carolina University College of Health and Human Performance.
2008-pres.	Fellow, American College of Sports Medicine.

Research Support:
Completed Research Support:
1. Experimental and Applied Sciences Investigator-initiated Research Grant: "Role of Nitric Oxide in Overload-induced Skeletal Muscle Hypertrophy" (3/03-12/04; S.E. Gordon, P.I.).
2. NIH Academic Research Enhancement Award (R15) Grant (PA-03-053): "Aging, AMP Kinase and Skeletal Muscle Overload" (9/05 – 8/09; S.E. Gordon, P.I.).
3. American Federation for Aging Research Grant: "Targeted Rescue of Protein Translation and Synthesis in Aged Skeletal Muscle" (7/06 – 6/08; S.E. Gordon, P.I.).
4. NIH Traditional Research Project (R01) Grant (PA-03-156): "Age-related Insulin Resistance, Muscle, and Exercise" (10/05 – 9/10; S.E. Gordon, Co-I, 5% Effort; Joseph A. Houmard, P.I.

Current Research Support:
1. UNC Charlotte College of Health and Human Services Start-up and Department of Kinesiology Research Support Funding to Dr. Gordon, ~$20,000 for 2016-2017. *These funds are exclusively dedicated to supporting the current research project, if needed.*

A3.1.4 List of Related Publications by the Principal Investigator/Student Investigator

Part A

11. List of Related Publications by the Principal Investigator/Student Investigator

Most relevant to the current application:

1. **Lawrence MM**, Myers BC, Shi R, Mixon WT, Whitworth HB, Gordon SE. Glycogen content and overload-induced hypertrophy in fast-twitch skeletal muscle of young adult and aged rats. *SEACSM Annual Meeting**, Conference Proceedings, Feb. 2014 (*Abstract accepted, but meeting cancelled due to inclement weather).
2. **Lawrence MM**, Shi R, Myers BC, Whitworth HB, Mixon WT, Gordon SE. Relationships between glycogen content, translational signaling, protein synthesis, and hypertrophy in overloaded fast-twitch skeletal muscles of young adult and aged rats. *Skeletal Muscle Biology in Health and Disease Bi-Annual Meeting*, Conference Proceedings, March 2014.

Additional recent peer-reviewed publications (Selected from 7 total):

1. Hardee JP, **Lawrence MM**, Utter AC, et al. Effect of inter-repetition rest on ratings of perceived exertion during multiple sets of the power clean. *Eur J Appl Physiol.* 2012;112(8): 3141-3147.
2. Jetton AM, **Lawrence MM,** Meucci M, et al. Dehydration and acute weight gain in mixed martial arts fighters prior competition. *J Strength Cond Res.* 2013;27(5): 1322-1326.
3. Zwetsloot KA, John CS, **Lawrence MM**, et al. High intensity interval training induces a modest systemic inflammatory response to active young men. *J Inflamm Res.* 2014;9(7): 9-17.
4. **Lawrence MM**, Cooley ID, Arthur ST, et al. Factors influencing isometric exercise training-induced reductions in resting blood pressure. *Scand J Med Sci Sports*. 2014; in press.
5. Arthur ST, Zwetsloot KA, **Lawrence MM**, et al. Ajuga turkestanica increases Notch and Wnt signaling in aged skeletal muscle. *Eur Rev Med Pharmacol Sci.* 2014;18(17): 2584-92.

Additional recent conference proceedings and published abstracts:

Conference Proceedings (Selected from 10 total):

1. **Lawrence MM**, Kirby T, McBride JM, et al. Acute leucine supplementation does not reduce inflammatory cytokines following eccentric resistance exercise. *SEACSM Annual Meeting*, Conference Proceedings, Feb. 2011.
2. Zwetsloot KA, Hardee J, **Lawrence MM**, et al. IL-6 increases in skeletal muscle interstitium of untrained young men in response to resistance exercise. *SEACSM Annual Meeting*, Conference Proceedings, Feb. 2011.
3. Arthur ST, Zwetsloot KA, **Lawrence MM**, et al. The effect of phytoecdysteroid treatment on notch and Wnt signaling in aged skeletal muscle. *SEACSM Annual Meeting*, Conference Proceedings, Feb. 2013.
4. **Lawrence MM**, Thomson DM, Fick CA, Gordon SE. Early translational signaling response to electrically stimulated eccentric vs. concentric resisted skeletal muscle contractions. *ACSM Integrative Physiology of Exercise Meeting*, Conference Proceeding, Sept. 2014.

Published Abstracts (Selected from 12 total):

1. **Lawrence MM**, Sevene-Adams PG, Berning JM, et al. Effect of overload sprint cycling on subsequent power output. NSCA Annual Meeting, *J Strength Cond Res* (Supp.): Aug. 2009.
2. Arthur ST, Zwetsloot KA, **Lawrence MM**, et al. Phytoecdysteroid treatment reduces Notch signaling in aged skeletal muscle. Experimental Biology Annual Meeting; Free Communication; *FASEB J.* 2012; 26:777.12.
3. **Lawrence MM**, Zwetsloot KA, Arthur ST, et al. Phytoecdysteroid treatment increases fiber size and PI3K-Akt signaling in aged skeletal muscle. Experimental Biology Annual Meeting; Free Communication; *FASEB J.* 2012; 26:777.12.
4. **Lawrence MM**, Triplett NT, Paul JA, et al. Relationship between jumping and running performance in middle and long distance runners. NSCA Annual Meeting, *J Strength Cond Res* (Supp.): July 2012.
5. Zwetsloot KA, **Lawrence MM**, Arthur ST, et al. Acute phytoecdysteroid treatment increases PI3k-Akt signaling in aged skeletal muscle. Experimental Biology Annual Meeting, Free Communication; *FASEB J.* 2013; 27:14.1.
6. **Lawrence MM**. Huot JR, Sherman CA, et al. Effect of Phytoecdysteroid Treatment on Fiber Type Percentage, Myostatin and Atrogenes Expression in Aged Mouse Skeletal Muscle. *Skeletal Muscle Biology in Health and Disease Bi-Annual Meeting*, January 2016 (Abstract accepted).

A3.1.5 List of Related Publications by Student Advisor

Part A

12. List of Related Publications by Student Advisor

Peer-Reviewed Manuscripts (Selected from 68 total):
Most relevant to the current application:

1. Thomson DM, **Gordon SE**. Diminished overload-induced hypertrophy in aged fast-twitch skeletal muscle is associated with AMPK hyperphosphorylation. *J Appl Physiol.* 2005;98(2): 557-564.
2. Thomson DM, **Gordon SE**. Impaired overload-induced muscle growth is associated with diminished translational signaling in aged rat fast-twitch skeletal muscle. *J Physiol.* 2006; 574(Pt 1): 291-305.
4. Thomson DM, Fick CA, **Gordon SE**. AMPK activation attenuates S6K1, 4E-BP1, and eEF2 signaling responses to high-frequency electrically stimulated skeletal muscle contractions. *J Appl Physiol.* 2008;104: 625-632.
5. **Gordon SE**, Lake JA, Westerkamp CM, et al. Does AMP-activated protein kinase negatively mediate aged fast-twitch skeletal muscle mass? *Exerc Sport Sci Rev.* 2008;36(4): 179-186.
6. Thomson DM, Brown JD, Fillmore N, Ellsworth SK, Jacobs DL, Winder WW, Fick CA, **Gordon SE**. AMP-Activated protein kinase response to contractions and AICAR treatment in young adult and old skeletal muscle. *J* Physiol. 2009;587: 2077-2086.

Additional recent Publications:

1. Kraemer WJ, **Gordon SE**, Fleck SJ, et al. Endogenous anabolic hormonal and growth factor responses to heavy resistance exercise in males and females. *Int. J. Sports Med.* 1991;12(2): 228-235.
2. **Gordon SE**, Davis BS, Carlson CJ, Booth FW. ANG II is required for optimal overload-induced skeletal muscle hypertrophy. *Am J Physiol Endocrinol Metab.* 2001;280: 150-159.
3. Deschenes MR, Tenny K, Eason MK, **Gordon SE**. Moderate aging does not modulate morphological responsiveness of the neuromuscular system to chronic overload in Fischer 344 rats. *Neuroscience.* 2007;148(4): 970-977.
4. Kraemer WJ, Fragala MS, van Henegouwen WR, **Gordon SE**, et al. Responses of proenkephalin Peptide F to aerobic exercise stress in the plasma and white blood cell biocompartments. *Peptides.* 2013; 42: 118–124.
5. **Gordon SE,** Kraemer WJ, Looney DP, et al. The influence of age and exercise modality on growth hormone bioactivity in women. *Growth Horm IGF Res.* 2014;24(2-3): 95–103

Relevant Published Abstracts (Selected from 114 total):

1. Gordon SE, Tharrington IH, Macesich JL, et al. Muscle Glycogen Content and the FOXO3A Response to Resistance Exercise in Young and Old Subjects. *ACSM Integrative Physiology of Exercise,* Sept. 2010.
2. Shi R, Macesich JL, Harper BM, Tharrington IH, Gavin TP, Heidal K, Hickner RC, **Gordon SE**. Muscle Glycogen Content and the eEF2 Response to Resistance Exercise in Young and Old Subjects. *Experimental Biology 2011, Washington, D.C.* April, 2011.
3. Gordon SE, Whitworth HB, Mixon WT, et al. Overload-Induced Skeletal Muscle Growth and Protein Translational Signaling are Partially Restored by Dietary Leucine Supplementation in Aged Animals. *Advances in Skeletal Muscle Biology in Health and Disease, Gainesville, FL.* February, 2012.
4. Lawrence MM, Myers BC, Shi R, Mixon WT, Whitworth HB, **Gordon SE**. Glycogen Content and Overload-induced Hypertrophy in Fast-Twitch skeletal muscle of Young Adult and Aged Rats. *Southeast Regional Chapter, American College of Sports Medicine, Greenville, SC.* February, 2014. (Abstract accepted by peer review; conference canceled due to weather)
5. Lawrence MM, Shi R, Myers BC, Whitworth HB, Mixon WT, **Gordon SE**. Relationships between Glycogen Content, Translational Signaling, Protein Synthesis, and Hypertrophy in Overloaded Fast-Twitch Skeletal Muscles of Young Adult and Aged Rats. *Advances in Skeletal Muscle Biology in Health and Disease, Gainesville, FL.* March, 2014.
6. Lawrence MM, Thomson DM, Fick CA, **Gordon SE**. Early Translational Signaling Response to Electrically Stimulated Eccentric vs. Concentric Resisted Skeletal Muscle Contractions. *ACSM Conference on Integrative Physiology of Exercise, Miami Beach, FL.* September 2014.

A3.1.6 Proposed Budget

Part A

13. Proposed Budget

Personnel

Name	Position/Title	%Effort	Salary	Fringe	Total
Not Applicable.				Sub Total	$0.00

Small Equipment (Itemize) — **Total**

None. — Sub Total $0.00

Supplies (Itemize)

1. **Chemicals:**
   - **a.** Muscle Processing/Homogenization and General Lab Supplies: $768.45
     - **i.** Buffer components (Tris., HEPES, Triton X-100, EGTA, EDTA, β-glycerophosphate, NaF, pepstatin A, aprotinin, leupeptin, sodium orthovanadate); protein assay reagents, and misc. buffer supplies, etc.
   - **b.** Glycogen Analysis Supplies: $304.00
     - **i.** Glucosidase, hexokinase kit, cuvettes.
   - **c.** Western Blotting and Histochemistry Antibodies and Other supplies: $2710.00
     - i. Antibodies for total Akt, mTOR, p70S6k, 4E-BP1, FOXO3A, MuRF1, MAFbx = $1440.00.
     - ii. Antibodies for phospho Akt^{Ser473}, Akt^{Thr308}, $mTOR^{Ser2448}$, $p70S6k^{Thr389}$, $p70S6k^{Ser421/Thr424}$, $FOXO3A^{Ser318/321}$, 4E-BP1β&γ/total = $660.00
     - iii. Secondary antibody ($150), PVDF membrane ($120), ECL detection agent ($240), film ($100) = $610.00
   - **d.** Protein Synthesis Assessment: $340.55
     - **i.** Puromycin
2. **Glassware**: $300.00
   - **a.** Muscle Processing/Homogenization and General Lab Supplies: Ground glass homogenizers, Latex gloves, eppendorf tubes, test tubes, pipette tips, serological pipettes, glassware, kimwipes, etc.

Sub Total $4423.00

3. **Animal Costs Detail**: (*All animals will be of the Fischer 344 or FBN strain – see Part B, P.18)*
   - a. Animal Numbers/Cost:
     - i. 10 rats/group x 1 young groups (male) = 10 young rats.
     - ii. 10 rats/group x 2 old groups (male; with and without glycogen enhancement) = 20 old rats.
     - iii. Animal costs and shipping free from NIA (see Appendix v.)
   - b. Animal Vivarium Charges (Per Diem/Rat):
     - i. $0.55/day/rat for ~1680 ratdays (30 rats x 35 days x $0.55) = $577.00

Sub Total $577.00

Grand Total $5000.00

A3.1.7 Budget Justification

1.) Supplies: Muscle Processing and Homogenization, General Lab Supplies, Glycogen Analysis Supplies, Western Blotting and Histochemistry Antibodies and Other Supplies, and Protein Synthesis Assessment: The Gordon lab already has most items needed for performing these techniques and analysis, however certain miscellaneous items still must be obtained as listed above.
1c.) For Western Blotting, we also plan to measure total AMPKα, ACC, eEF2, eEF2k and phospho AMPKThr172, ACCSer79, eEF2Thr56, eEF2kSer398, but did not list in the budget as we currently have those antibodies.
3.) Animal Costs Detail: Animals are no cost, due to new policy implemented by NIA in January of 2014.
3a&3b.) NOTE: If animals cannot be obtained for any reason from NIA, the cost of animals/shipping from a private vendor will be funded through Dr. Gordon's startup funds or department funds dedicated to research from the University (See Part B, P.18 #2).

A3.1.8 Institutional Resources and Environment

All equipment necessary for the proposed research is located at UNC Charlotte's Dept. of Kinesiology's Laboratory of Systems Physiology (LSP) that occupies ~3100 ft2 of dedicated space and is designed for basic and applied research (both rodent and human) with the following relevant major equipment: Cryostat-microtome, NanoDrop™ Spectrophometer, 5 x 4°C/ -20°C refrigerators/freezers, 4 x - 86°C sub freezers, UV Spectrophotometer, BioRad™ Criterion XT kit for SDS PAGE, Licor™ Odyssey CLx Infrared Imager and Konica Minolta™ SRX-101A Film Processor for western blot analysis, IX71 inverted fluorescent microscope (Olympus™), Thermo Scientific™ Sorvall ST 40 Refrigerated centrifuge, 2 x 4ft biological safety cabinet, Midsci Incubated shaker, and BTX ECM 830 Square Wave Electroporation System. The LSP also occupies space in the University vivarium. The research environment of the LSP is enhanced by 6 faculty members occupying the contiguous lab space and will provide Mr. Lawrence direct and indirect mentoring both within the lab environment and in bi-weekly lab meetings. Mr. Lawrence will be further developed through attendance at Dept. of Kinesiology monthly seminars along with frequent seminars in other departments and programs such as Biology, Health Psychology, Nursing, Public Health, Biomedical Engineering, and Bioinformatics. Dr. Scott Gordon will provide the primary mentorship and hands on guidance to Mr. Lawrence for all protocols and analysis. Importantly, Mr. Lawrence has already begun performing these procedures in the Gordon laboratory (Fig.4-5).

A3.2 PART B: RESEARCH PLAN

A3.2.1 Introduction

Part B: Research Plan

Introduction: (Resubmissions Only)

I would like to thank the reviewers of my previously submitted Doctoral Student Research Grant entitled "Enhancing Muscle Glycogen Content to Rescue Skeletal Muscle Growth" for their insightful comments and concerns. Overall, both reviewers found that my approach of using a mutant glycogen synthase plasmid to enhance muscle glycogen and thus restore overload-induced anabolic signaling and growth in aged rat skeletal muscle to be a significant strength that should produce compelling and convincing data. However, they also identified suggestions for improvement that I have addressed in the revised proposal. Below is a summary of changes in response to these concerns, and I feel that the proposal is greatly enhanced.

Both Reviewers' Concerns:
1) Both reviewers viewed the Specific Aims as redundant and unclear.
Response: The Specific Aims (Part B, P.13) have been updated to clarify the overall goal of the project including the hypotheses, specific objectives, impact on the field, and expected results to strengthen the proposal.
2) The reviewers both felt that more rationale was needed for the chosen dependent variables, especially the chosen anabolic signaling markers.
Response: Additional rationale has been added to help clarify the chosen dependent variables (Approach, P.17 & Budget/Budget Narrative).
3) The reviewers requested survival rates following invasive surgeries in rats of this age to be addressed.
Response: New rationale has been added for the chosen animal numbers, including specifically addressing survival rates (P.18, #2), which have been historically extremely low in the Gordon lab in the ablation model in aged rats.

Reviewer A Concerns:
1) Reviewer A felt that the Research Plan and entire proposal did not convincingly convey a detailed understanding of the concepts involved in the grant.
Response: The entire Research Plan (Part B., P.13-19) has been significantly revised to be more concise and provide additional rationale where needed including adding additional information regarding 5'-AMP-activated protein kinase (AMPK) potential interaction with well-known anabolic and catabolic signaling, including adding a new figure (Fig.1).
2) Reviewer A commented that our preliminary data did not present convincing potential for delineation of the response between young and old.
Response: I appreciate the reviewer's comments, and agree that more pilot data is always helpful. Given the fact that this is a doctoral dissertation grant, and the fact that additional recent pilot data have been added (Fig.4-5) to the data previously compiled (Fig.2-3), it is hoped that enough evidence is presented to enhance the case that the proposed experiment is worth pursuing.

Reviewer B Concerns:
1) Reviewer B appreciated the NIA or private vendor rat colony resource approach, but requested additional assurance that rats can be obtained via those resources.
Response: The description for obtaining Fischer344/Brown Norway (FBN) F1 Hybrid rats from the NIA (P.18, #2) has been edited, as well as alternative strategies for obtaining a parent strain of the FBN rats from a private vendor, if needed. Additionally, there is provided documentation of the ability to obtain free animals from NIA (see Appendix v.).

Additional Changes:
1) The reviewers viewed the inclusion of aged female rats as a strength. However, it is necessary to remove female animals altogether, as obtaining aged FBN female rats from the very limited female NIA colony would occur too slowly to support the grant timeline (Heidi Brogdon, NIA, personal communication). Exploring sex differences may be an important future direction if the current project is promising.
2) As evidenced by our recent pilot work (Fig.4-5), all procedures outlined in this proposal, including plasmid preparation, electroporation, and synergistic ablation, have now been successfully performed by Mr. Lawrence. Thus, it was no longer necessary to solicit the previous consultants for the proposal.
3) The above-mentioned pilot work was added to demonstrate very preliminary effects of the mutant GS plasmid on enhancing muscle growth and muscle protein synthesis in rat skeletal muscle, which we view with enthusiasm for use in aged skeletal muscle in the current proposal.

A3.2.2 Specific Aims

Part B: Research Plan

Specific Aims

Specific Aim: The aim of this proposal is to determine whether enhancing intramuscular glycogen content will enhance overload-induced skeletal muscle growth by altering the intramuscular anabolic and catabolic balance in aged rats.

We hypothesize that enhancing intramuscular glycogen content in aged rat skeletal muscle via the plasmid DNA expression of active glycogen synthase will rescue overload-induced muscle growth to levels observed in young adult muscle and to levels significantly greater than age-matched controls lacking glycogen enhancement. We further hypothesize that the mechanisms underlying this effect in the glycogen-enhanced, overloaded muscles of aged animals will be suppressed AMPK activity, enhanced anabolic protein translational signaling and muscle protein synthesis (MPS) rates, and suppressed catabolic protein signaling compared to the age-matched controls. Our anticipated results are presented in Table 1.

Specific objectives:

1) Determine the effects of 21-day overload-induced fast-twitch (plantaris) muscle growth with and without glycogen enhancement in aged rat skeletal muscle as compared to normal young adult muscle (i.e., young adult muscle without glycogen manipulation).
2) Elucidate any potential mechanism(s)/link(s) between muscle glycogen content, AMPK, MPS, muscle protein breakdown(MPB), growth, and associated signaling following chronic overload in aged skeletal muscle.
3) Provide potential mechanistic evidence that suppression of AMPK through enhancing skeletal muscle glycogen content (or any other mechanism elucidated in this study) can enhance muscle mass and/or overload-induced growth in older adult rats.

Impact of Research Results on Field:

1) The findings from the currently proposed project will help to elucidate the roles of glycogen and AMPK on overload-induced growth, anabolic signaling, and MPS in aged skeletal muscle.
2) If our hypothesis is supported, the current project would provide evidence that muscle glycogen enhancement can restore overload-induced muscle growth in aged muscle. Such findings would support further research potentially examining dietary or gene delivery therapy modalities to enhance muscle glycogen in aged animals or, ultimately, humans. Future work could also determine whether enhanced glycogen content increases muscle mass in aged individuals even in the absence of overloading or any anabolic stimuli. Other work could determine whether glycogen enhancement has the potential to benefit muscle mass in conditions other than sarcopenia, such as spinal cord injury, limb immobilization, AIDS, and other states of severe muscle wasting.

Potential Pitfalls and Alternative Outcomes: All experimental procedures have been performed by Mr. Lawrence or others in the Gordon lab. Thus we anticipate no experimental difficulties that cannot be overcome. However, there is a potential experimental outcome that may affect our interpretation of the results:

The mutant GS plasmid proposed for use in the current experiments has been previously utilized to enhance glycogen content in young rodent skeletal muscle (19). We anticipate that glycogen content will be similarly enhanced in aged rat skeletal muscle in this investigation. However, it is possible that glycogen will be enhanced to a lesser (albeit still significant) level or to a greater level than the normal endogenous glycogen content in the young adult animals. Nevertheless, either of these alternative possibilities will still enable the determination of whether enhancing intramuscular glycogen content enhances overload-induced skeletal muscle growth by altering the intramuscular anabolic and catabolic balance in aged rats.

+/- Glycogen Enhancement:	-	-	+
Age Group:	8 months	33 months	33 months
Glycogen Content:	100%	↓	=
Muscle AMPK Phosphorylation & Activity:	100%	↑	=
Catabolic Protein Signaling*:	100%	↑	=
Anabolic Protein Translational Signaling*:	100%	↓	=
Muscle Protein Synthesis Rate:	100%	↓	=
Increase in Muscle Mass & Fiber Size with 21-day Overload:	100%	↓	=

Table 1: Experimental Design with Expected Results. *Results presented only in overloaded muscles, relative to the young adult (8-mo.) group set to 100%.* AMPK, 5'-AMP-activated protein kinase; MPB, muscle protein breakdown; MPS, muscle protein synthesis (MPS). *The rationale for the specific anabolic and catabolic signaling markers chosen are outlined in the "Approach" section below.

A3.2.3 Research Strategy

Part B: Research Plan

Research Strategy

Significance: *Skeletal muscle mass and strength decline greatly with age; known interventions are relatively ineffective in combatting this problem*. Skeletal muscle wasting (atrophy) with age, or "sarcopenia", is a significant clinical problem and a major component of the age-related decline in mobility, ability to accomplish basic activities of daily living, and overall quality of life in the elderly (31). The resultant impact on functional independence, institutionalization, and health care costs in our rapidly expanding older adult population is enormous; sarcopenia-related disabilities are estimated to cost $300 billion per year in the U.S. (4). Unfortunately, interventions such as resistance exercise training (loading of the muscle) are relatively ineffective at increasing muscle mass in the elderly when compared to healthy young adults (10, 41). Our laboratory has observed highly similar detriments in muscle hypertrophy in response to chronic loading of the muscle (i.e., synergistic ablation/tenotomy, a model of resistance exercise training) in aged rats (12, 39, 40).

Aged skeletal muscle displays a blunted protein turnover. Skeletal muscle mass is maintained by the intricate balance of protein turnover that involves muscle protein synthesis (MPS) and muscle protein breakdown (MPB) (41). Aged skeletal muscle is associated with a reduction in MPS and anabolic protein translational signaling (i.e., intermediate signaling such as the Akt-mTOR-p70S6k pathway – see Fig. 1 for pathway details and acronym definitions) and an upregulation of MPB and catabolic signaling (e.g., "atrogenes" such as FOXO3A, MuRF1, and MAFbx; Fig.1), leading to a net protein loss. Moreover, these losses have been predominantly found to affect fast-twitch (i.e., type II) skeletal muscle fibers (18). Additionally, in response to anabolic stimuli (i.e., resistance training, growth factors, etc.) aged skeletal muscle has a blunted ability to hypertrophy (7, 9). Further, the inability to maintain or increase muscle fiber size occurs both in aged humans (23) and in rats (25). Importantly, the Gordon lab found that an enzyme within skeletal muscle fibers called 5'-AMP-activated protein kinase (AMPK) plays a major role in the suppression of MPS and associated signaling (8, 12, 39, 40), upregulation of MPB signaling (36) and thus, impaired growth in aged muscle (12, 39, 40).

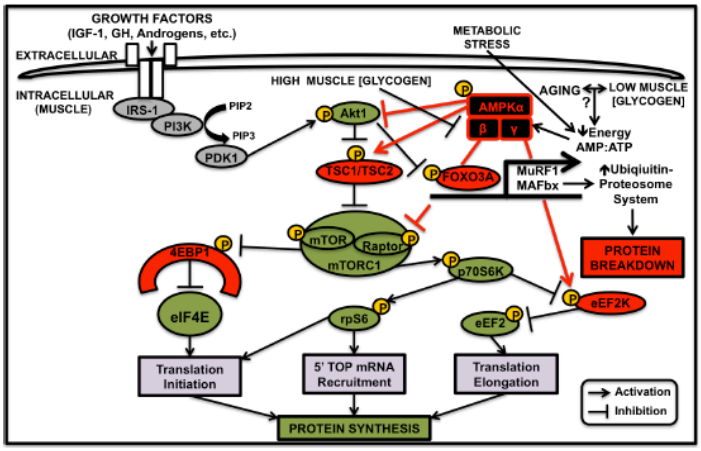

Figure 1. Overview of potential muscle protein synthesis (MPS) and muscle protein breakdown (MPB) regulation by 5'-AMP-activated protein kinase (AMPK). Note: red arrows and lines indicate direct effects of AMPK. IGF-1, insulin-like growth factor 1; GH, growth hormone; IRS-1, insulin receptor substrate 1; PI3k, phosphoinositide 3-kinase; PIP2, phosphatidylinositol (3,4)-bisphosphate; PIP3, phosphatidylinositol (3,4,5)-triphosphate; PDK1, 3-phosphoinositide-dependent protein kinase 1; Akt1, protein kinase B 1; TSC1/TSC2, tuberous sclerosis complex; FOXO3A, forkhead box transcription factor 3A; mTOR, mechanistic (formerly mammalian) target of rapamycin; mTORC1, mTOR complex 1; MuRF1, muscle ring-finger 1; MAFbx, muscle atrophy F-box; eIF4E, eukaryotic initiation factor 4E; 4EBP1, eIF4E binding protein; p70S6k, 70-kDa ribosomal protein S6 (rpS6) kinase; eEF2K, eukaryotic elongation factor 2 (eEF2) kinase; 5' TOP, 5' terminal oligopyrimidine tract. Factors that inhibit protein synthesis and/or lead to protein breakdown are in red, whereas, factors involved in protein synthesis and/or inhibit protein breakdown are in green. Note: Aging is associated with low muscle [glycogen], which may be the cause of the negative energy (high AMP:ATP) balance leading to activation of AMPK.

Negative energy balance in aged skeletal muscle chronically activates AMPK. Aged skeletal muscle displays a negative energy balance (i.e., a high ratio of AMP to ATP), which is known to activate AMPK (14), and may do so on a chronic basis in aged muscle (39). AMPK exists in a heterotrimeric complex containing 7 isoforms: α_1, α_2, β_1, β_2, γ_1, γ_2, γ_3. In addition to being activated allosterically by elevated AMP (on its γ subunit), AMPK is also activated by phosphorylation at Threonine-172 (Thr^{172}) by upstream kinases (e.g., AMPK kinase) on its catalytic α subunit. Moreover, AMPK can conversely be strongly inhibited by glycogen binding to a glycogen-binding domain (GBD) on its β subunit (14, 20, 21). When activated, AMPK acutely upregulates pathways to supply short-term energy via glucose uptake and fat oxidation (14), and chronic AMPK activation leads to long-term energy supply pathways being increased, such as mitochondrial biogenesis (14), to restore cellular energy homeostasis.

AMPK also inhibits ATP-expensive pathways such as MPS. Specifically, AMPK directly activates (via phosphorylation) TSC2 allowing for the TSC1/TSC2 (TSC) complex to form, which in turn inhibits mTOR complex 1 [mTORC1; (32); Fig.1]. AMPK also directly inhibits mTORC1 by phosphorylating and inhibiting the mTORC1 protein Raptor [(32); Fig.1]. mTORC1 inactivation leads to suppression of protein translation

initiation by not allowing mTORC1 to activate (via phosphorylation) both p70S6k and being unable to remove (via phosphorylation) 4E-BP1 inhibitory binding on eIF-4E (Fig.1). The inhibition of p70S6k by AMPK also inhibits p70S6k from recruiting 5' TOP mRNA as well as phosphorylating rpS6 (15, 32) further inhibiting protein translation initiation (Fig.1). Further, the inhibition of p70S6k by AMPK leads to inhibition of protein elongation by not allowing p70S6k to remove eEF2k inhibition of eEF2 (15) ; Fig.1]. AMPK has been found to directly inhibit elongation by phosphorylating eEF2k [(16); Fig.1]. AMPK also blocks Akt inhibition (via phosphorylation) of FOXO3A, allowing for FOXO3A translocation to the nucleus and subsequent upregulation of MuRF1 and MAFbx, leading to MPB [(15); Fig.1]. The Gordon lab has observed a similar elevation of AMPK activity and inhibition of protein translation initiation and elongation anabolic (MPS) signaling following an acute bout of RE (37) and following chronic muscle overload (12, 39, 40), in conjunction with a blunted hypertrophy in aged rat skeletal muscle (12, 39, 40). The elevated AMPK activity in older muscle is likely due in part to age-related deficits in cellular energy status, such as compromised high-energy phosphate molecules and reduced carbohydrate (i.e., glycogen; Fig.1) stores (3).

Proposed restoration of muscle glycogen content to suppress AMPK and rescue overload-induced growth in aged skeletal muscle. Glycogen, the stored form of glucose, makes up ~500 g of total skeletal muscle mass, and serves as a critical energy reserve for ATP production during states of reduced cellular energy (5, 26). Glycogen is synthesized by the main enzyme glycogen synthase (GS) and is degraded by the enzyme glycogen phosphorylase, and both work in conjunction with other enzymes (30). Not surprisingly, glycogen content is diminished in aged skeletal muscle at rest in both rats (3, 5) and humans (5). Moreover, the contraction-induced depletion of glycogen is significantly greater in aged skeletal muscle (5) and there is a substantially blunted ability to increase glycogen levels with training when compared to young adult muscle in both rats (6) and humans (22). Further, as stated above, AMPK has a direct interaction with glycogen through its β subunit containing a GBD (20). AMPK's activity has been found to be inversely related with the level of glycogen in muscle *in vivo*, with its activity being dramatically suppressed with high levels of glycogen and an increased AMPK activity with low levels of glycogen in both rats (42) and humans (35). These findings have also been supported *in vitro*, where large synthesized branched oligosaccharides (i.e., large glycogen-mimicking molecules) inhibited AMPK's activity up to 90%, and as the oligosaccharides decreased in their amount of branching (i.e., smaller glycogen-mimicking molecules) there were concomitant increases in AMPK's activity as well as suppression on glycogen synthesis (20). Additionally, AMPK directly acts upon GS to inhibit it during states of increased energy requirements (i.e., low energy status) and this may be a critical factor involved with the inability to store glycogen in aging skeletal muscle (i.e., chronic activation of AMPK).

Low glycogen content (i.e., a diminished energy reserve) directly enhances AMPK's activity, which in turn suppresses protein synthesis as part of an attempt to restore immediate energy balance (13). It is not surprising that glycogen content is diminished in aged muscle at rest (3, 5), but the link between glycogen content and muscle growth during overload has not been previously examined in humans or animals of any age. Preliminary data (see Fig. 2-3) in our lab indicate that glycogen increases in overloaded fast-twitch skeletal muscle (i.e., plantaris) in young adult, but not old, rats (Fig.2), resulting in lower absolute glycogen levels in aged rat skeletal muscle during overload. Moreover, this diminished increase in glycogen content was associated, albeit not all significantly, with higher AMPK activity (significant; data not shown), lower protein synthesis (approaching significance, data not shown), and reduced muscle growth (Fig.3) in the old animals. We thus postulate that reduced muscle glycogen content and responsiveness is an important cause of suppressed overload-induced growth in aged muscle. We hypothesize that enhancing intramuscular glycogen content in aged rat skeletal muscle via the plasmid DNA expression of active glycogen synthase will rescue overload-induced muscle growth to levels observed in young adult muscle and to levels significantly greater than age-matched controls lacking glycogen enhancement. We further hypothesize that the mechanisms underlying this effect in the glycogen-enhanced, overloaded muscles of aged animals will be suppressed AMPK

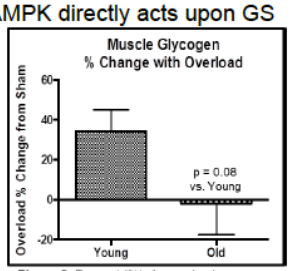

Figure 2: Percent (%) change in glycogen content of 7-day overloaded vs. sham-operated plantaris muscles in young adult (8 mo.) vs. old (33 mo.) rats.

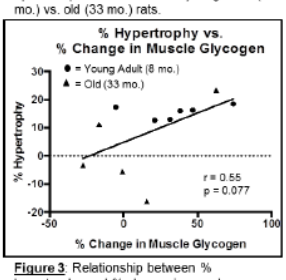

Figure 3: Relationship between % hypertrophy and % change in muscle glycogen content in overloaded-limb with 7 days of overload in plantaris muscles of young adult (8 mo.) and old (33 mo.) rats.

activity, enhanced anabolic protein translational signaling and MPS rates, and suppressed catabolic protein signaling compared to the age-matched controls.

Innovation: Previous experiments in the Gordon lab (12, 38-40) have highlighted the role of AMPK in diminished overload-induced growth in aged skeletal muscle. In addition, our preliminary data (Fig. 2-3) finding moderate-to-good relationship trends between the amount of intramuscular glycogen during overload-induced hypertrophy and AMPK activity, protein synthesis rate, and muscle growth highlights a potential role of glycogen in suppressing AMPK and restoring overload-induced growth in aged skeletal muscle. Therefore, this study is innovative in that this is the first time that the effect of variable glycogen levels on overload-induced growth will be examined in aged skeletal muscle. If our hypotheses are supported, the proposed research will lead to a greater understanding of the role of glycogen content and AMPK on muscle growth in aged skeletal muscle. This would warrant further examination into different approaches (e.g., dietary, gene therapy, or others) of enhancing muscle glycogen in aged rat, or eventually, human muscle with and without muscle overload.

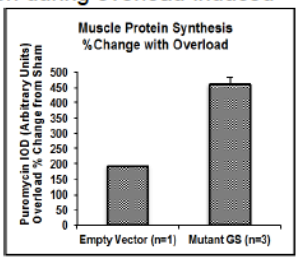

Figure 4: Percent (%) change in puromycin IOD protein synthesis of 21-day overloaded vs. sham-operated plantaris muscles in young adult rats with empty vs. mutant glycogen synthase (GS) plasmid treatment.

The use of plasmid DNA to enhance intramuscular glycogen in this investigation (as opposed to increasing dietary carbohydrate intake) is due to the fact that it is very difficult to increase muscle glycogen through dietary manipulation alone in rat or mouse skeletal muscle (R.C. Hickner, Ph.D., personal communication). Important to this proposal, employing the exact methodology as outlined in the "Approach" section, very recent pilot work (Fig. 4-5) in our lab has found that the introduction of the mutant GS plasmid vector prior to 3 weeks of overload-induced growth had a profound increase on MPS (Fig. 4) and wet weight (Fig.5) in the plantaris muscle as compared to an empty (no glycogen manipulation) vector plasmid in young adult (8 mo.) rats. Further analyses for glycogen content, AMPK phosphorylation and activity, and protein anabolic and catabolic signaling are currently ongoing and being validated in our laboratory. The small sample size (*n* of 1) for the empty vector was due to an error by a veterinary staff member during initial survival surgery inducing a fatal combination of anesthetic and analgesic that was identified and corrected for all future animals (remaining *n* of 4 in Fig.4-5).

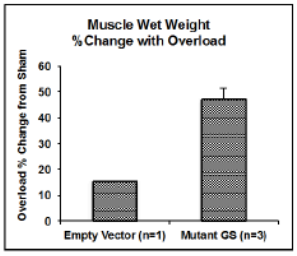

Figure 5: Percent (%) change in muscle wet weight of 21-day overloaded vs. sham-operated plantaris muscles in young adult rats with empty vs. mutant glycogen synthase (GS) plasmid treatment.

Approach: *Experimental Groups, Surgical Procedures, and Glycogen Enhancement*. Young adult (8 mo.) and old (33 mo.) male FBN rats (*n* = 10/group, 30 total – Fig.6) will be housed at the UNC Charlotte vivarium under standard animal care. All procedures will be performed by Mr. Lawrence, under the direct supervision of Dr. Gordon. Under general anesthesia (2-3% isofluorane and supplemental O_2), unilateral hindlimb surgical ablation of the gastrocnemius muscle in each animal will be performed to enable compensatory overload of the synergistic plantaris and soleus muscles for 3 weeks as described by Thomson and Gordon (39, 40). A sham (non-overload) surgery will be performed on the contralateral control hindlimb.

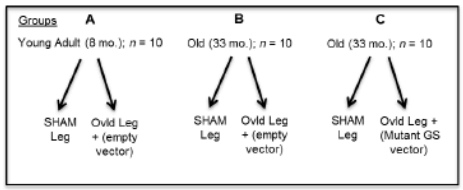

Figure 6: Overview of proposed experimental design. Using 3-week unilateral synergistic ablation (Ovld) with respective Groups' plasmid (empty or mutant glycogen synthase; GS) treatment in the Ovld limb and the contralateral limb receiving sham surgery. Groups A and B will be injected with the empty control vector plasmid DNA, inducing a normal glycogen response. Group C will be injected with mutant GS plasmid DNA, inducing an enhancement in intramuscular glycogen.

During the ablation surgery, 120 µL of plasmid DNA (either mutant GS or empty vector) for each muscle will be introduced into the plantaris muscle to be overloaded (but not the contralateral sham-operated muscle) using a 27-gauge needle and syringe following the protocol of Wu and Kandarian (43). Briefly, the needle will be inserted near the distal myotendinous junction of the muscles, and slowing pushed in ~1cm rostrally to the proximal end of the muscle. 120 µL (at 1.5 µg/µL) of the plasmid DNA (in warm sterile saline solution) will be injected evenly along the longitudinal axis of the muscles while slowly withdrawing the syringe. Following a 1-min wait period, electroporation will be performed. Briefly, the surface of the muscles will be moistened with sterile saline. Then, the electrodes (Tweezerodes, Harvard Apparatus) will be placed on either

side of the muscle. Next, 5 square-wave electrical pulses at 75-100 V/cm, 20 ms at 1 Hz, with 200 ms interpulse intervals will be applied using a BTX Electro Square Porator (Harvard Apparatus). *Importantly, these procedures have already been successfully performed by Mr. Lawrence and Dr. Gordon (Fig.4-5).*

We have obtained a constitutively active mutant (mutated from serine to alanine on two key phosphorylation sites of the enzyme to keep enzyme constantly active) glycogen synthase (mutant GS) cDNA insert (from Dr. Peter Roach, Indiana University) that was ligated into the pCAGIG vector (pCAGIG-GS). The mutant GS cDNA on a similar vector backbone (pCMV4) has been found to enhance muscle glycogen in rodents (19). Animals intended for glycogen enhancement (see Table 1 and Fig. 6) will receive mutant pCAGIG-GS plasmids that expresses constitutively active glycogen synthase (resulting in elevated muscle glycogen content). The rest of the animals will receive "empty vector" DNA plasmids with no glycogen synthase expression (resulting in the animals own endogenous glycogen). Both the mutant GS and empty vector plasmids have already been prepared numerous times for electroporation by Mr. Lawrence utilizing the following protocols (34, 43) *and have been employed in our recent pilot work (Fig.4-5)*. All DNA plasmids will be injected into the plantaris muscle designated for overload only (i.e., not into the sham limb). After recovery from anesthesia (< 1 hour), all animals will be allowed to walk normally on the limbs for 3 weeks (choice for 3 week time point discussed below), inducing compensatory growth in the overloaded plantaris muscles; growth is severely diminished in normal aged animals without glycogen enhancement (39).

Muscle and Blood Harvesting. Three weeks after ablation surgery, animals will be again anesthetized. Three weeks is the chosen time point for ablation surgery to allow for inflammatory processes to subside and for MPS rates and muscle growth to be optimized (1, 2, 27). During anesthesia, one jugular vein of the animal will be exposed by incision through the skin of the neck. The vein will then be slowly injected with 0.040 µmol puromycin/ g BW dissolved in sterile PBS using a 25-gauge needle (17). Puromycin is incorporated into synthesizing proteins within the muscle and can be used in determining rate of protein synthesis by western blotting in harvested muscle samples [(11); Fig. 4]. At 20 min. after injection, the plantaris muscles will be very quickly harvested, weighed, and frozen in liquid N_2-chilled isopentane for immunohistochemistry (IHC), western blotting, and other analyses. After which, the abdominal cavity will be carefully opened via incision and 2-3 mL of whole blood will be collected via venipuncture of the inferior vena cava (for any potential serum analyses that may be needed). Other muscles may also be harvested if time permits.

Experimental Analyses. Analyses and expected results are summarized in Table 1. All experimental analyses techniques have been previously performed by Mr. Lawrence, or are currently being validated (pilot work Fig.4-5) by Mr. Lawrence. Glycogen content will be measured in subportions of each harvested plantaris muscle as previously performed in the Gordon lab (37). Also as performed in the Gordon lab (12, 37-40) and by Mr. Lawrence, standard western blotting techniques will be employed to analyze phosphorylation and total for AMPKα and AMPK's *in vivo* activity marker [Acetyl CoA Carboxylase (ACC) Ser^{79}; (24)] in muscle homogenates; along with phosphorylation and total for several other anabolic protein translational signaling regulating anabolic protein translation initiation (specifically Akt, mTOR, p70S6k, 4E-BP1; Fig.1) and elongation (specifically eEF2 and eEF2K); as well as, catabolic protein signaling (specifically FOXO3A, MuRF1, MAFbx) that are known to be regulated or influenced by AMPK (Fig.1). Importantly, the Gordon lab (8, 12, 36-40) has found the anabolic translational signaling markers of Akt, mTOR, p70S6k, 4E-BP1, eEF2, eEF2k and the catabolic signaling markers of FOXO3A, MuRF1, MAFbx (specific phospho-sites are detailed in the "Budget"/"Budget Narrative") to be intricately involved with AMPK, MPS, MPB, and growth in aged muscle. Protein synthesis will be also analyzed by standard western blotting for puromycin as previously described (11, 17). Whole muscle mass will be assessed by wet weight and muscle fiber cross-sectional area (CSA; via laminin staining) will be assessed via IHC in muscle cross-sections. In addition to whole muscle measurements, we will also specifically analyze cross-sections for individual fibers expressing the plasmid for CSA, protein synthesis (11), glycogen content (33), and signaling intermediates where necessary.

Statistical Analyses. A two-way analysis of variance will be used (Treatment Group x Overload, with repeated measures for overload between contralateral limbs). Post-hoc comparisons will be accomplished via a Fisher's LSD test, with statistical significance being set *apriori* at $p \leq 0.05$.

A3.2.4 Description of Risks for the Protection of Human Subjects or Vertebrate Animals

Part B: Research Plan

Descriptions of Risks for the Protection of Human Subjects or Vertebrate Animals

---

1. Young adult (8 mo.) and old (33 mo.) male FBN rats (*n* = 10/group; 30/total) will be used in the current study. The rationale for the use of animals within the current proposal is because the use of plasmid DNA to enhance glycogen content in rat skeletal muscle is a fairly standard and simple technique that is not readily available in humans.

2. The minimum calculated sample sizes for a power level of 0.80 and an alpha level of 0.05 is 8 rats per group (SigmaStat, Saugus, MA). As outlined in Appendix v attached, the NIA provides FBN rats at no cost to grantees funded by U.S. private foundations and limits non-NIA grantees to 10 rats per month. Therefore, we plan to request the maximum of 10 rats per month until we reach our *n* of 10 for each group. This strategy is our only option for FBN of any age as they are not available from private vendors. We foresee reaching our full sample sizes for each group in ~3-5 months, while simultaneously performing group-matched experiments and analyses. Importantly, previous work in the Gordon lab (8, 12, 39, 40) has found <5% mortality rates in all FBN's (both 8 mo. and 30+ mo. old) in surgical ablation studies. However, we will order 10/group to account for potential unforeseen losses and ensure at least 8/group. Although highly unlikely, if we do experience mortality >25% we will request more animals as needed to meet our *n* of 8/group (the powered sample size). The skeletal muscle aging characteristics of the FBN rat closely model human skeletal muscle aging (29), and has been found to be the best rodent model with respect to aging human skeletal muscle. Furthermore, the use of 8 mo. old rats as "young adult", and 33 mo. old rats as "old" coincides with the human age equivalents of peak muscle mass (i.e., 8 mo. old rat or ~25 human years) and when the incidence of sarcopenia is over 50% of that aged population [(28); i.e., 33 mo. old rat or ~80+ human years]. Additionally, if the FBN's cannot be obtained within our given timeline for any reason, we will use the parent strain of Fischer344, the next best strain for aging muscle (29), for all experiments as this strain is available from multiple private vendors.

3. All procedures will be approved by the UNC Charlotte Animal Care and Use Committee. Animals will be housed and all animal experiments will be performed at the UNC Charlotte Vivarium, an AAALAC accredited facility. Animals will be kept in a room maintained at 21°C, 50% humidity, with a 12:12-hour light cycle. Muscle harvesting times will be controlled and matched amongst groups to account for variations in protein synthesis through the circadian and feeding cycle. Food and water will be provided *ad libitum*. The UNC Charlotte Vivarium is staffed by full-time professionals, including a full-time Director and Veterinarian, all of who participate in ongoing training and professional development, and are independently certified.

4. For survival surgery, including unilateral synergistic ablation and plasmid injection and electroporation, animals will be anesthetized (2-3% isofluorane and supplemental O_2). Proper level of anesthesia will be assessed by the pedal and corneal reflexes and breathing patterns before and every few min. during surgery. Surgery will be performed using standard sterile techniques and instruments in the Vivarium surgical suite. Prior to surgery, the surgical sites will be prepared (shaved and scrubbed with iodine solution). Under aseptic conditions, incisions will be made in the distal posterior hindlimbs to expose the gastrocnemius muscle, which will be surgically ablated. After ablation, the underlying plantaris muscle will be subjected to electroporation to introduce the desired plasmids into the muscle fibers. Plasmids and electroporation will be administered following the protocol outlined above in the "Approach" section, using the previously published protocol (43). Importantly, in our recent pilot work (Fig.4-5) we have found no deleterious effects, including muscle damage or infection following the same protocol outlined the "Approach" section above. After electroporation, the incision will be closed using sterile stainless steel surgical clips. Animals will be kept on a water-circulation heating pad during surgery, and subcutaneously injected with warm sterile saline after surgery. During surgery while still under anesthesia, the animals will be given subcutaneous injections of analgesic (buprenorphine, 0.05 mg/kg BW). Animals will be injected with buprenorphine as needed every 8-12 hrs for the following 24-72 hrs. We have observed very little or no post-operative complications (including infection), in prior surgeries, regardless of age. Animals are typically ambulatory and active immediately upon recovery from anesthesia, and display no signs of pain of discomfort.

5. For non-survival surgery/euthanasia, with animals still alive, but at a terminal anesthetic plane achieved by isofluorane, one jugular vein of the animals will exposed for puromycin injection as outlined in the "Approach" section. After tissue and blood harvesting, animals will be sacrificed by opening of the thoracic cavity and excision of the heart while still under terminal anesthesia, which is an approved AVMA procedure.